Quantum phase transitions: from antiferromagnets and superconductors to black holes

Reviews:
arXiv:0907.0008
arXiv:0810.3005 (with Markus Mueller)

Talk online: sachdev.physics.harvard.edu

PHYSICS
VE RI TAS
HARVARD

Lars Fritz, Harvard
Victor Galitski, Maryland
Max Metlitski, Harvard
Eun Gook Moon, Harvard
Markus Mueller, Trieste
Joerg Schmalian, Iowa

Frederik Denef, Harvard+Leuven
Sean Hartnoll, Harvard
Christopher Herzog, Princeton
Pavel Kovtun, Victoria
Dam Son, Washington

PHYSICS
HARVARD

Outline

1. Coupled dimer antiferromagnets

   Order parameters and Landau-Ginzburg criticality

2. Graphene

   `Topological' Fermi surface transitions

3. Quantum criticality and black holes

   AdS_4 theory of compressible quantum liquids

4. Quantum criticality in the cuprates

   Global phase diagram and the spin density wave transition in metals

Outline

1. Coupled dimer antiferromagnets
   Order parameters and Landau-Ginzburg criticality

2. Graphene
   `Topological' Fermi surface transitions

3. Quantum criticality and black holes
   AdS_4 theory of compressible quantum liquids

4. Quantum criticality in the cuprates
   Global phase diagram and the spin density wave transition in metals

$TlCuCl_3$

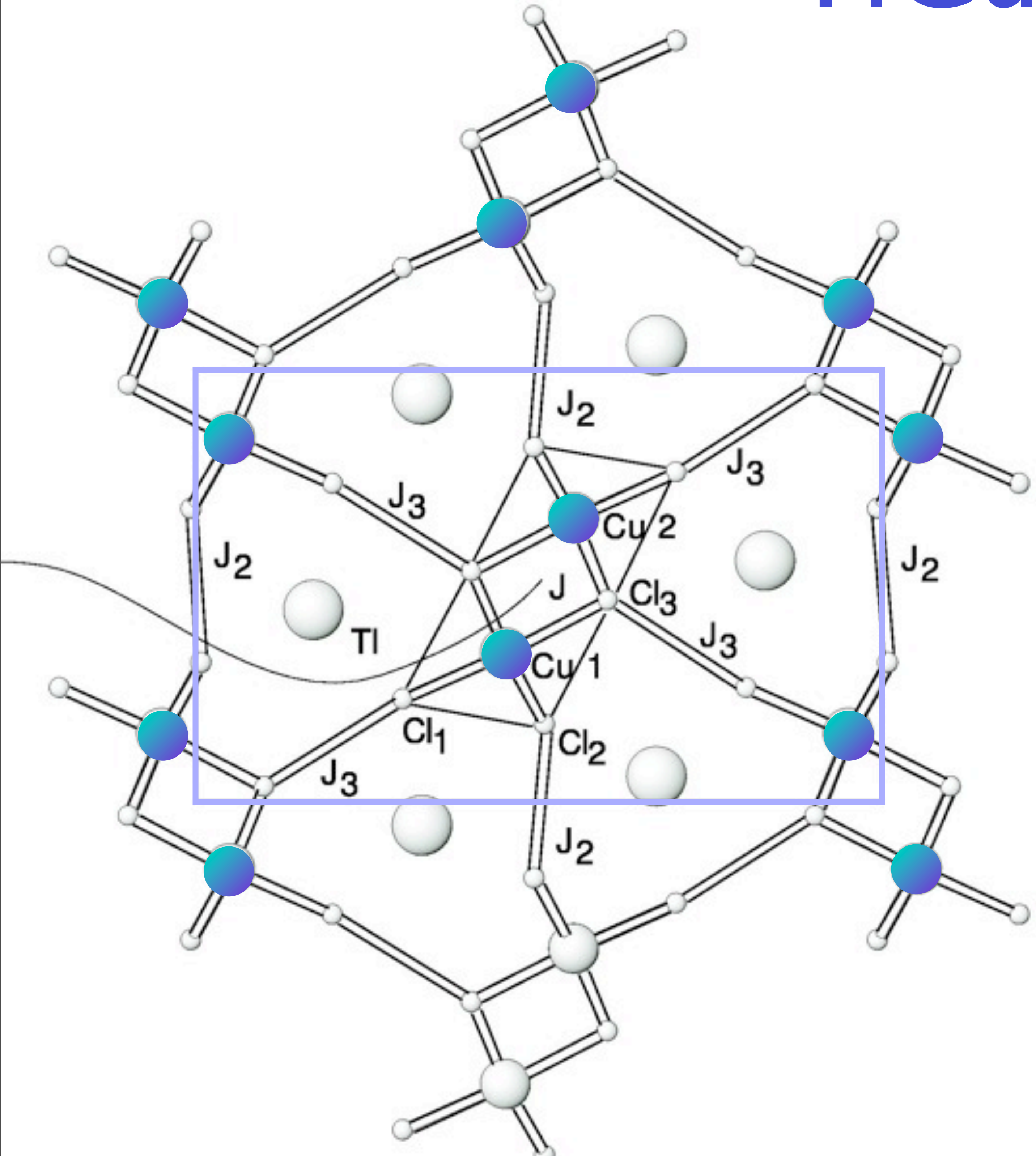

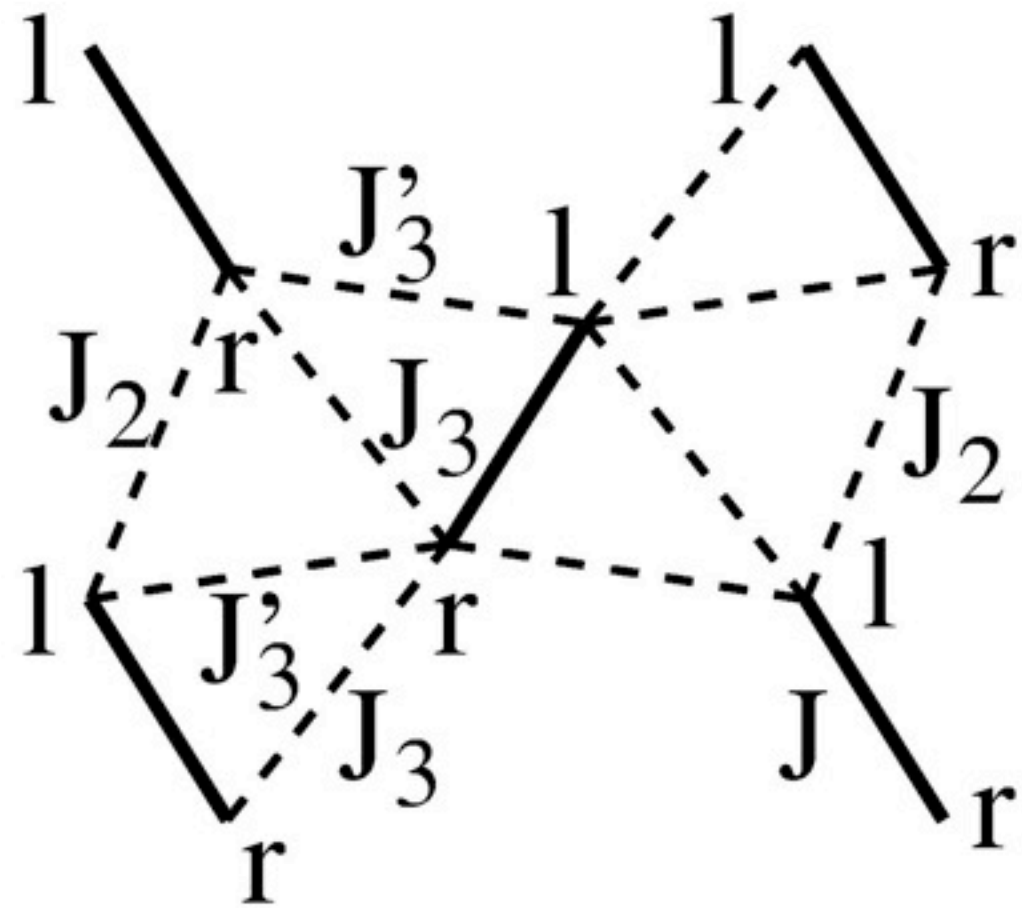

$TlCuCl_3$

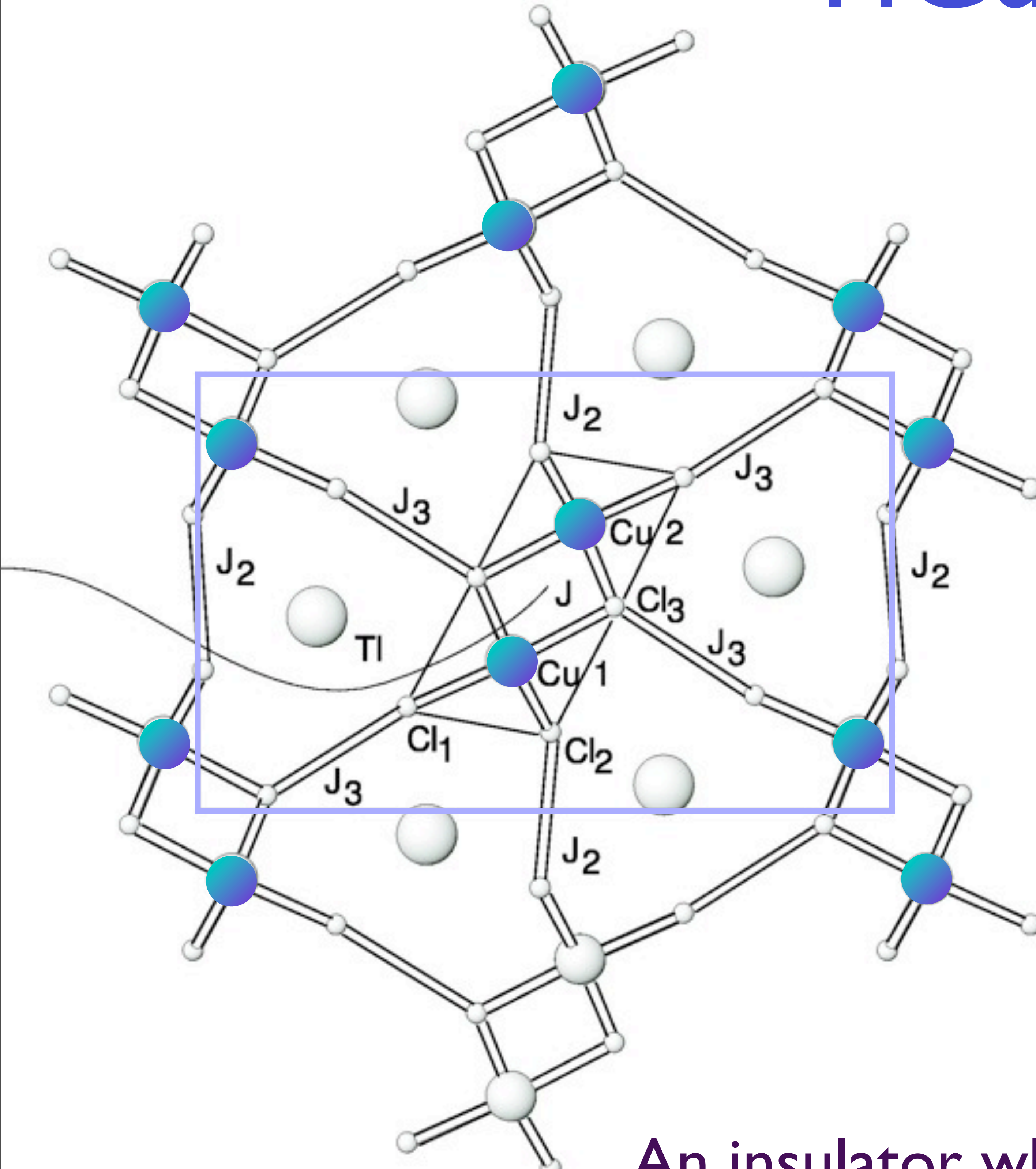

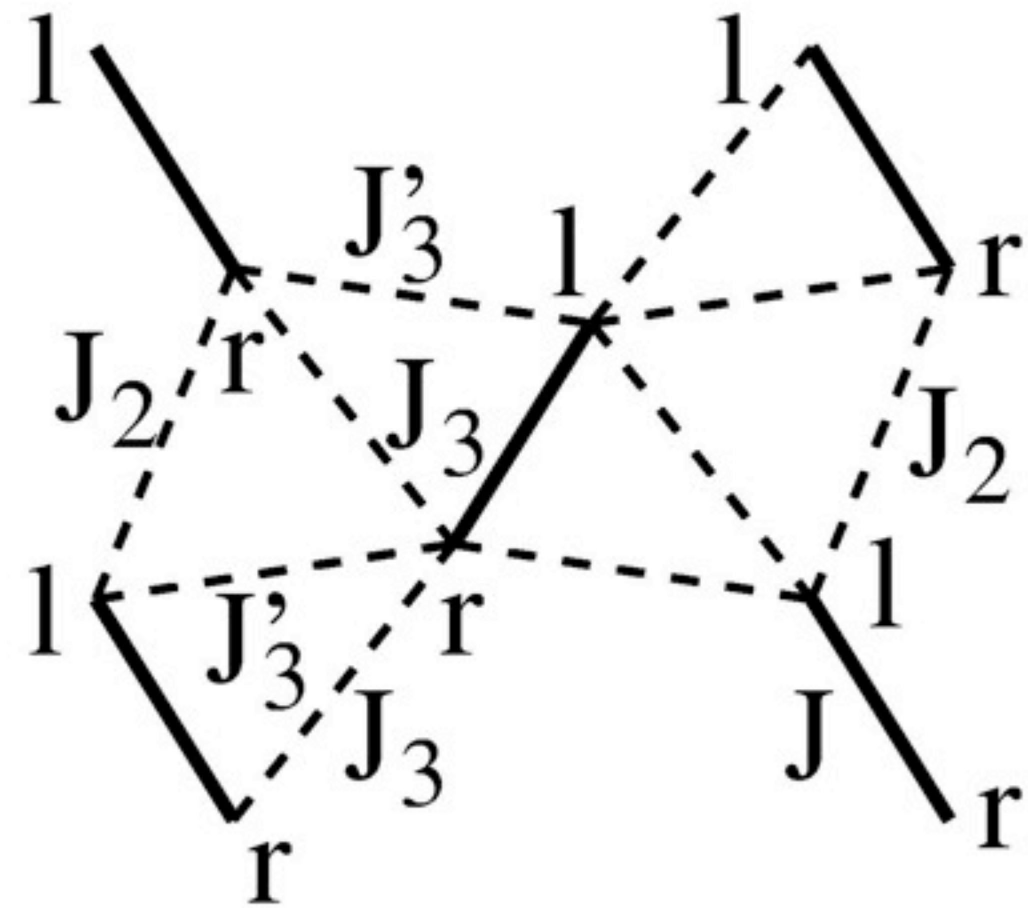

An insulator whose spin susceptibility vanishes exponentially as the temperature T tends to zero.

Square lattice antiferromagnet

$$H = \sum_{\langle ij \rangle} J_{ij} \vec{S}_i \cdot \vec{S}_j$$

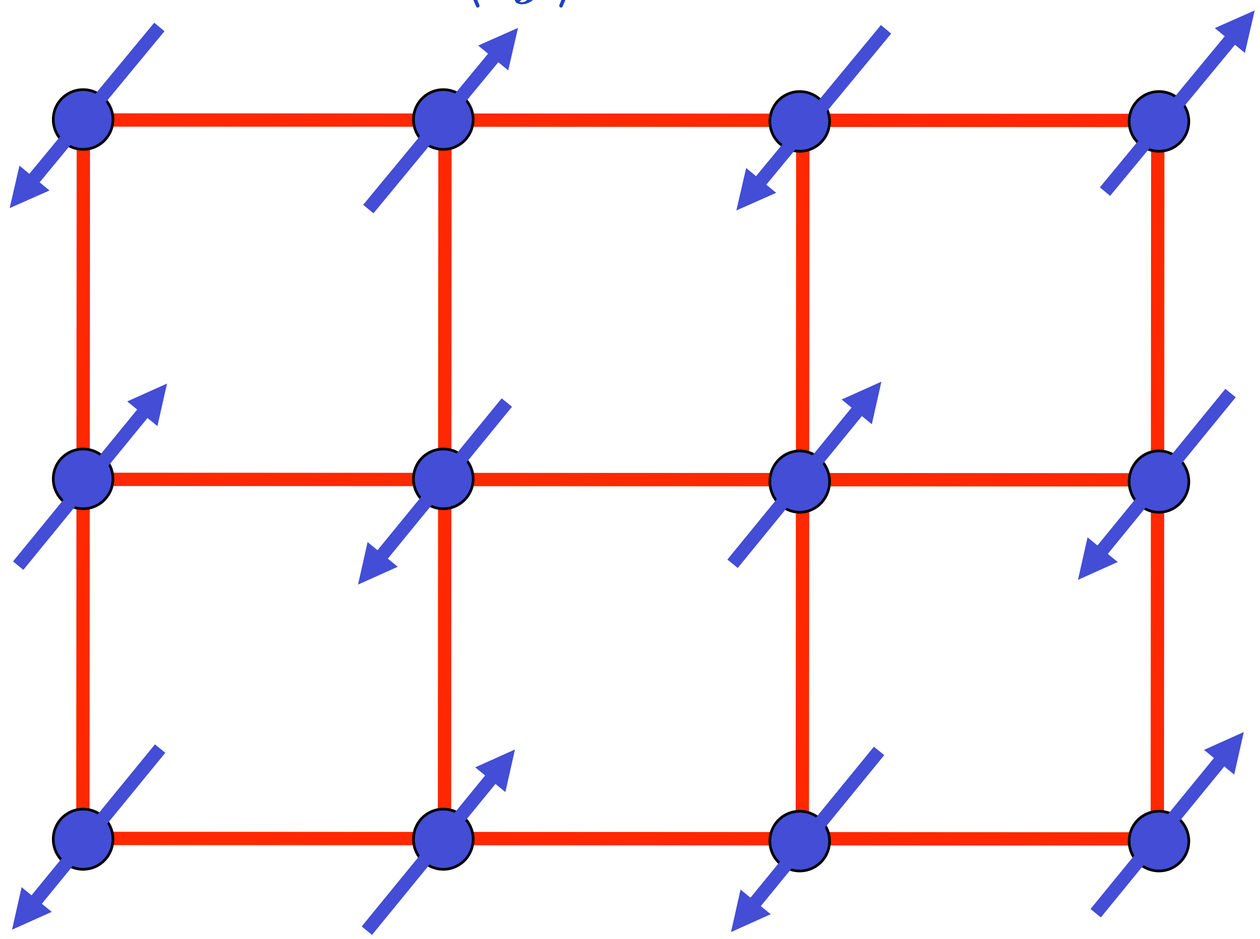

Ground state has long-range Néel order

Order parameter is a single vector field $\vec{\varphi} = \eta_i \vec{S}_i$

$\eta_i = \pm 1$ on two sublattices

$\langle \vec{\varphi} \rangle \neq 0$ in Néel state.

Square lattice antiferromagnet

$$H = \sum_{\langle ij \rangle} J_{ij} \vec{S}_i \cdot \vec{S}_j$$

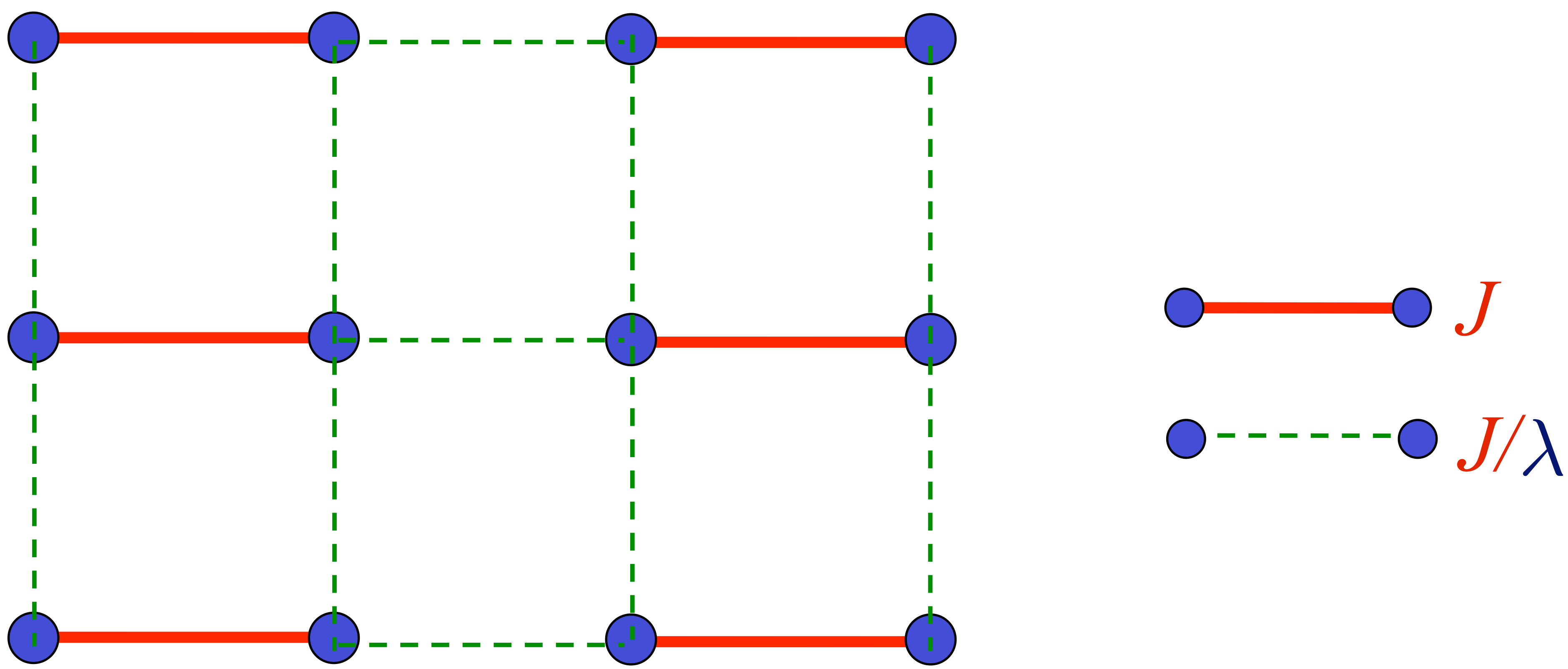

Weaken some bonds to induce spin entanglement in a new quantum phase

Square lattice antiferromagnet

$$H = \sum_{\langle ij \rangle} J_{ij} \vec{S}_i \cdot \vec{S}_j$$

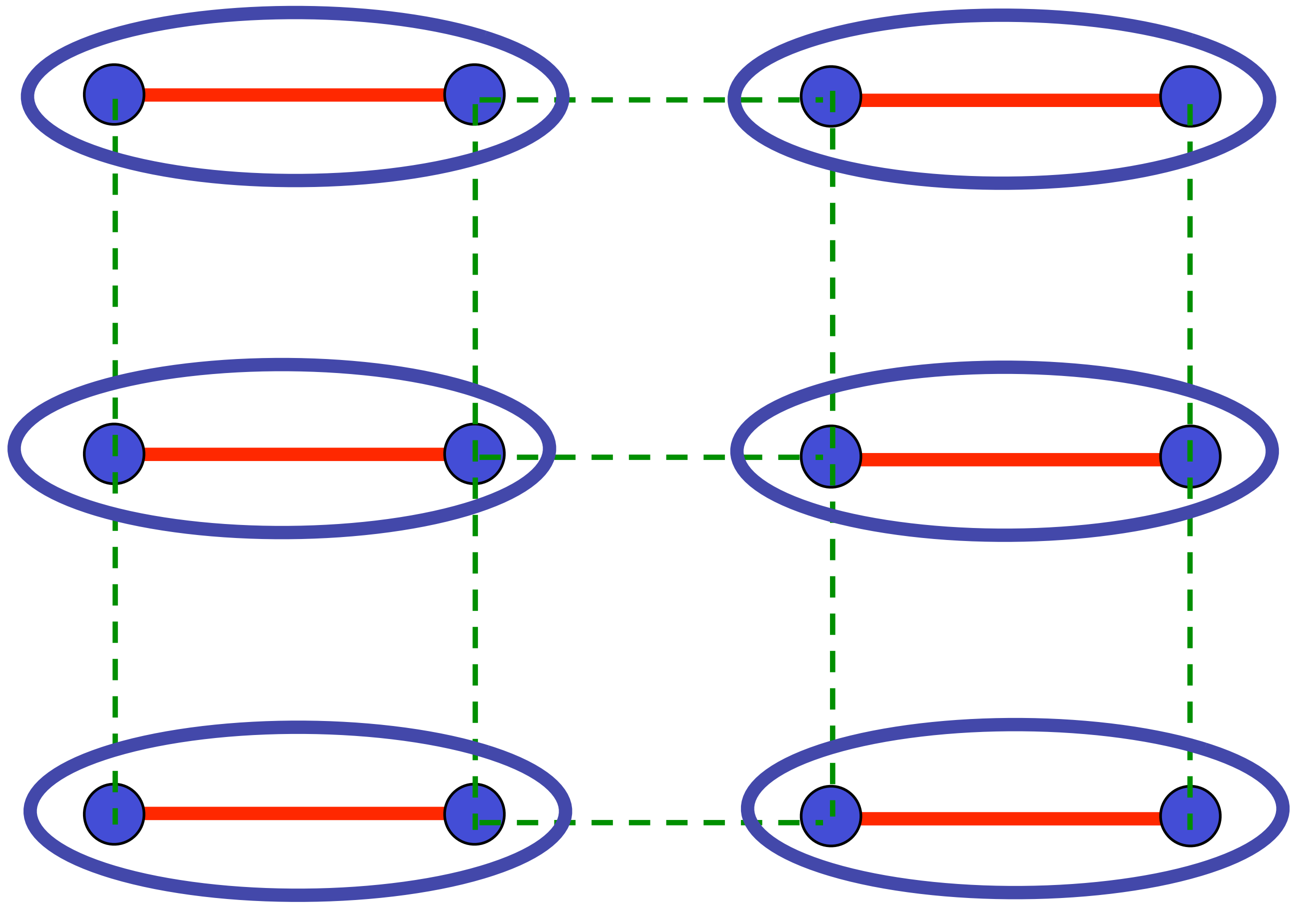

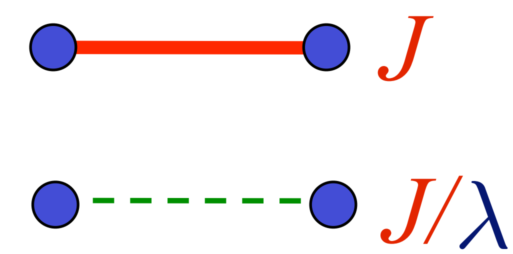

Ground state is a "quantum paramagnet"
with spins locked in valence bond singlets

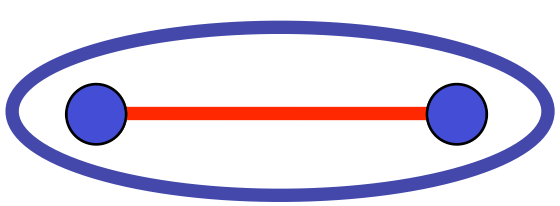

$$= \frac{1}{\sqrt{2}} \left(\left| \uparrow\downarrow \right\rangle - \left| \downarrow\uparrow \right\rangle \right)$$

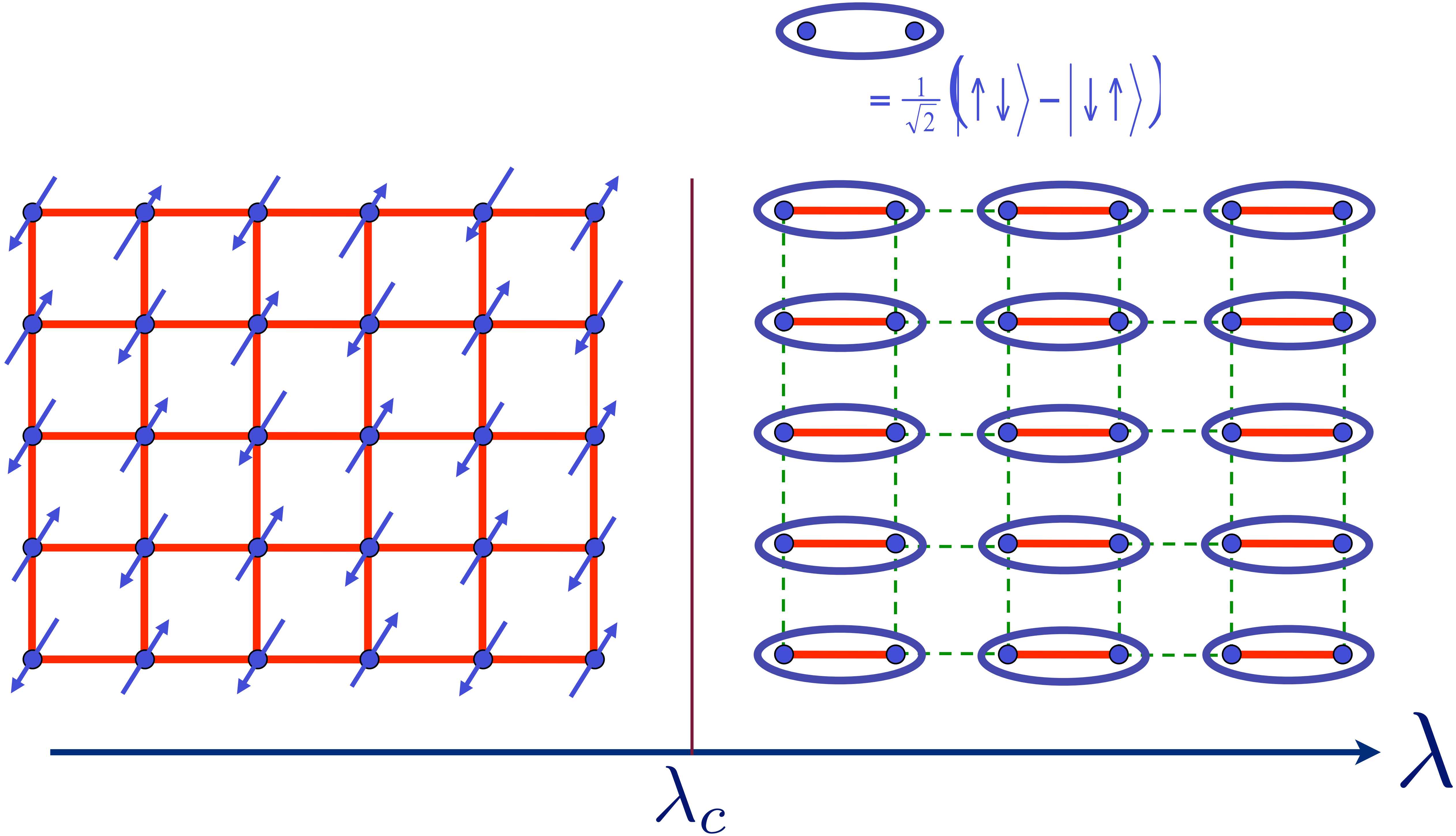

Pressure in $TlCuCl_3$

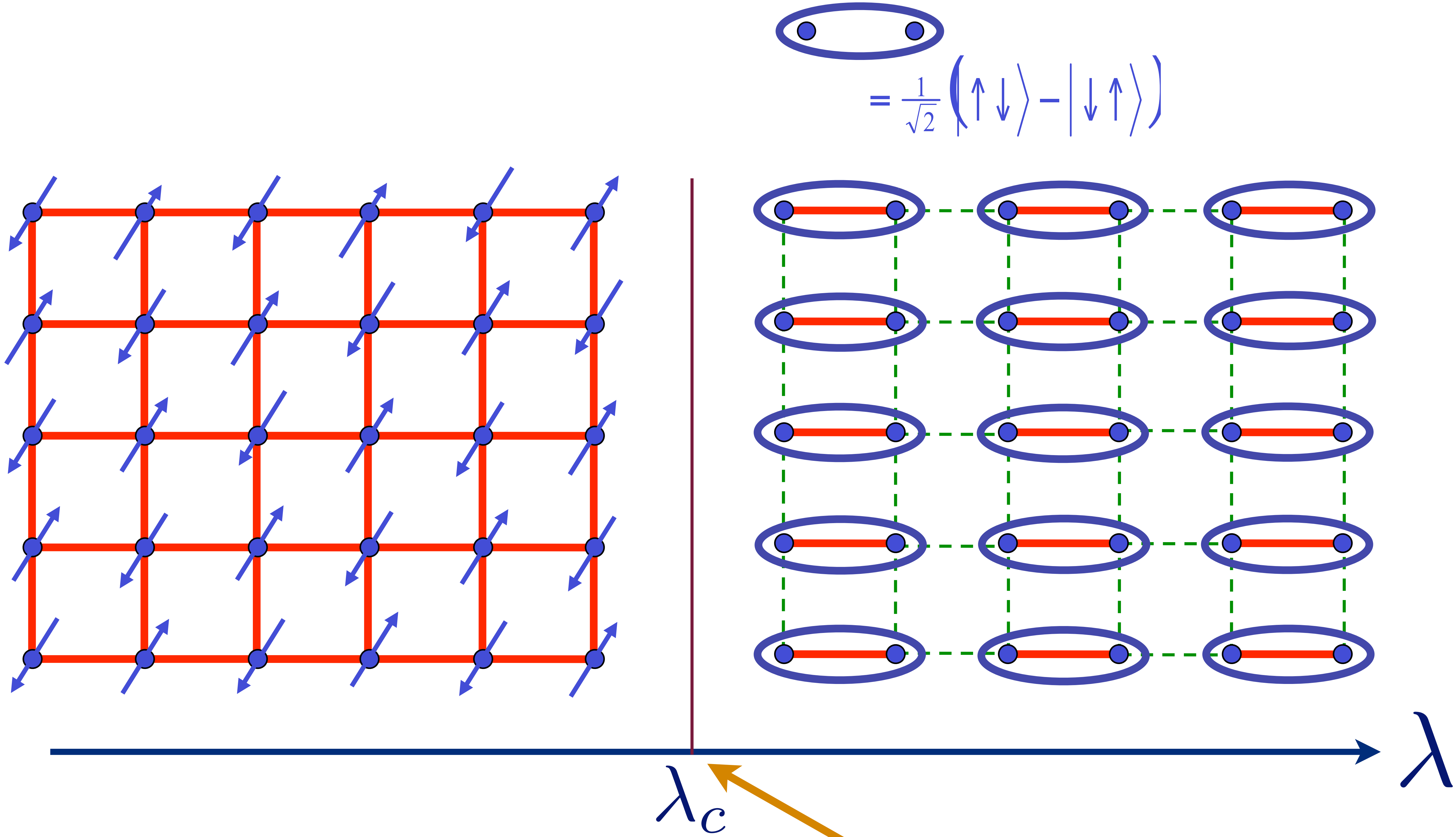

Quantum critical point with non-local entanglement in spin wavefunction

Excitation spectrum in the paramagnetic phase

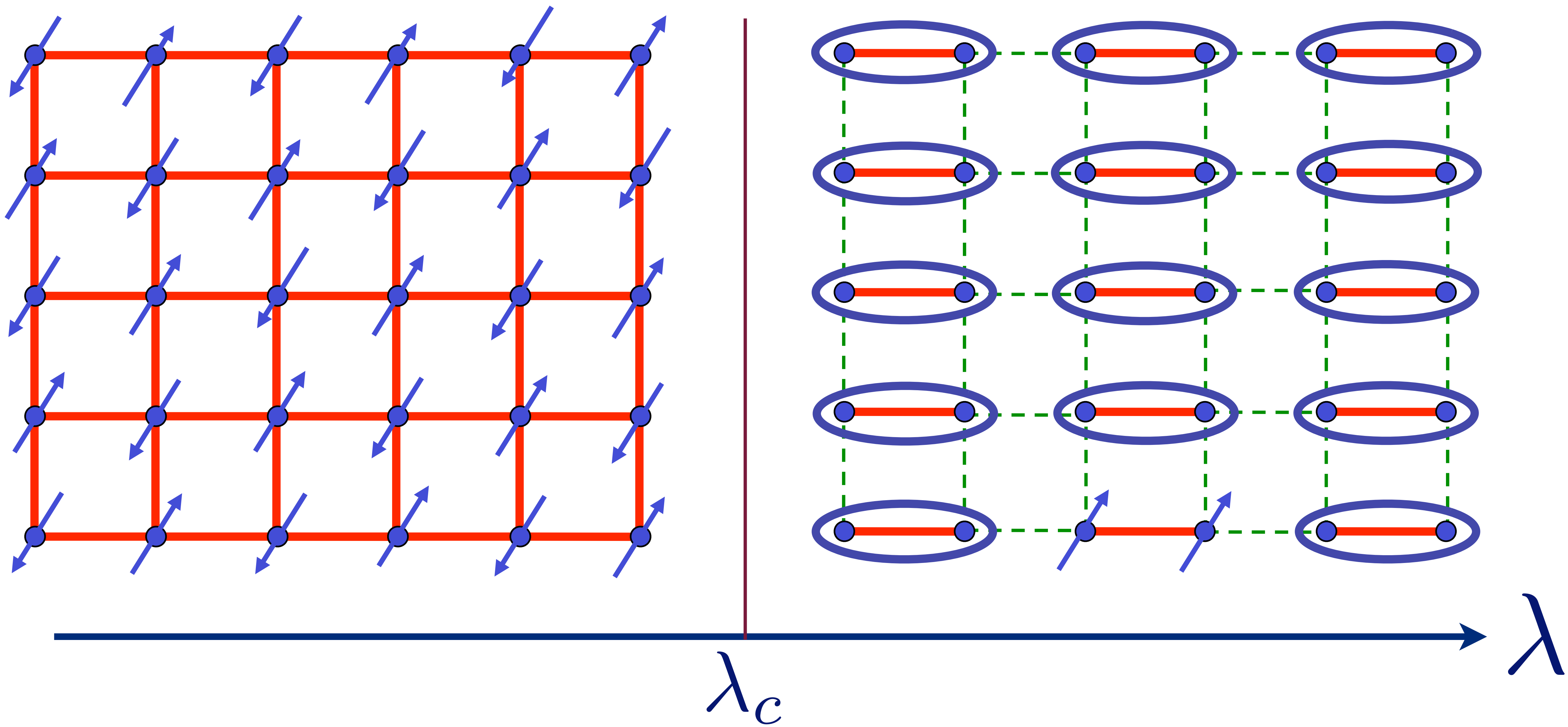

Excitation spectrum in the paramagnetic phase

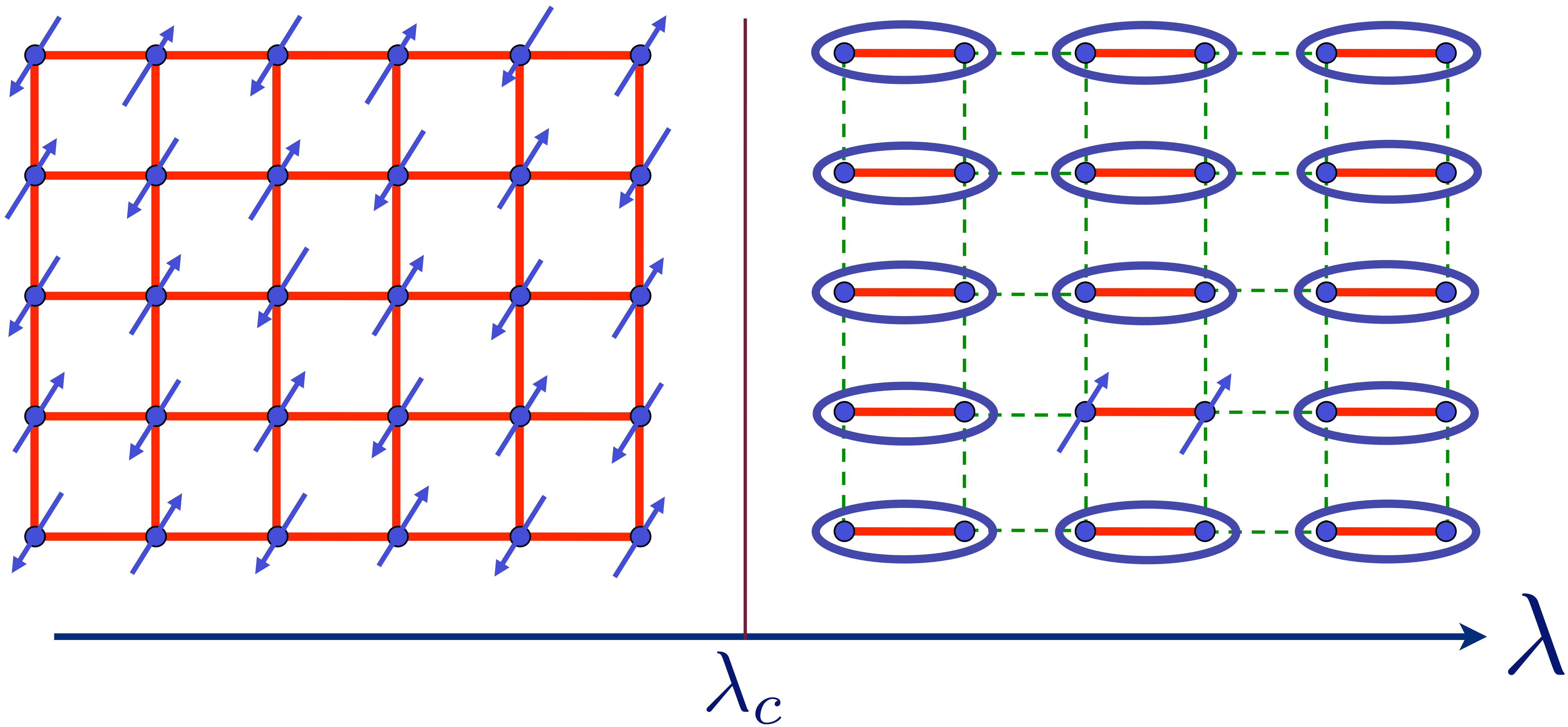

Excitation spectrum in the paramagnetic phase

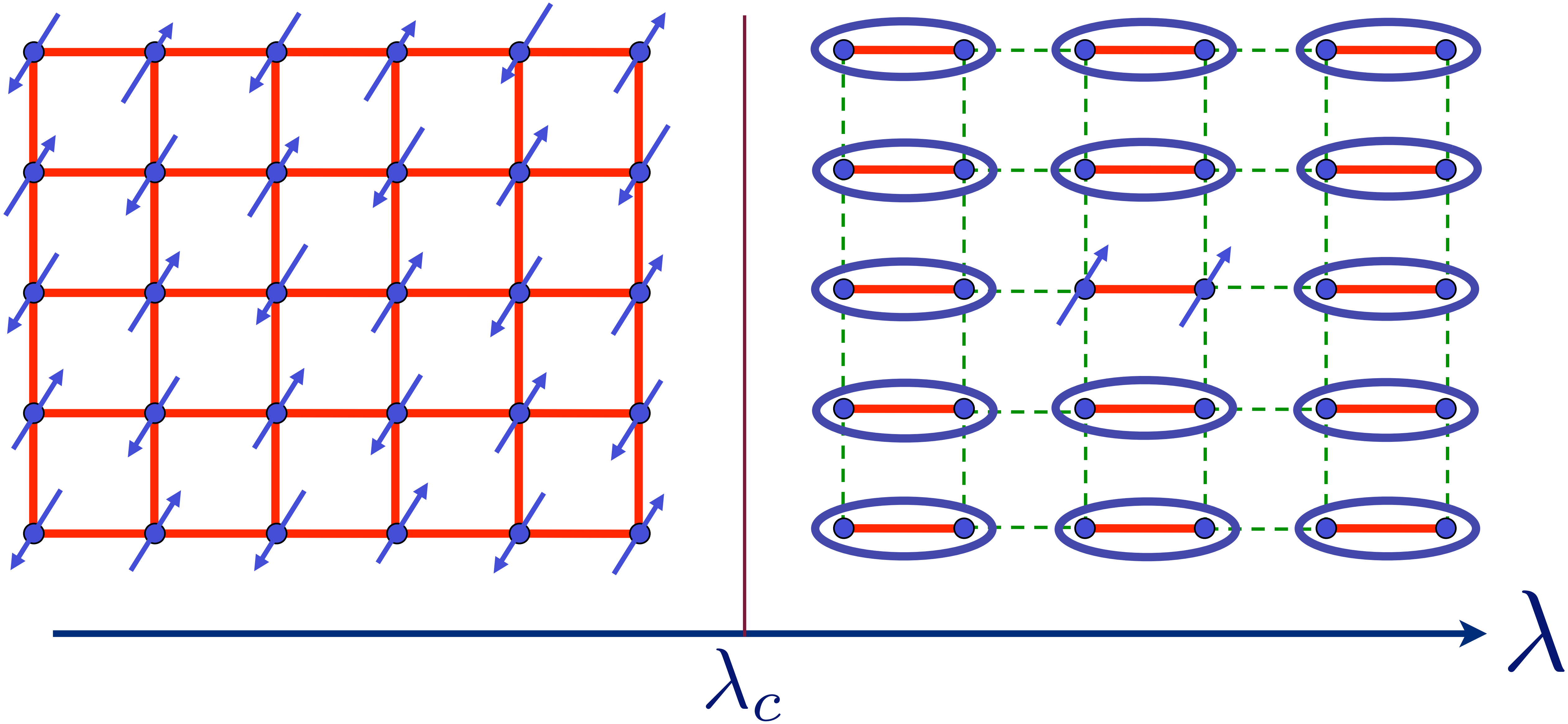

Excitation spectrum in the paramagnetic phase

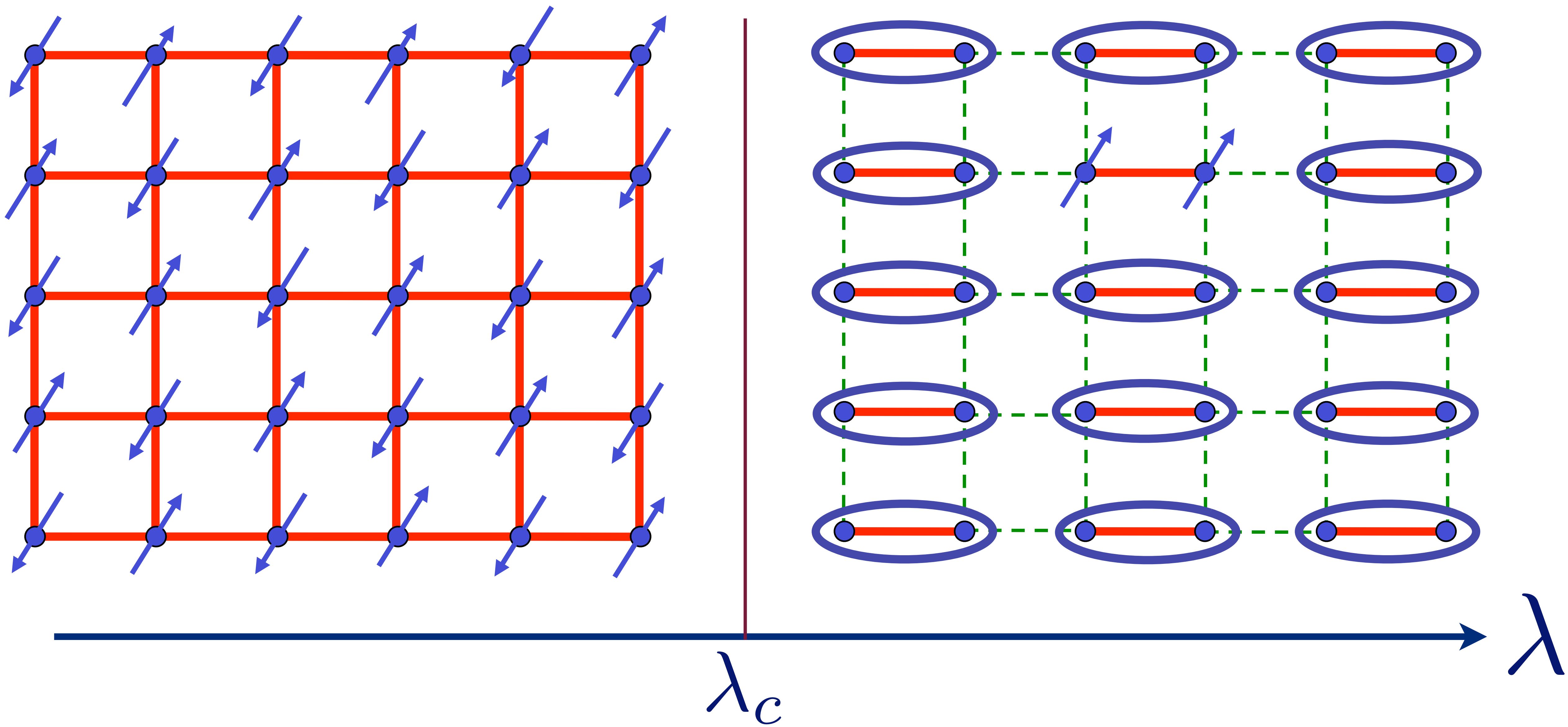

Excitation spectrum in the paramagnetic phase

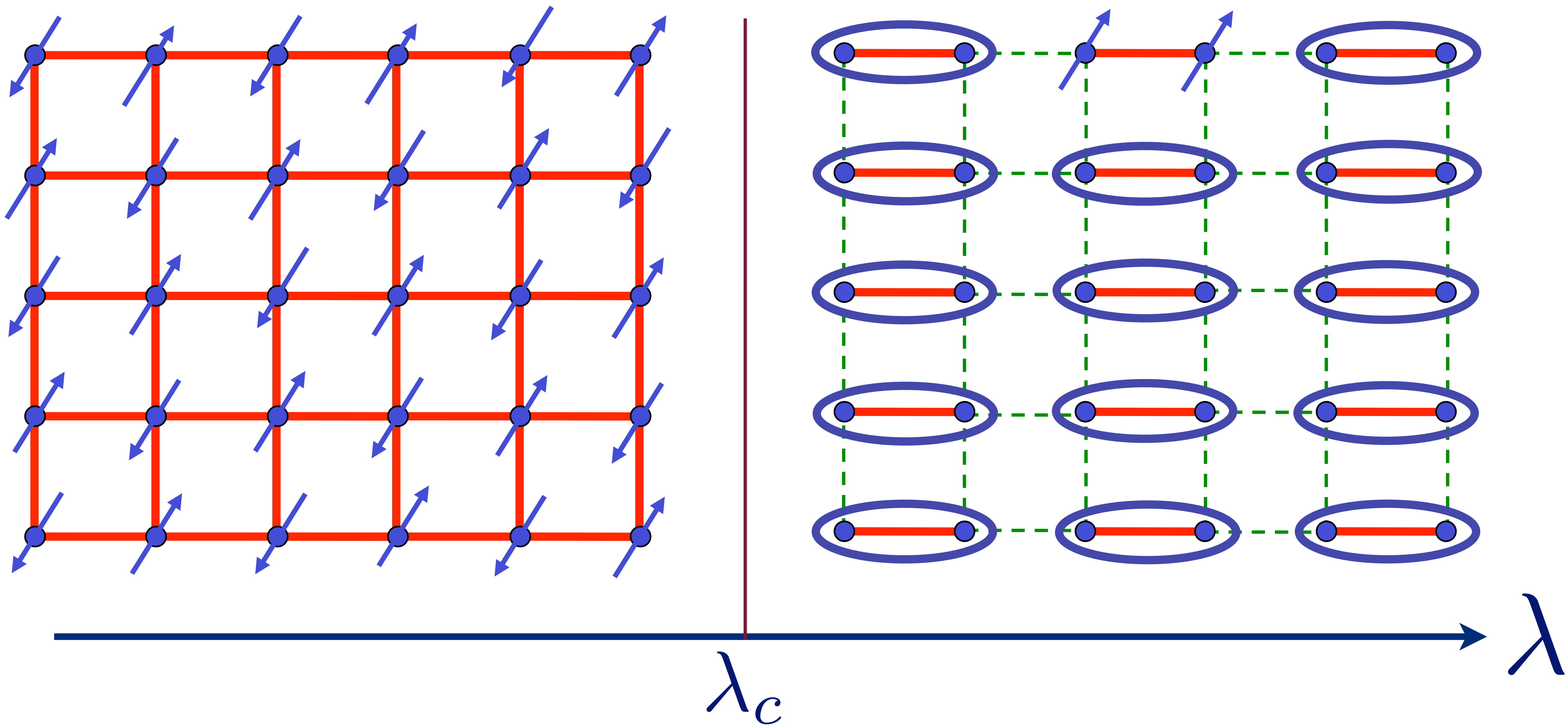

$TlCuCl_3$ at ambient pressure

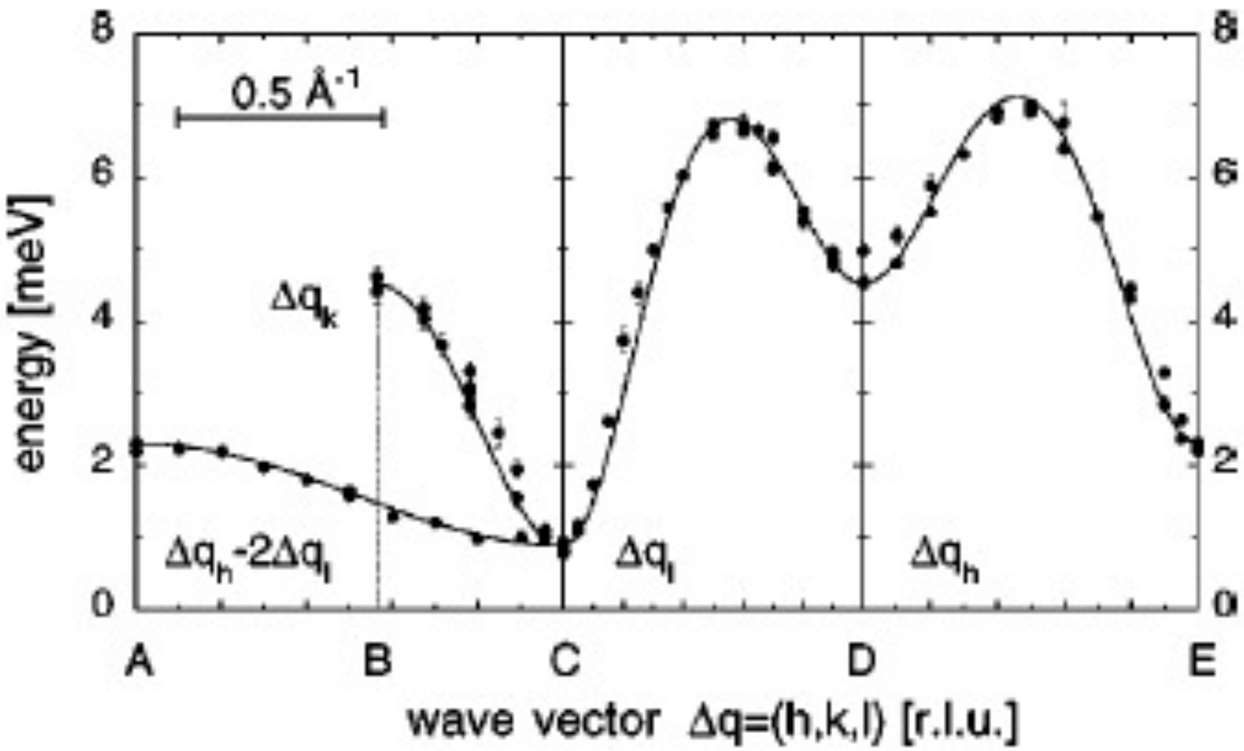

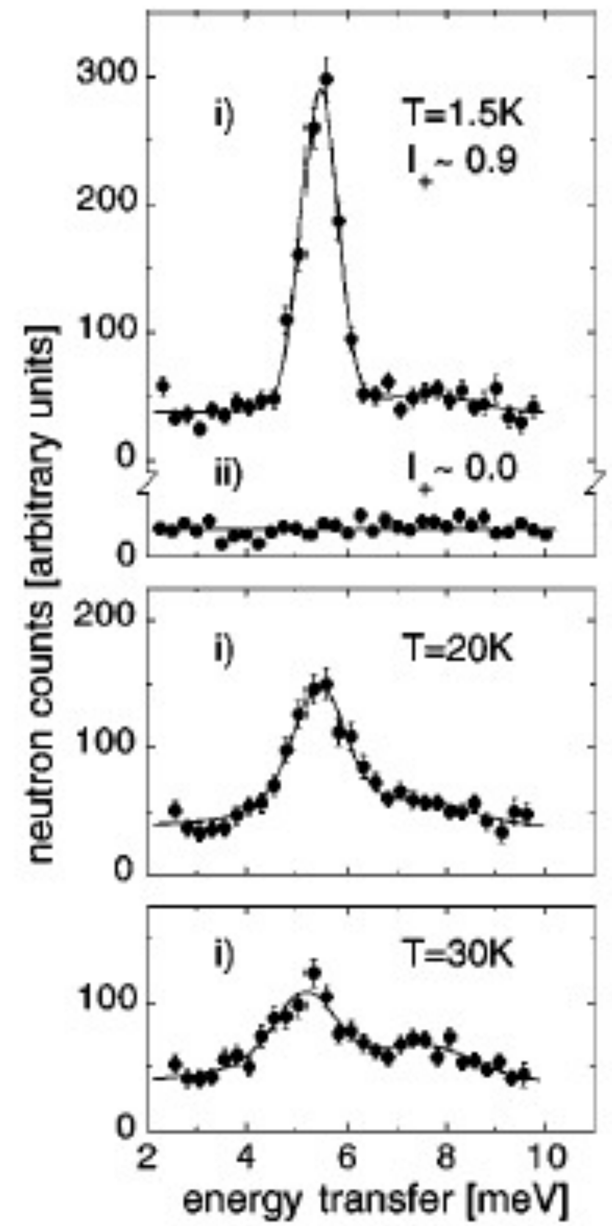

FIG. 1. Measured neutron profiles in the a^*c^* plane of $TlCuCl_3$ for $i=(1.35,0,0)$, $ii=(0,0,3.15)$ [r.l.u]. The spectrum at $T=1.5$ K

N. Cavadini, G. Heigold, W. Henggeler, A. Furrer, H.-U. Güdel, K. Krämer and H. Mutka, *Phys. Rev.* B 63 172414 (2001).

$TlCuCl_3$ at ambient pressure

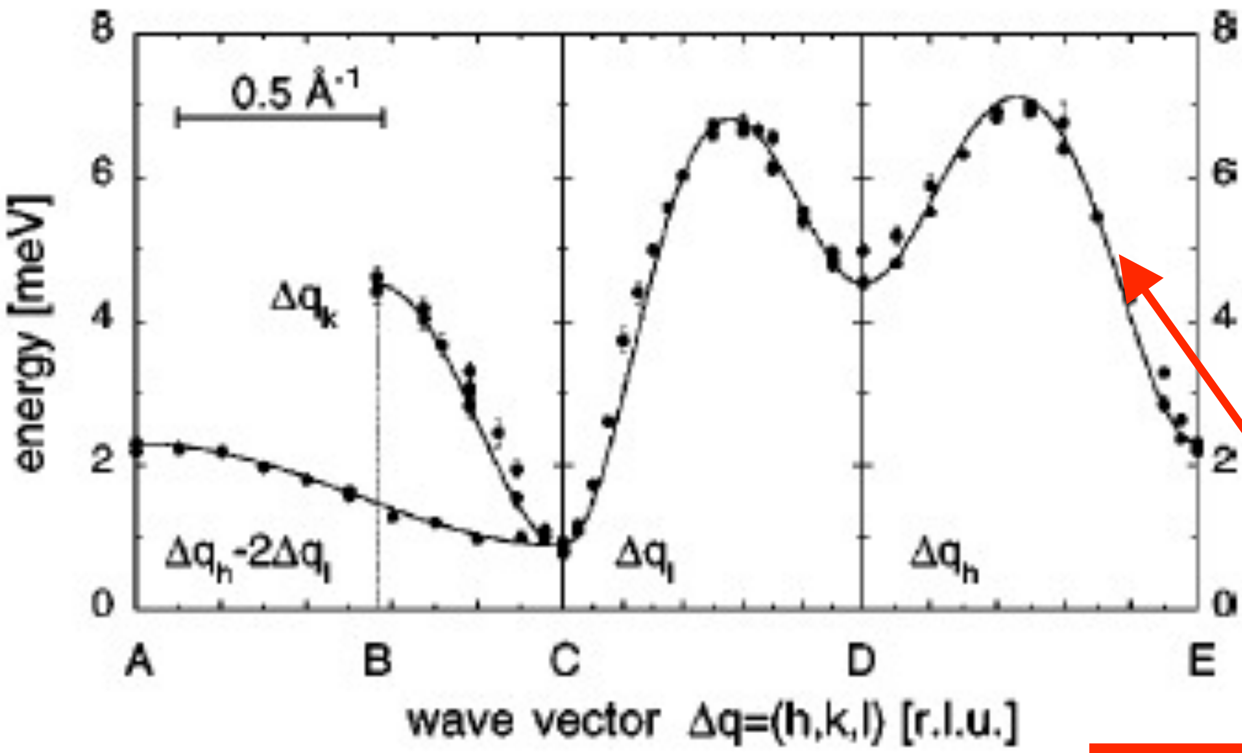

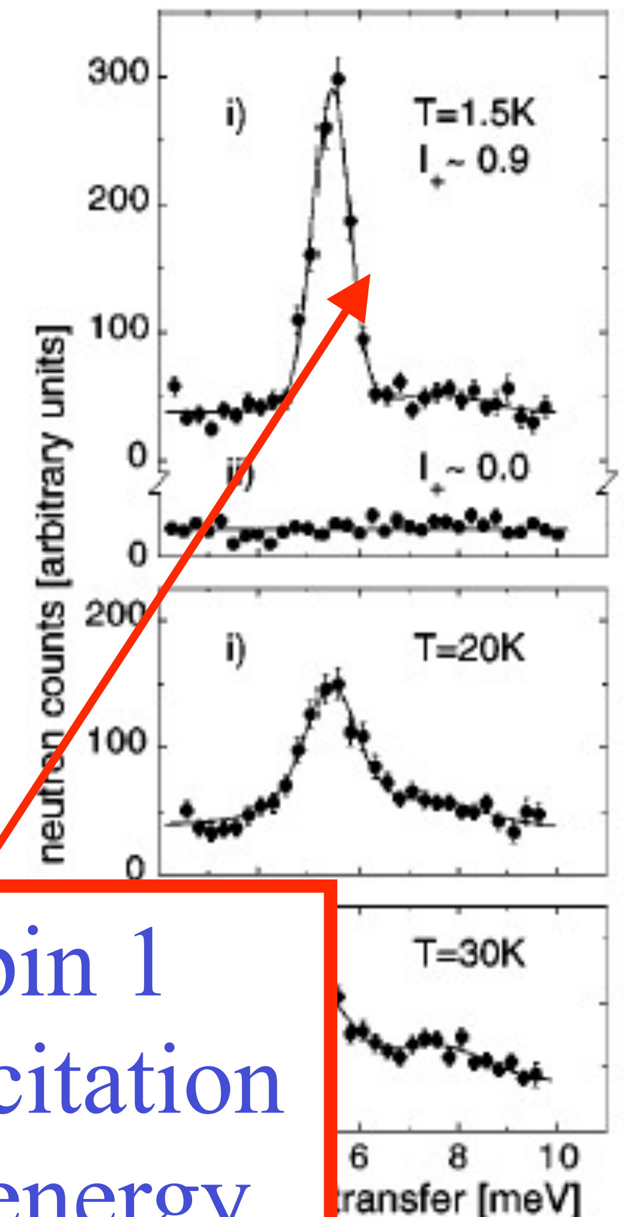

Sharp spin 1 particle excitation above an energy gap (spin gap)

...iles in the a^*c^* plane of $TlCuCl_3$ ...r.l.u]. The spectrum at $T = 1.5$ K

N. Cavadini, G. Heigold, W. Henggeler, A. Furrer, H.-U. Güdel, K. Krämer and H. Mutka, *Phys. Rev.* B 63 172414 (2001).

Excitation spectrum in the Néel phase

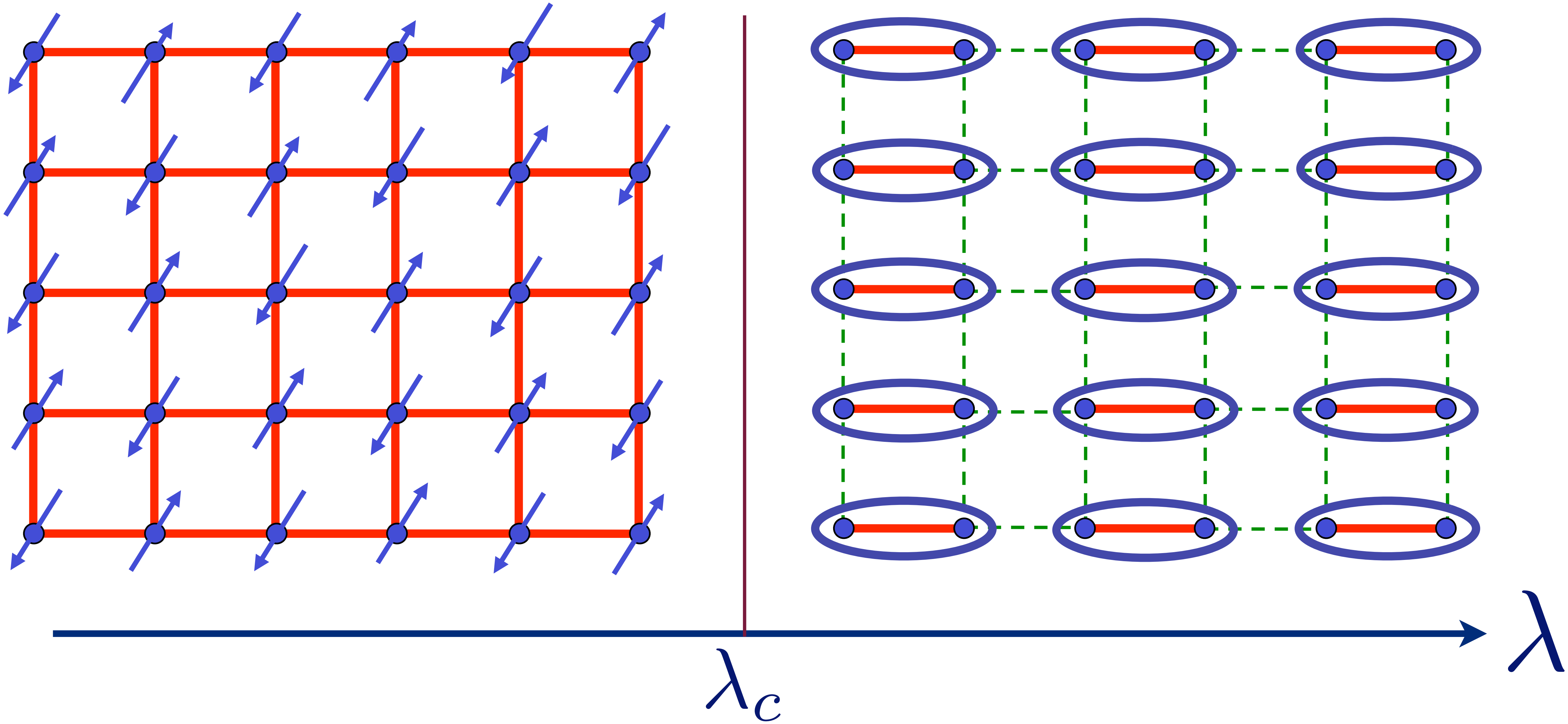

Excitation spectrum in the Néel phase

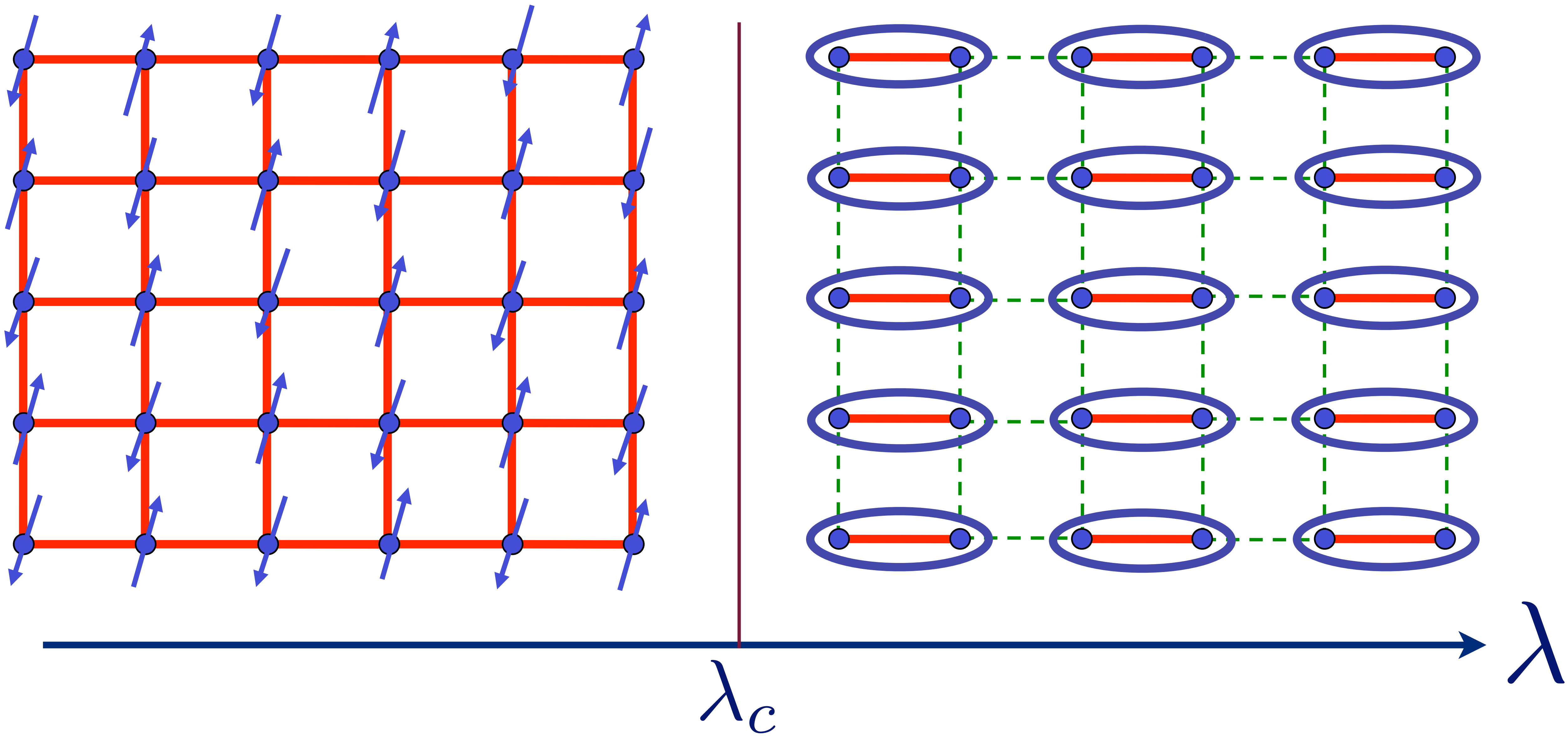

Spin waves

Excitation spectrum in the Néel phase

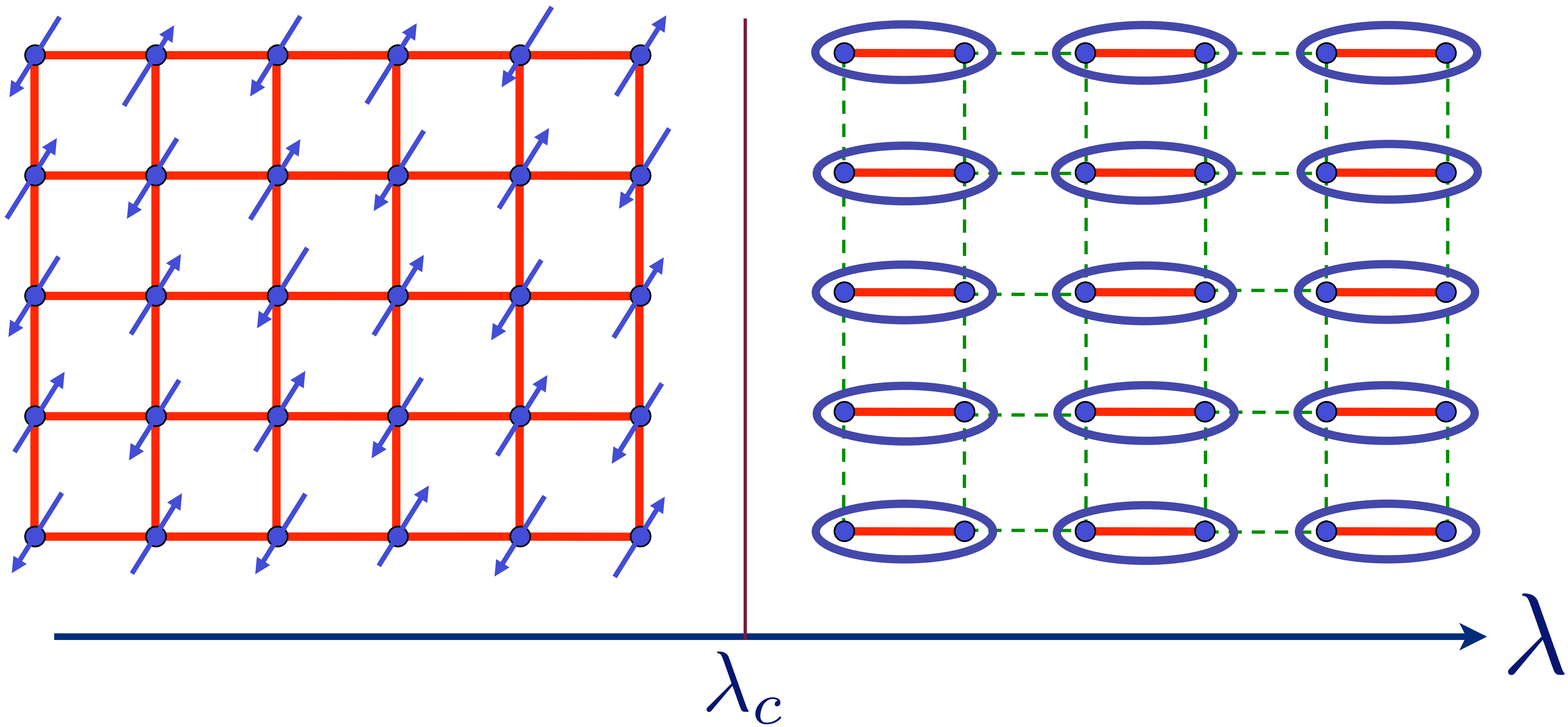

Spin waves

Description using Landau-Ginzburg field theory

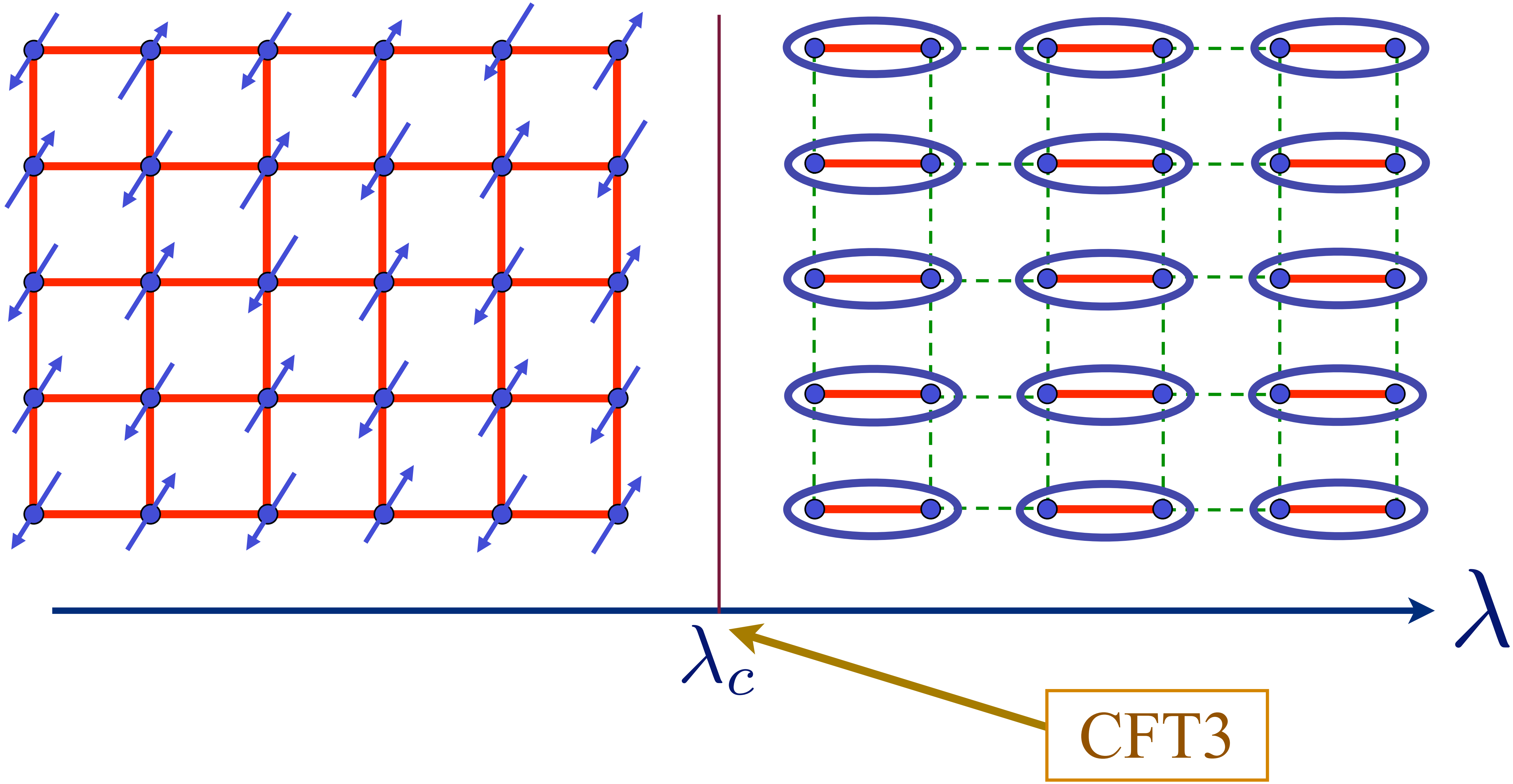

O(3) order parameter $\vec{\varphi}$

$$\mathcal{S} = \int d^2r d\tau \left[(\partial_\tau \varphi)^2 + c^2 (\nabla_r \vec{\varphi})^2 + (\lambda - \lambda_c) \vec{\varphi}^2 + u \left(\vec{\varphi}^2 \right)^2 \right]$$

Excitation spectrum in the paramagnetic phase

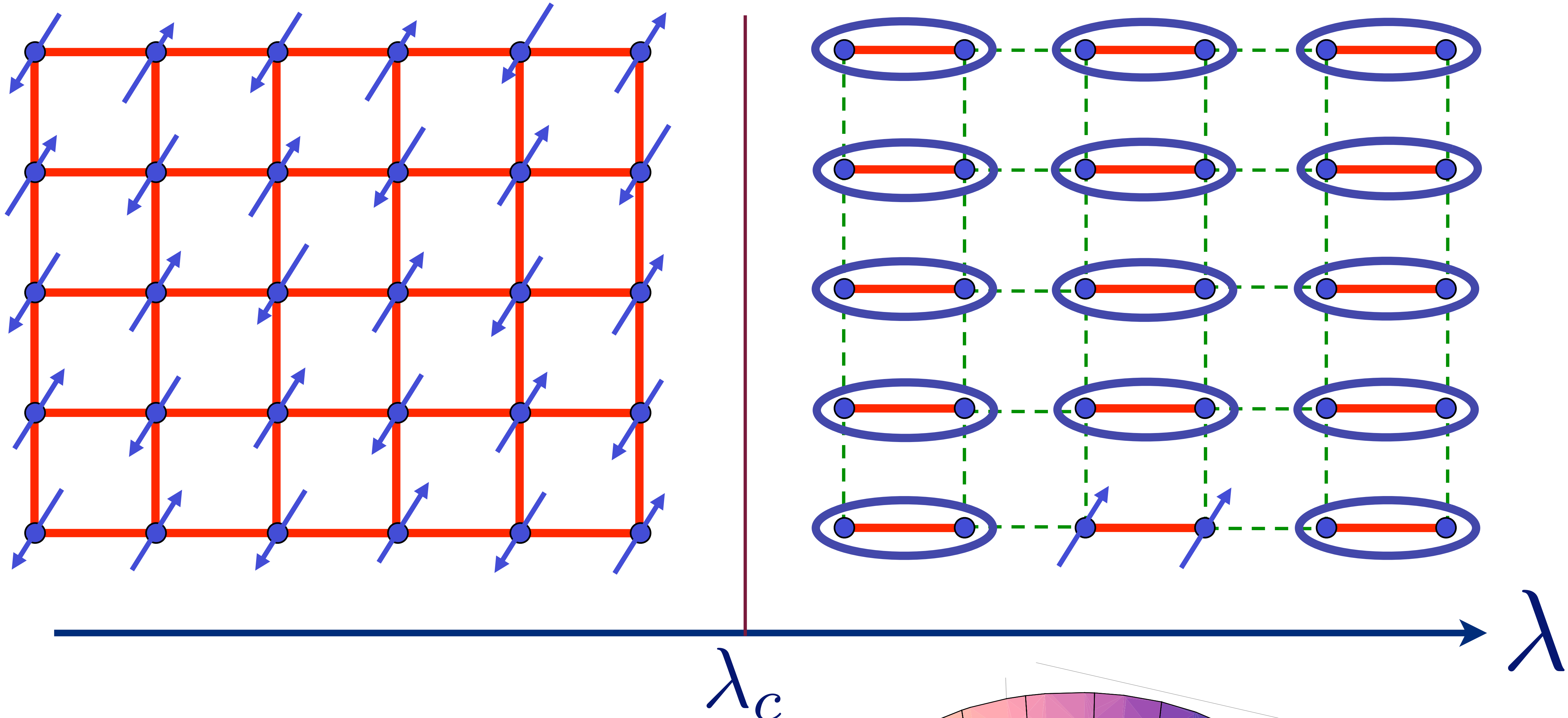

$$V(\vec{\varphi}) = (\lambda - \lambda_c)\vec{\varphi}^2 + u\left(\vec{\varphi}^2\right)^2$$

$$\lambda > \lambda_c$$

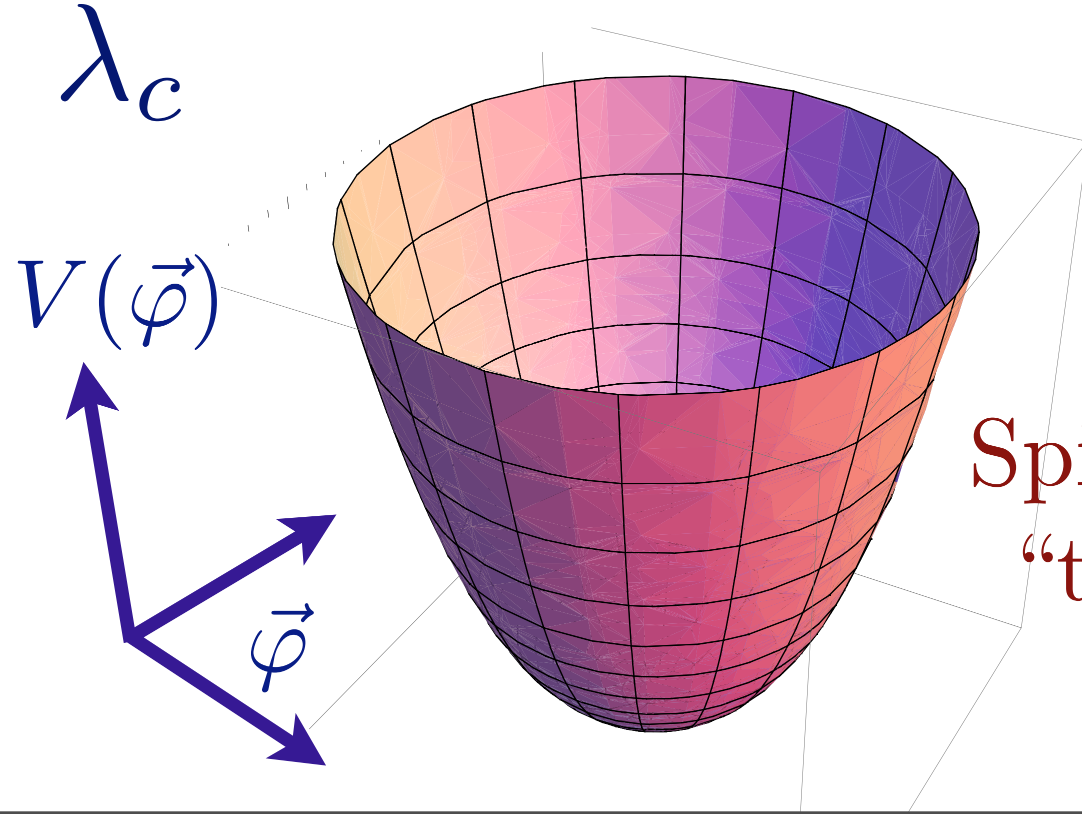

Spin $S = 1$
"triplon"

Excitation spectrum in the paramagnetic phase

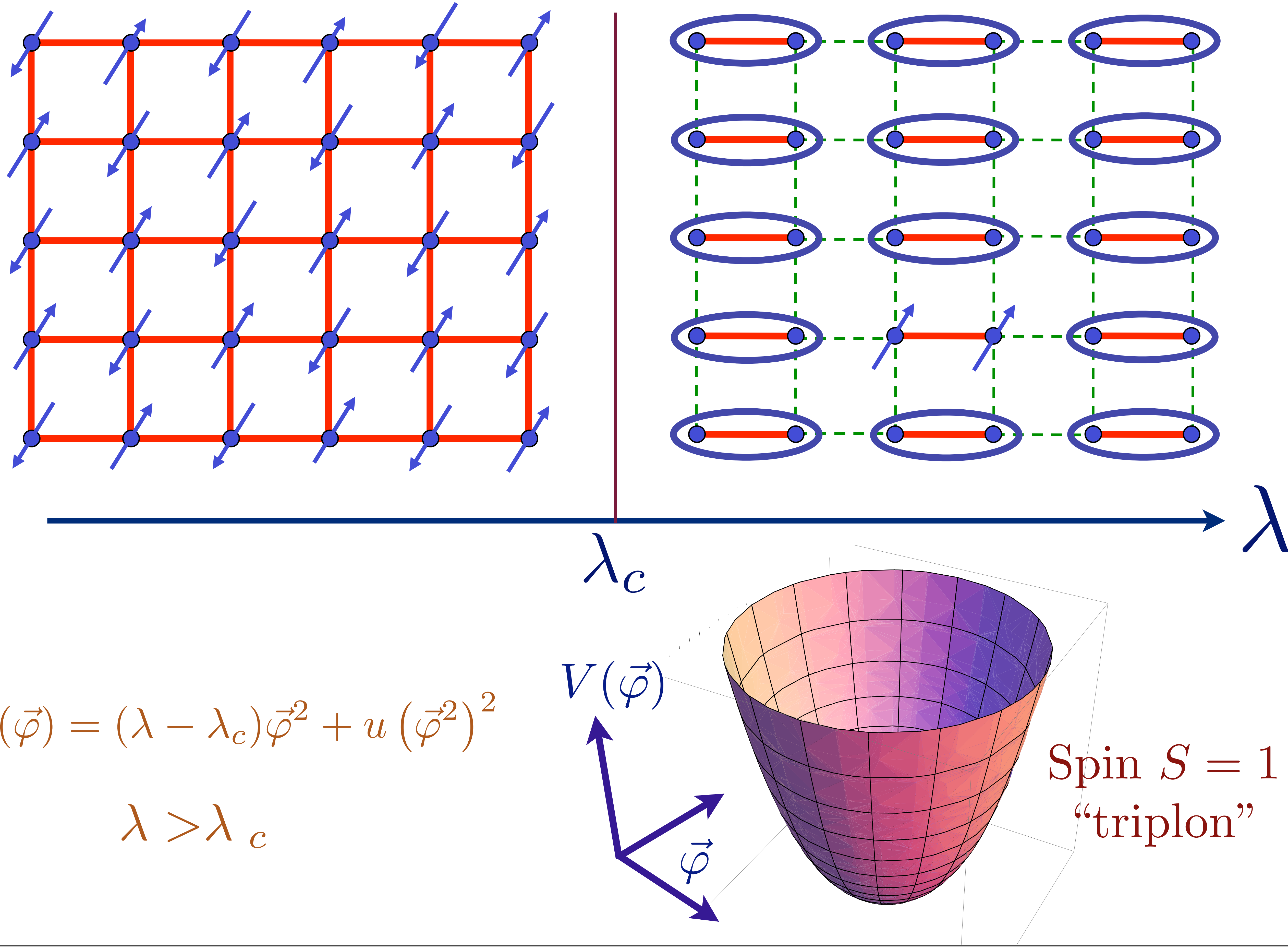

$$V(\vec{\varphi}) = (\lambda - \lambda_c)\vec{\varphi}^2 + u\left(\vec{\varphi}^2\right)^2$$

$$\lambda > \lambda_c$$

Excitation spectrum in the paramagnetic phase

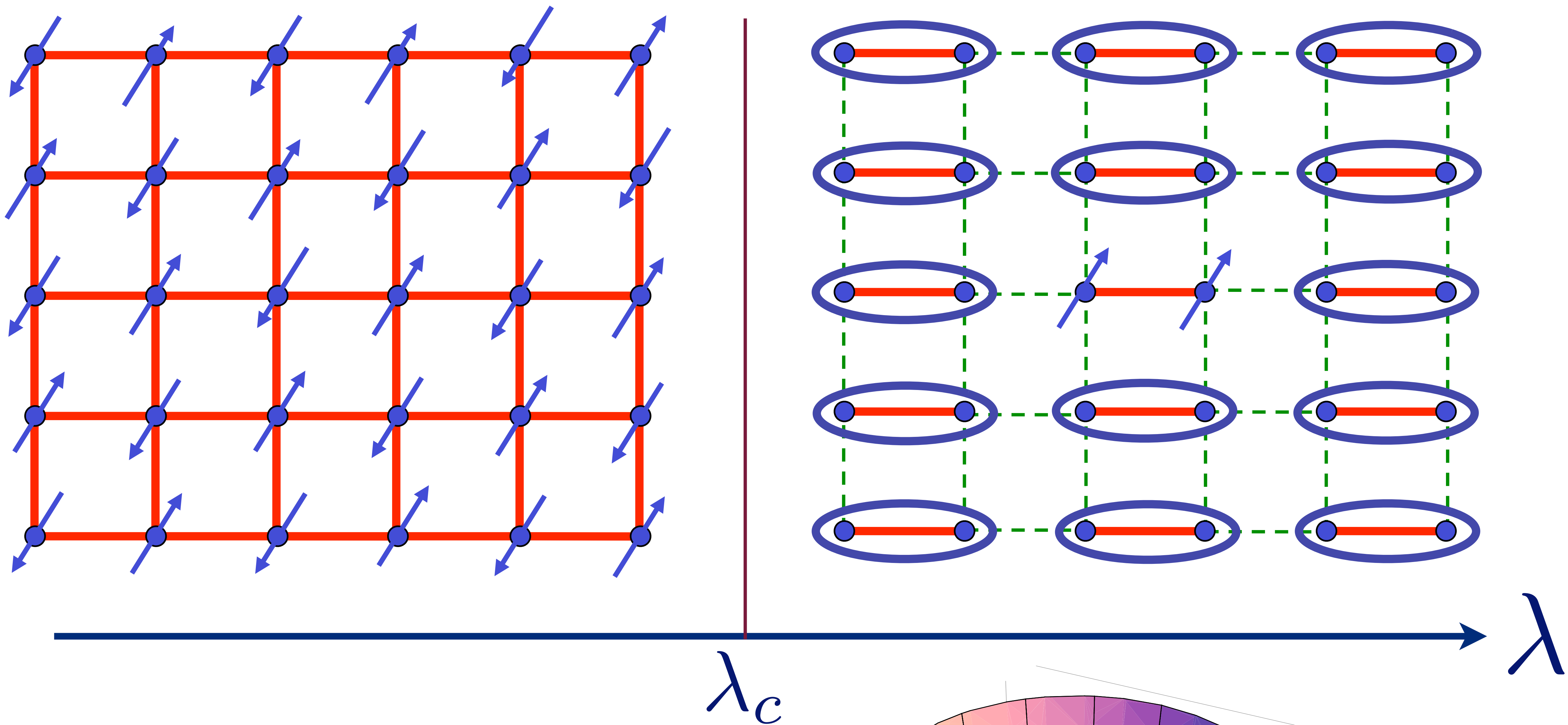

$$V(\vec{\varphi}) = (\lambda - \lambda_c)\vec{\varphi}^2 + u\left(\vec{\varphi}^2\right)^2$$

$$\lambda > \lambda_c$$

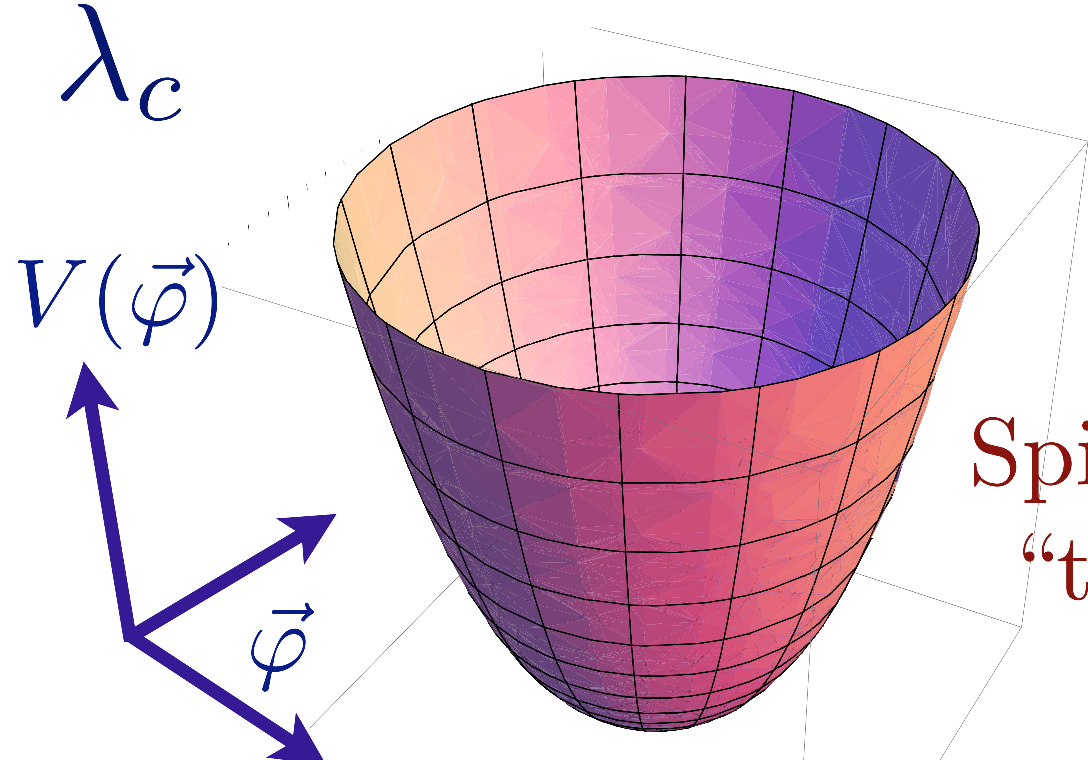

Spin $S = 1$
"triplon"

Excitation spectrum in the paramagnetic phase

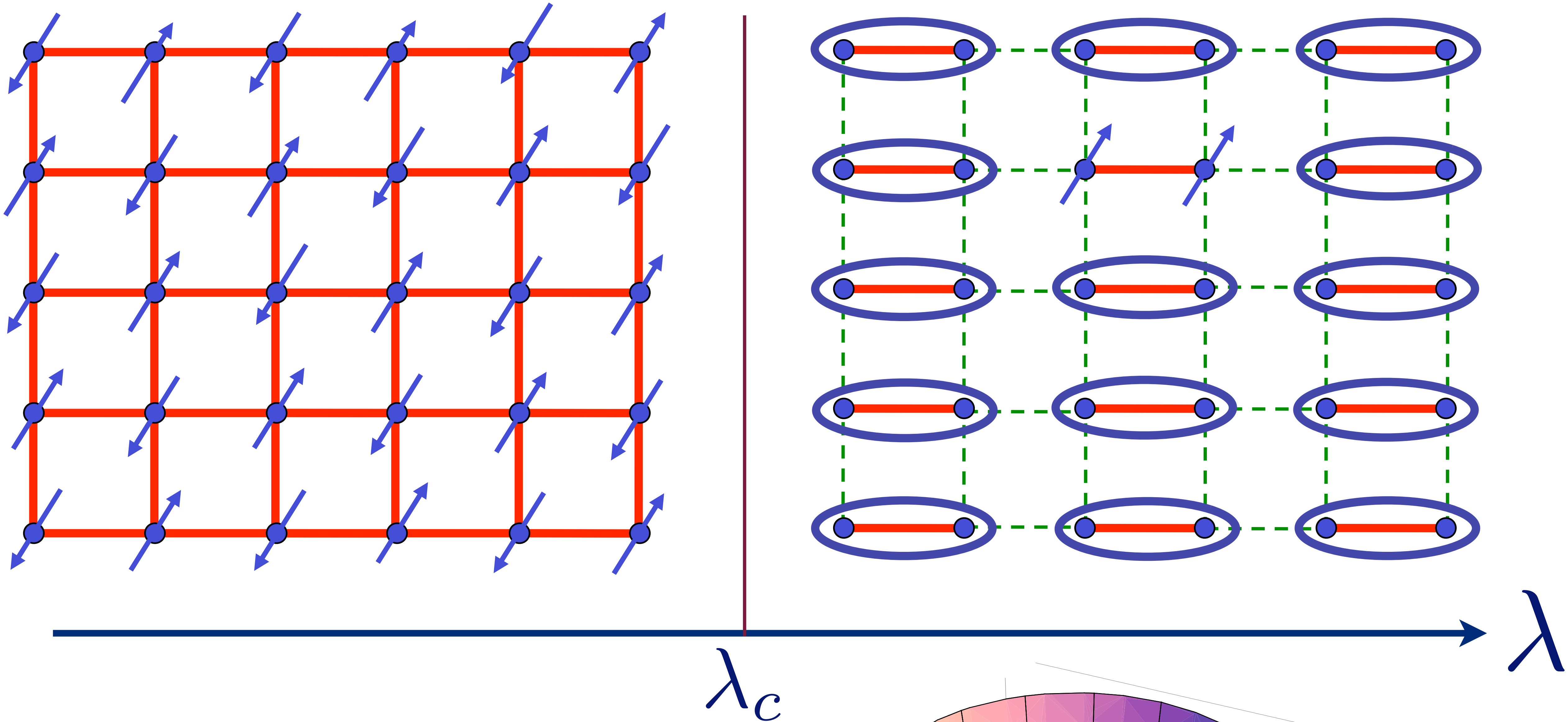

$$V(\vec{\varphi}) = (\lambda - \lambda_c)\vec{\varphi}^2 + u\left(\vec{\varphi}^2\right)^2$$

$$\lambda > \lambda_c$$

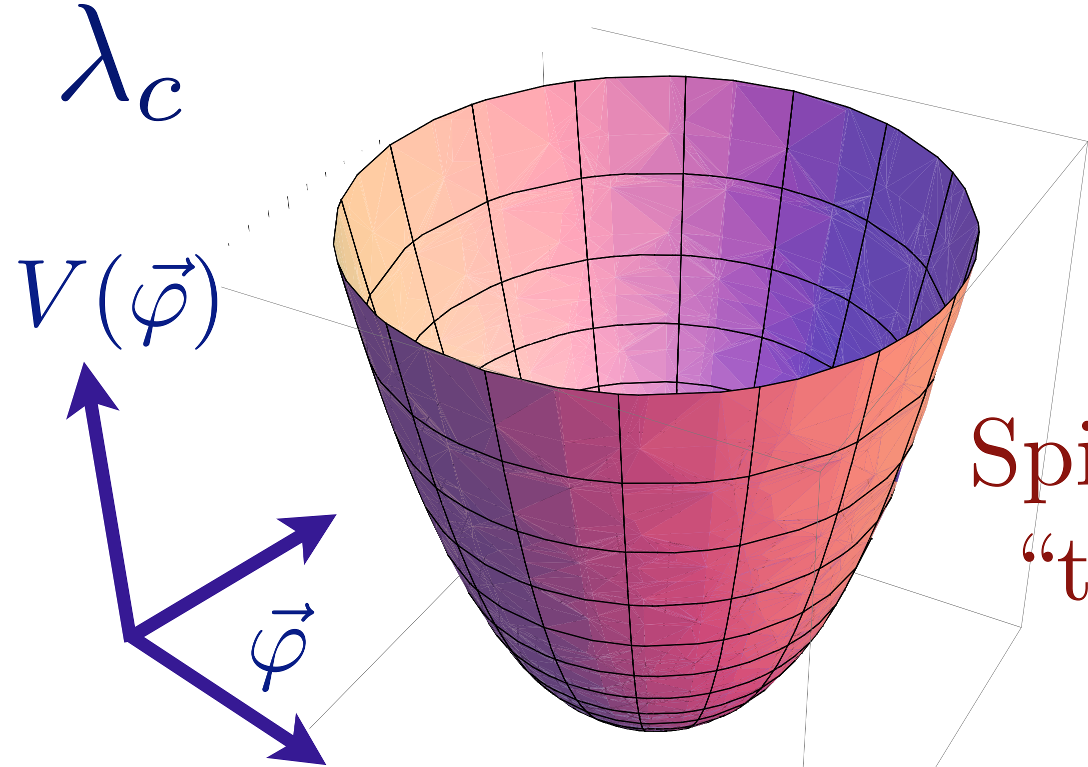

Spin $S = 1$
"triplon"

Excitation spectrum in the paramagnetic phase

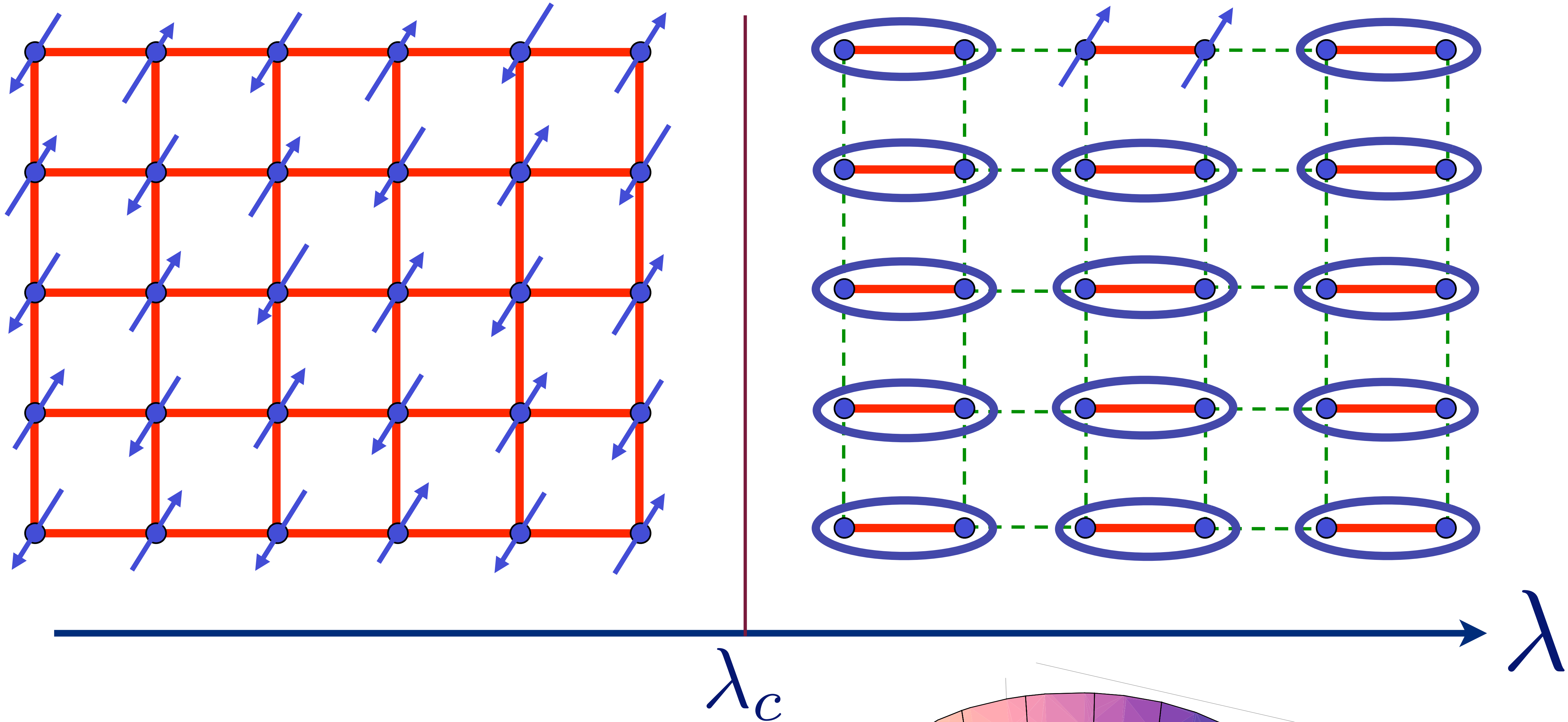

$$V(\vec{\varphi}) = (\lambda - \lambda_c)\vec{\varphi}^2 + u\left(\vec{\varphi}^2\right)^2$$

$$\lambda > \lambda_c$$

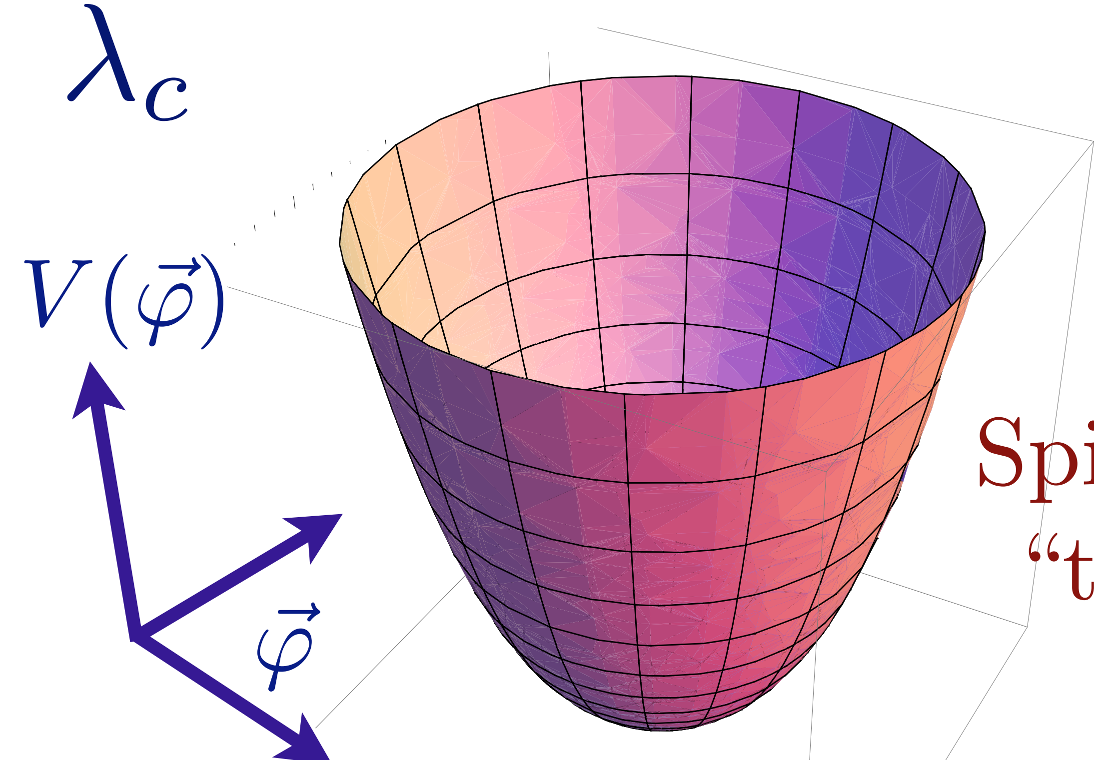

Spin $S = 1$
"triplon"

Excitation spectrum in the Néel phase

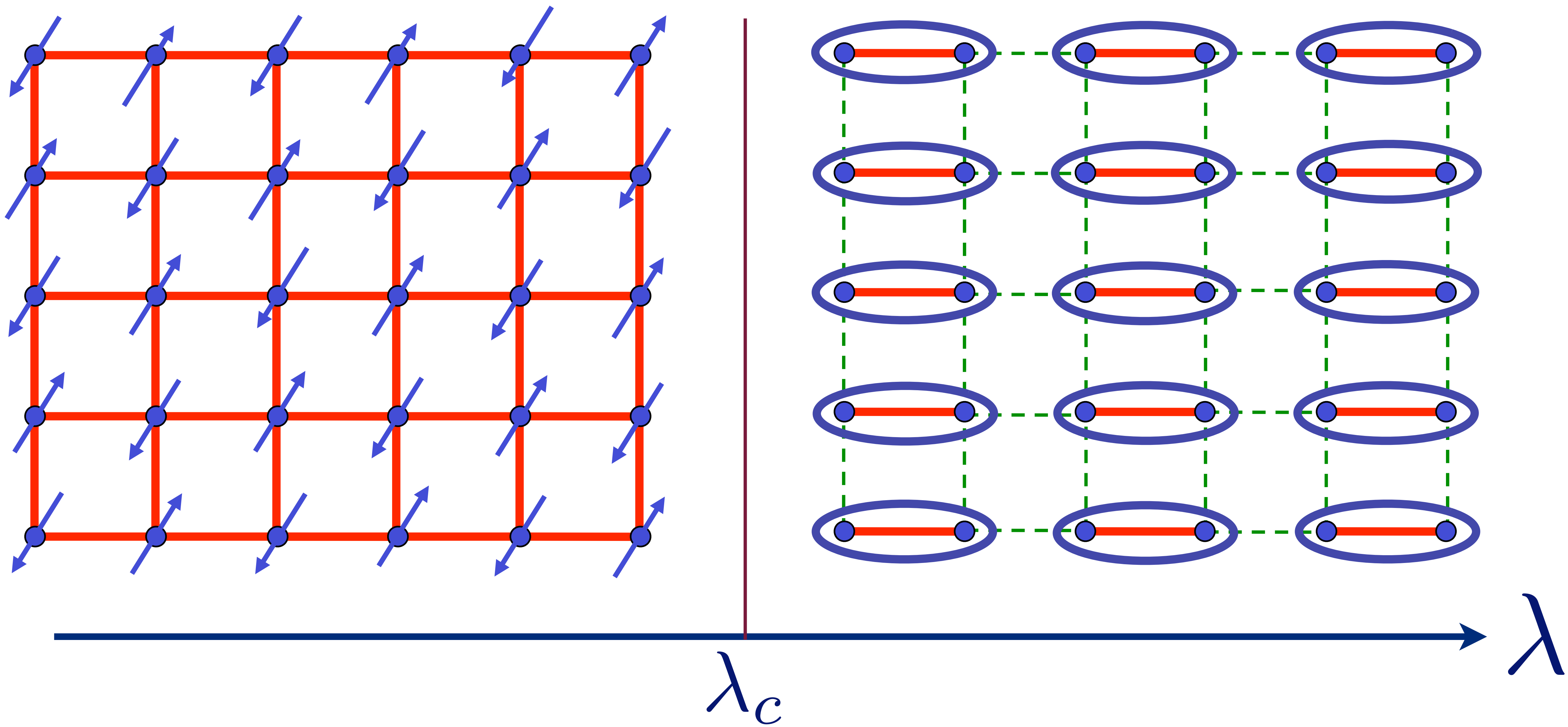

Excitation spectrum in the Néel phase

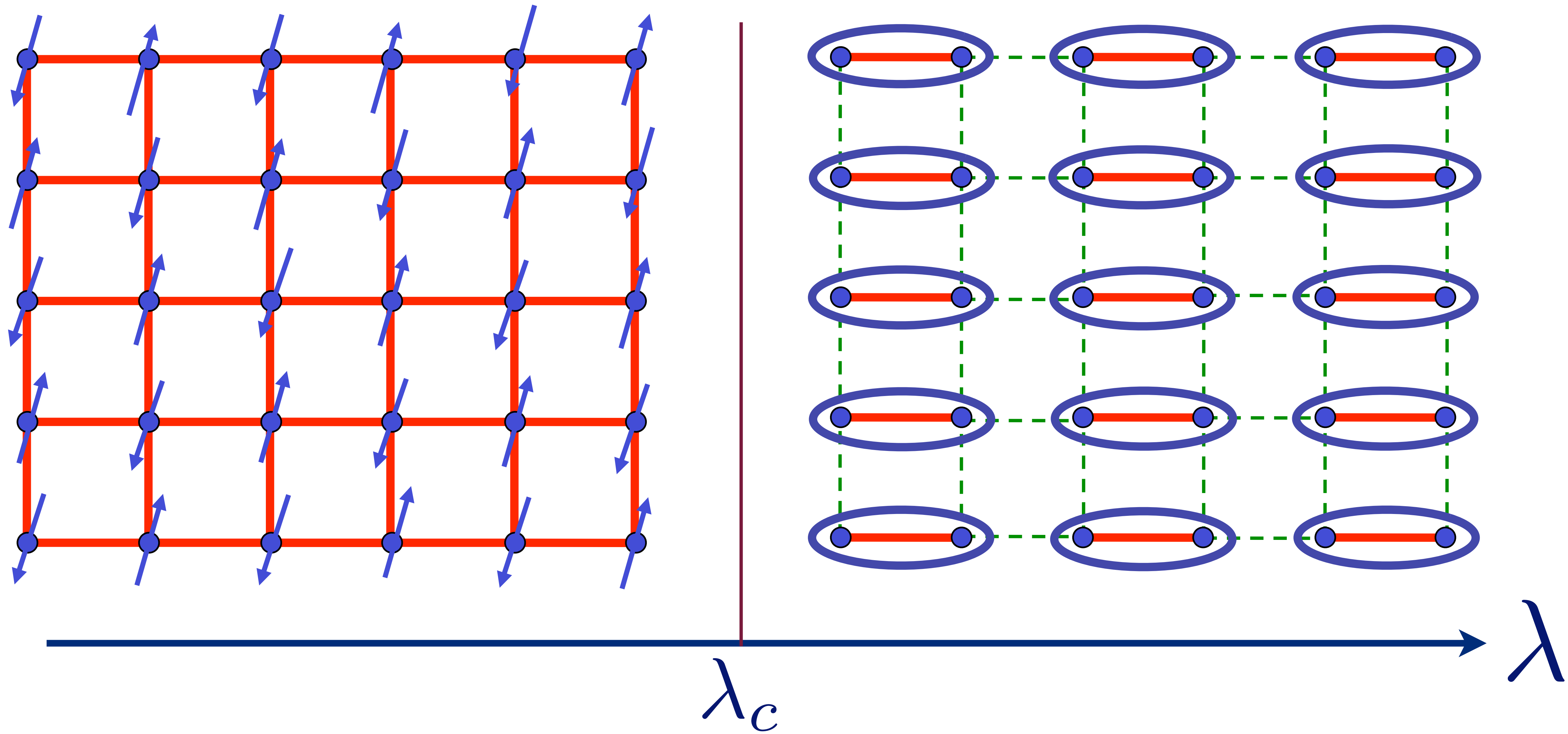

Spin waves

Excitation spectrum in the Néel phase

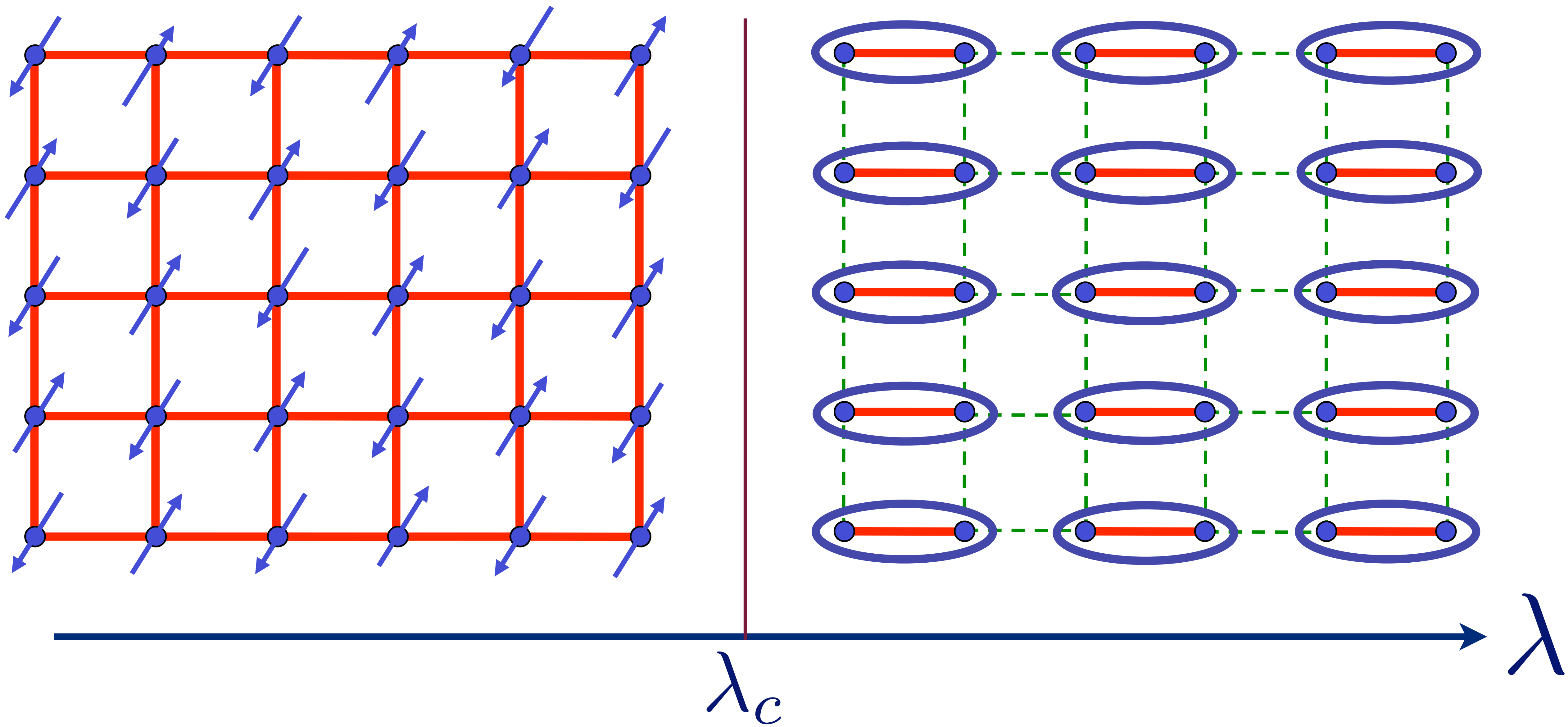

Spin waves

Excitation spectrum in the Néel phase

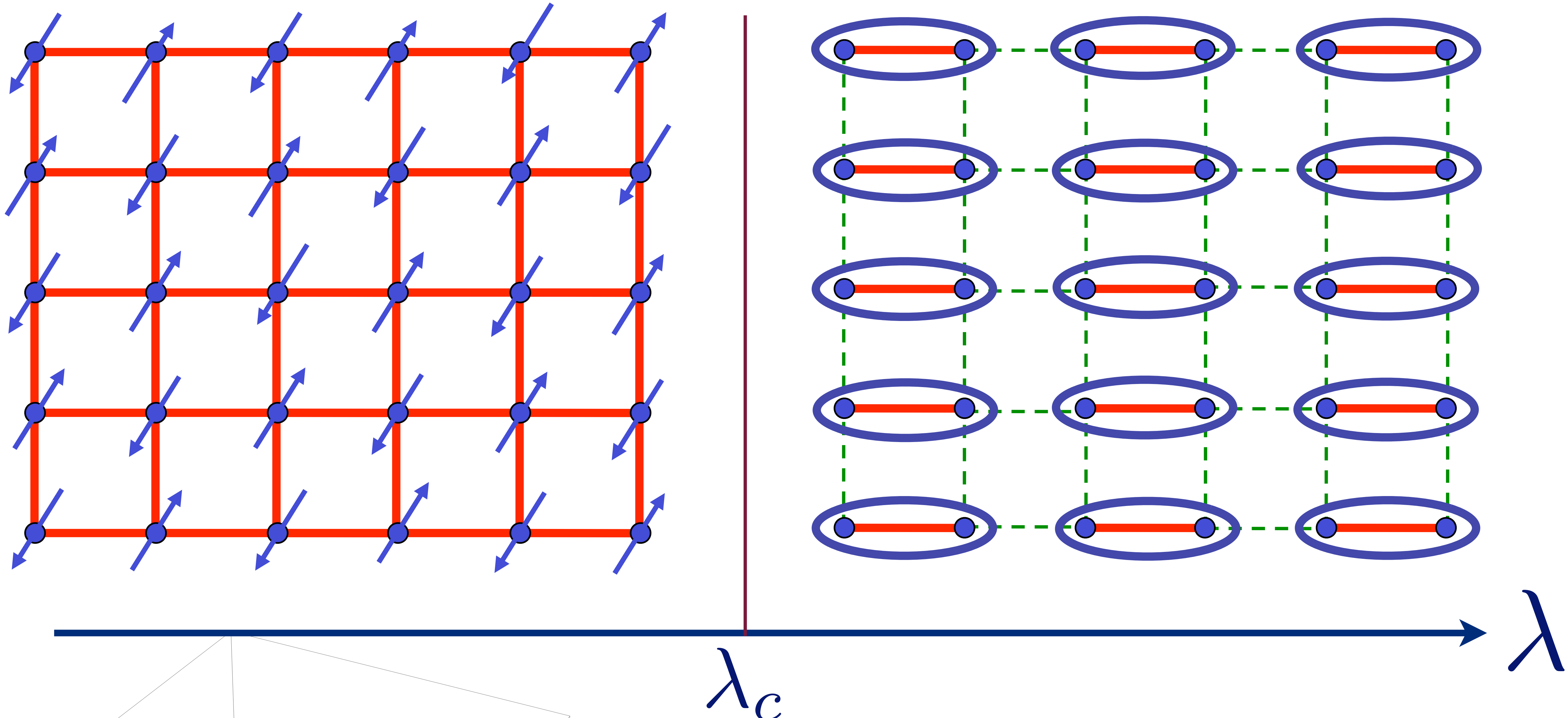

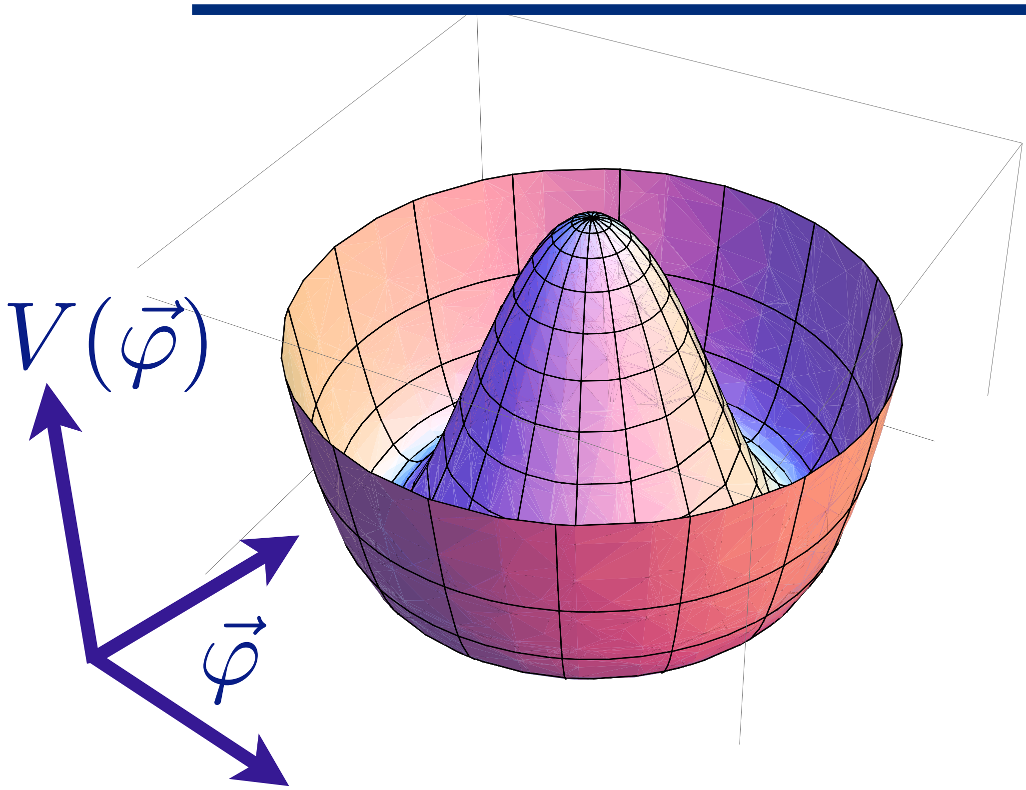

$$V(\vec{\varphi}) = (\lambda - \lambda_c)\vec{\varphi}^2 + u\left(\vec{\varphi}^2\right)^2$$

$$\lambda < \lambda_c$$

Excitation spectrum in the Néel phase

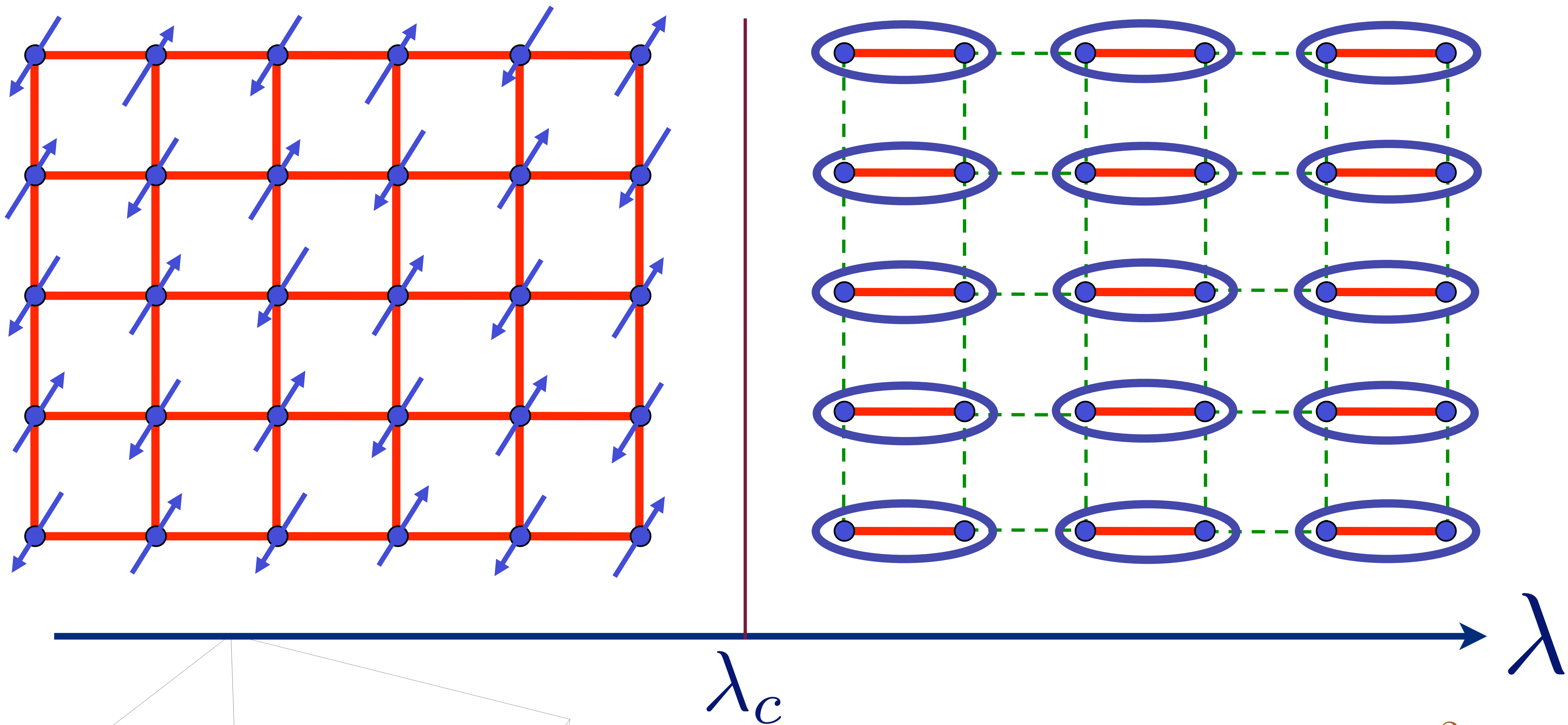

$$V(\vec{\varphi}) = (\lambda - \lambda_c)\vec{\varphi}^2 + u\left(\vec{\varphi}^2\right)^2$$

$$\lambda < \lambda_c$$

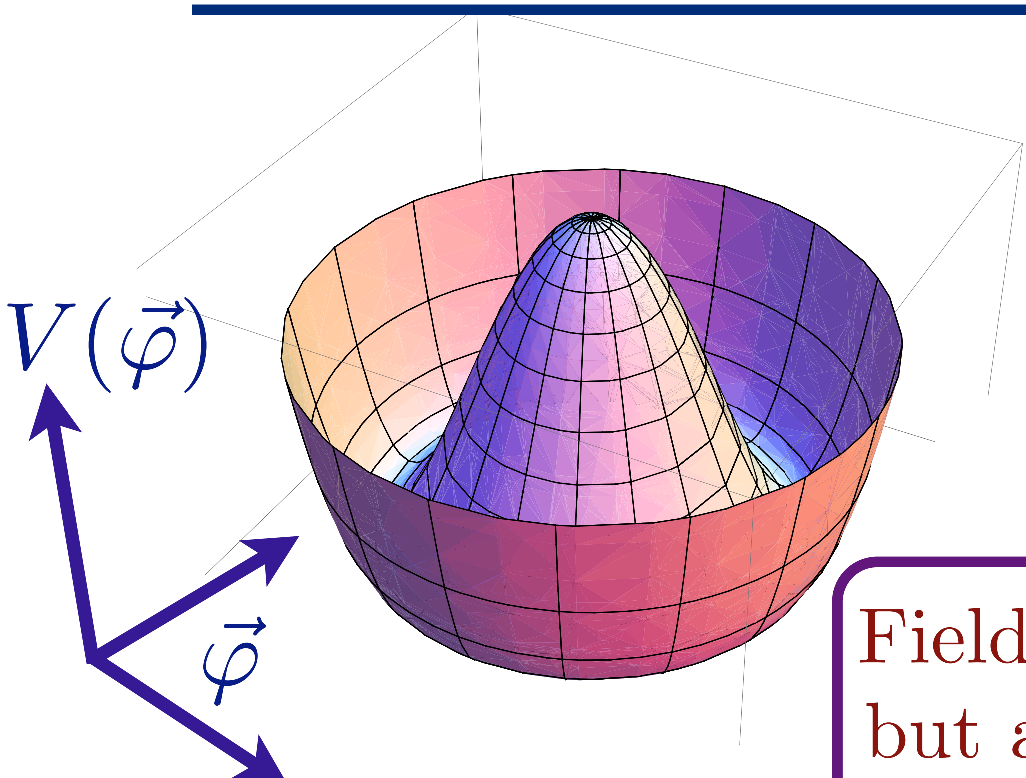

Field theory yields spin waves ("Goldstone" modes) but also an additional longitudinal "Higgs" particle

Excitation spectrum in the Néel phase

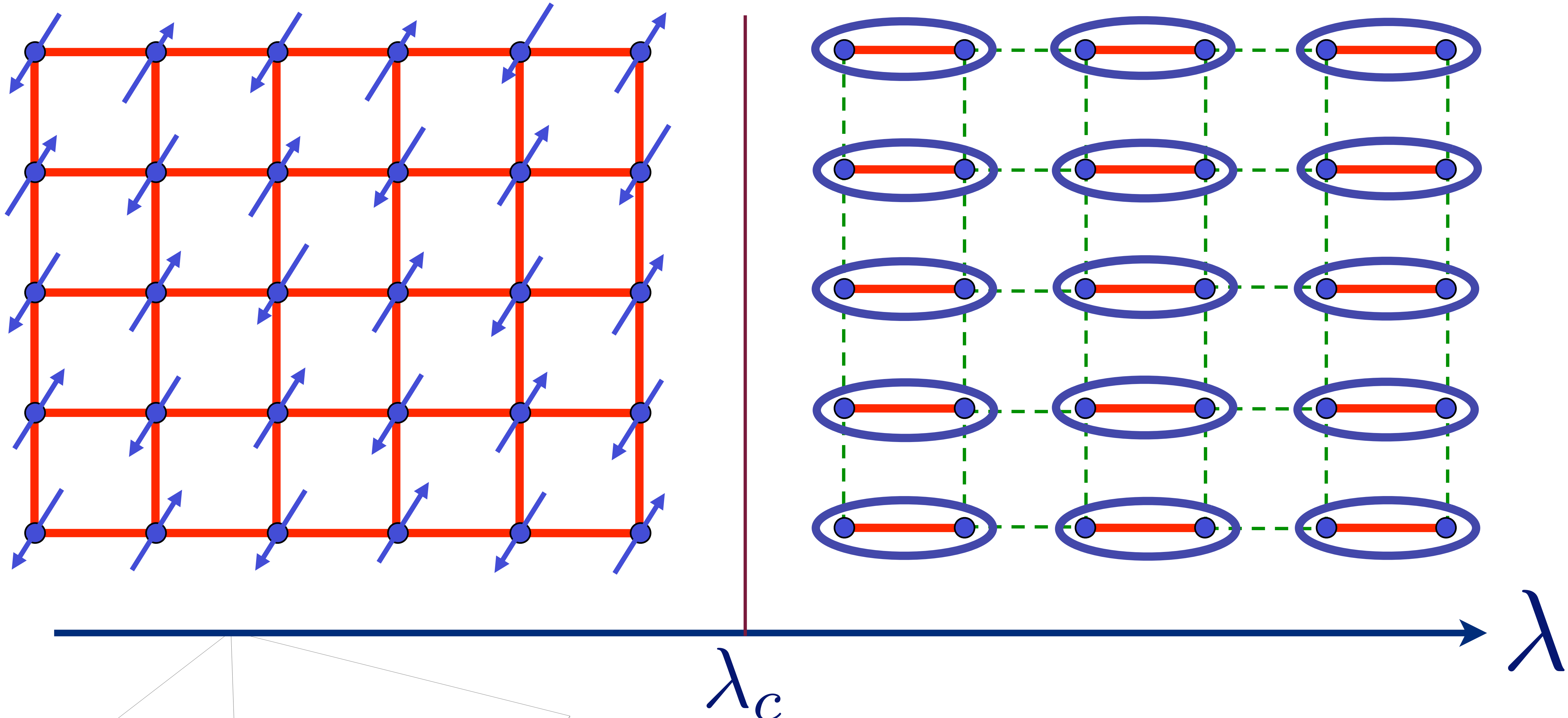

$$V(\vec{\varphi}) = (\lambda - \lambda_c)\vec{\varphi}^2 + u\left(\vec{\varphi}^2\right)^2$$

$$\lambda < \lambda_c$$

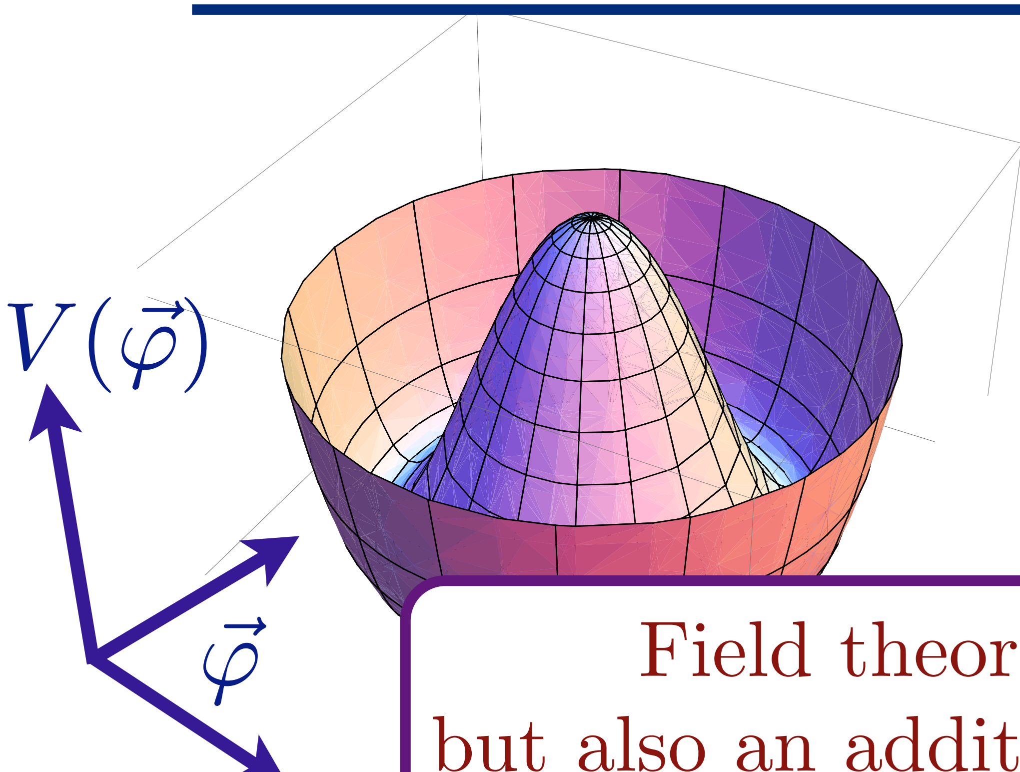

Field theory yields spin waves ("Goldstone" modes)
but also an additional longitudinal Higgs-Englert-Brout particle

$TlCuCl_3$ with varying pressure

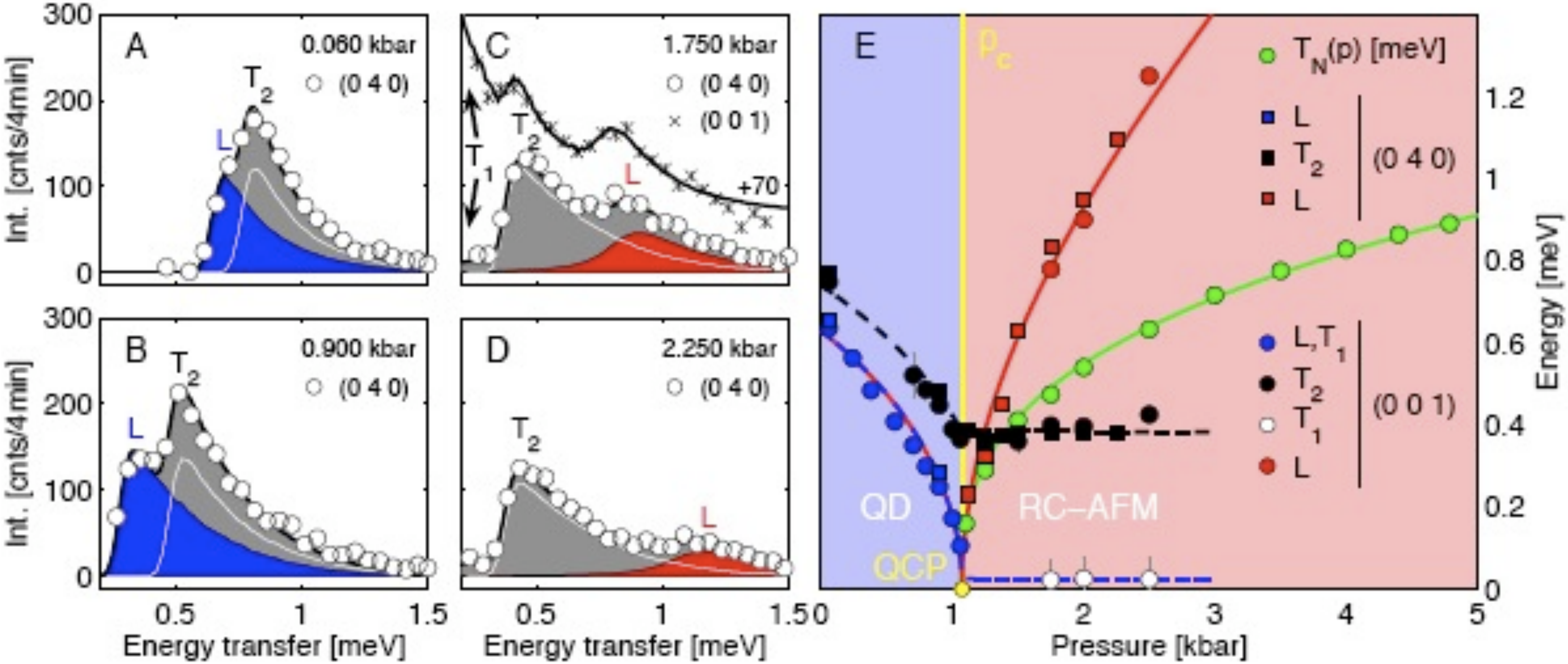

Observation of 3 → 2 low energy modes,
emergence of new Higgs-Englert-Brout particle in the Néel phase,
and vanishing of Néel temperature at the quantum critical point

Christian Ruegg, Bruce Normand, Masashige Matsumoto, Albert Furrer, Desmond McMorrow, Karl Kramer, Hans–Ulrich Gudel, Severian Gvasaliya, Hannu Mutka, and Martin Boehm, *Phys. Rev. Lett.* **100**, 205701 (2008)

Prediction of quantum field theory

Potential for $\vec{\varphi}$ fluctuations: $V(\vec{\varphi}) = (\lambda - \lambda_c)\vec{\varphi}^2 + u\left(\vec{\varphi}^2\right)^2$

Paramagnetic phase, $\lambda > \lambda_c$

Expand about $\vec{\varphi} = 0$:

$$V(\vec{\varphi}) \approx (\lambda - \lambda_c)\vec{\varphi}^2$$

Yields 3 particles with energy gap $\sim \sqrt{(\lambda - \lambda_c)}$

Prediction of quantum field theory

Potential for $\vec{\varphi}$ fluctuations: $V(\vec{\varphi}) = (\lambda - \lambda_c)\vec{\varphi}^2 + u\left(\vec{\varphi}^2\right)^2$

Paramagnetic phase, $\lambda > \lambda_c$

Expand about $\vec{\varphi} = 0$:

$$V(\vec{\varphi}) \approx (\lambda - \lambda_c)\vec{\varphi}^2$$

Yields 3 particles with energy gap $\sim \sqrt{(\lambda - \lambda_c)}$

Néel phase, $\lambda < \lambda_c$

Expand $\vec{\varphi} = \left(0, 0, \sqrt{(\lambda_c - \lambda)/(2u)}\right) + \vec{\varphi}_1$:

$$V(\vec{\varphi}) \approx 2(\lambda_c - \lambda)\varphi_{1z}^2$$

Yields 2 gapless spin waves and one Higgs-Englert-Brout particle with energy gap $\sim \sqrt{2(\lambda_c - \lambda)}$

Prediction of quantum field theory

$$\frac{\text{Energy of Higgs-Englert-Brout particle}}{\text{Energy of triplon}} = \sqrt{2}$$

$$V(\vec{\varphi}) = (\lambda - \lambda_c)\vec{\varphi}^2 + u\left(\vec{\varphi}^2\right)^2$$

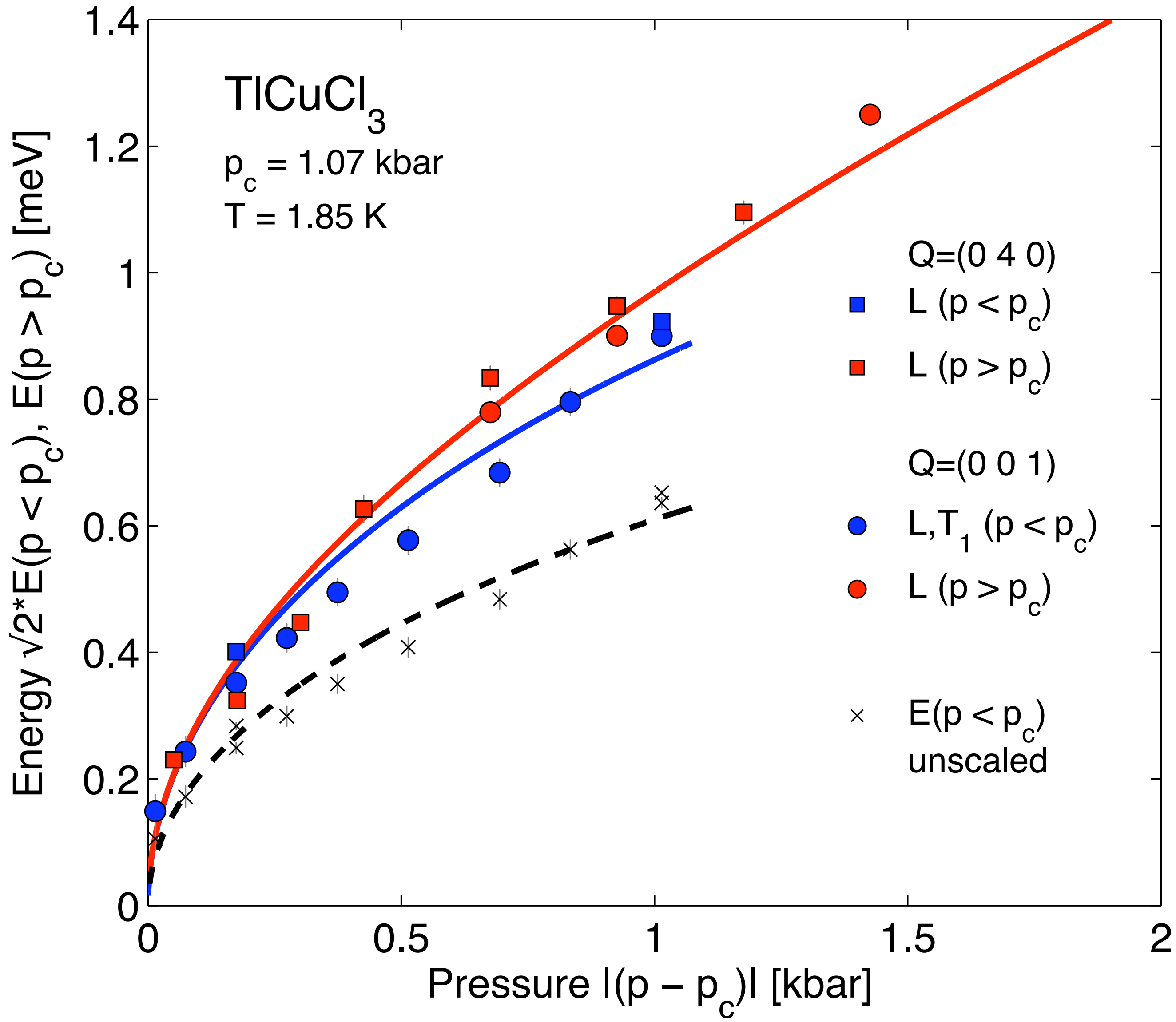

Christian Ruegg, Bruce Normand, Masashige Matsumoto, Albert Furrer, Desmond McMorrow, Karl Kramer, Hans-Ulrich Gudel, Severian Gvasaliya, Hannu Mutka, and Martin Boehm, *Phys. Rev. Lett.* **100**, 205701 (2008)

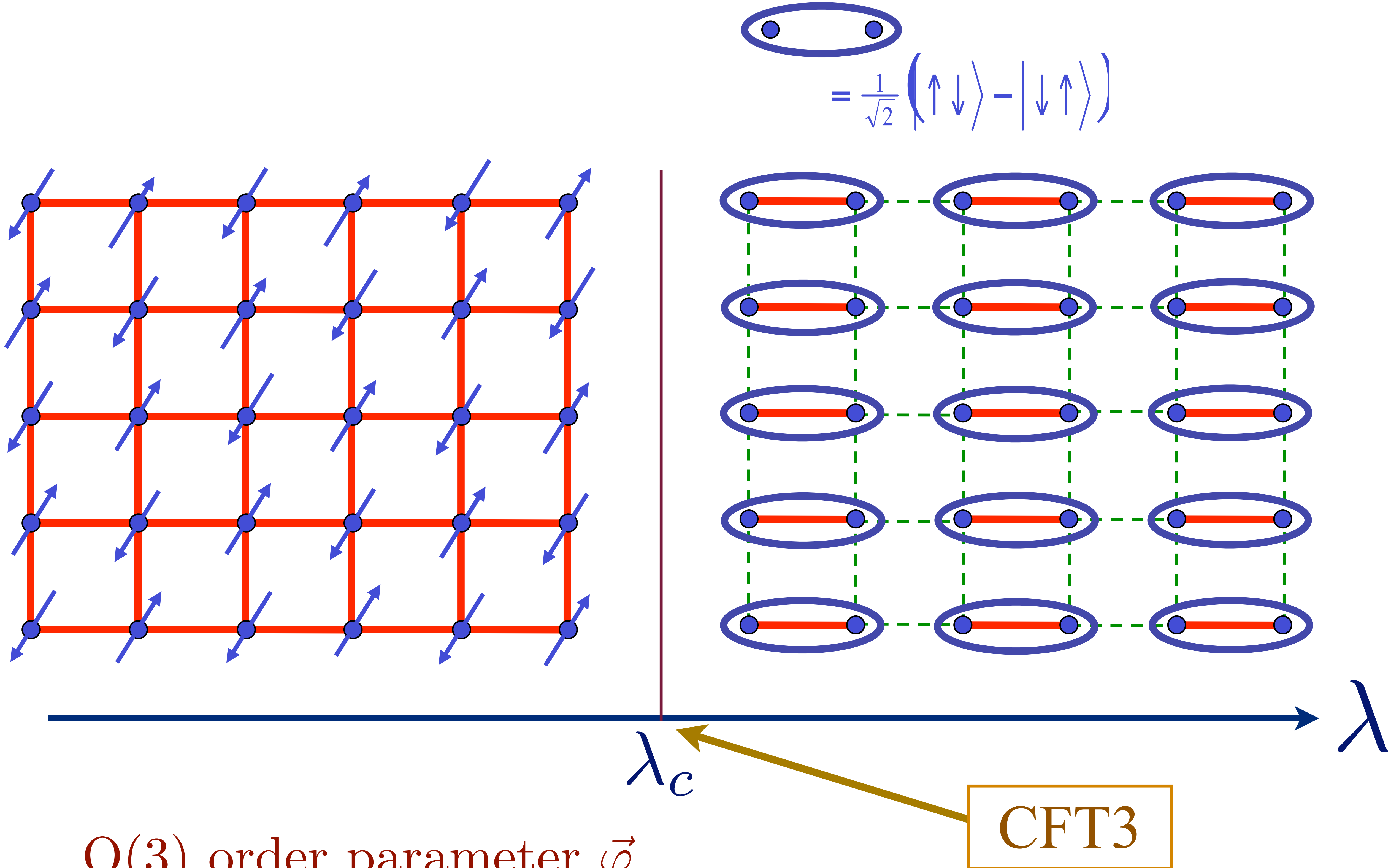

O(3) order parameter $\vec{\varphi}$

$$\mathcal{S} = \int d^2 r d\tau \left[(\partial_\tau \varphi)^2 + c^2 (\nabla_r \vec{\varphi})^2 + s\vec{\varphi}^2 + u \left(\vec{\varphi}^2\right)^2 \right]$$

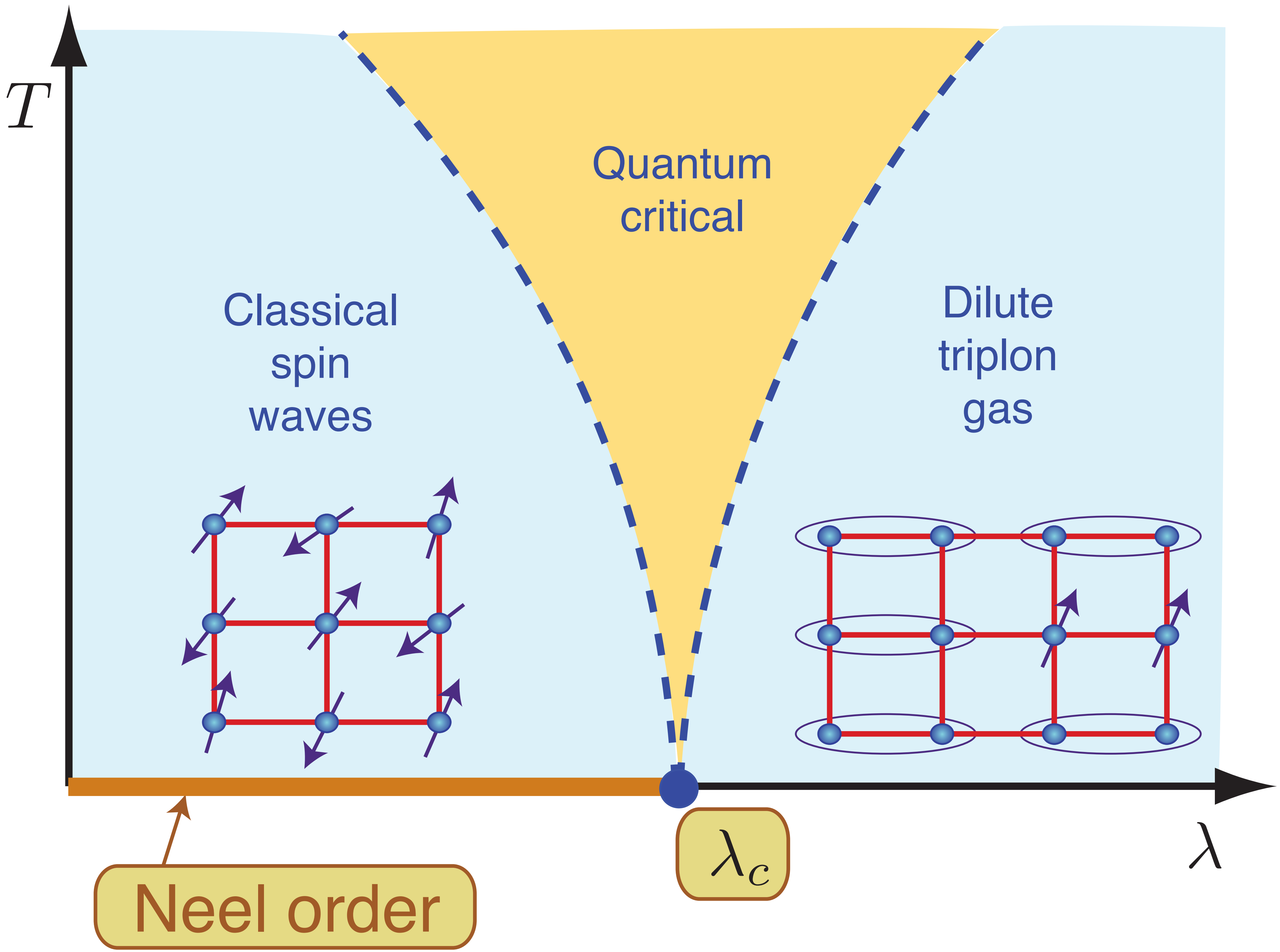

T
Quantum critical
Classical spin waves
Dilute triplon gas
λ
λ_c
Neel order

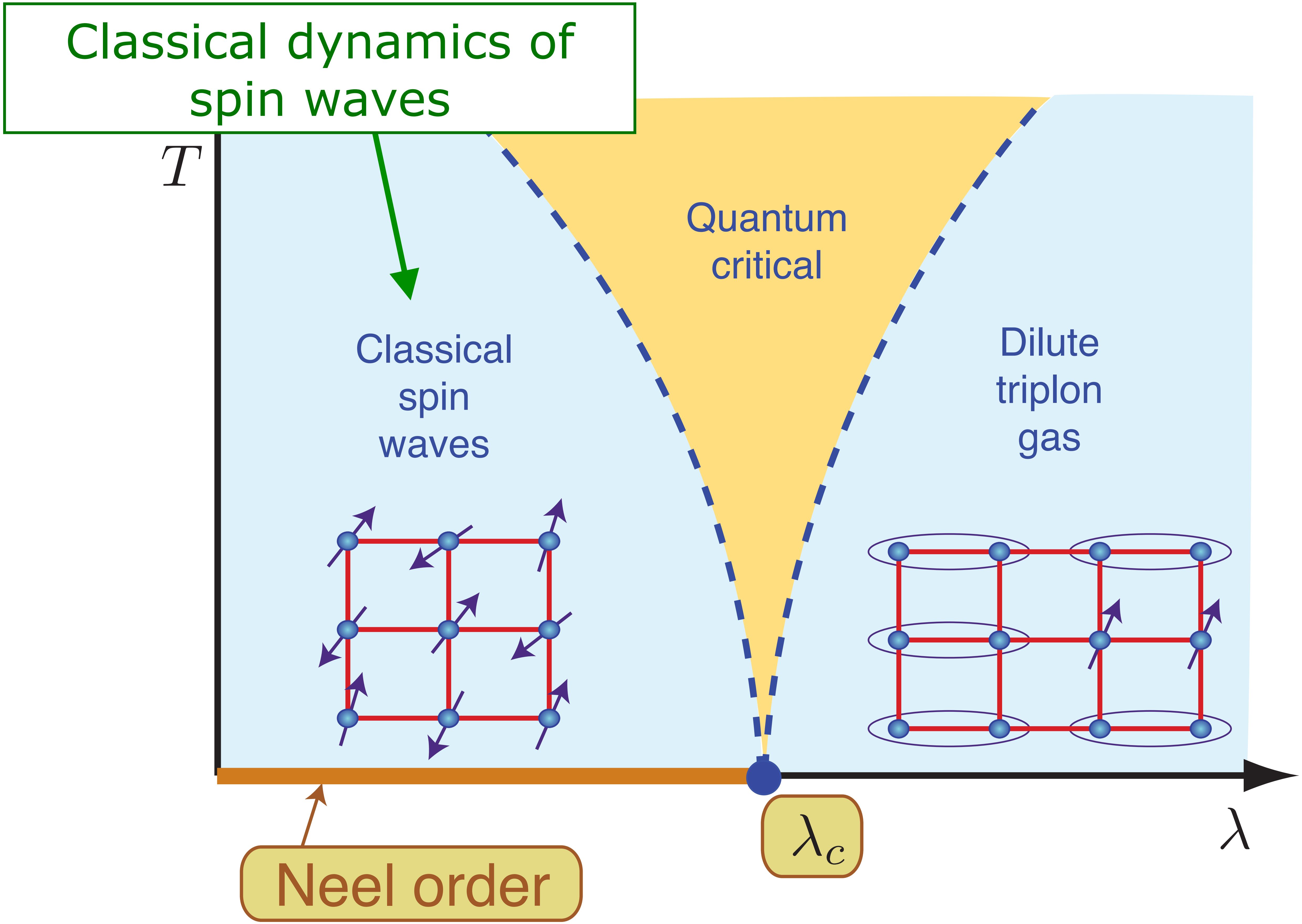

Classical dynamics of spin waves
T
Quantum critical
Classical spin waves
Dilute triplon gas
λ
λ_c
Neel order

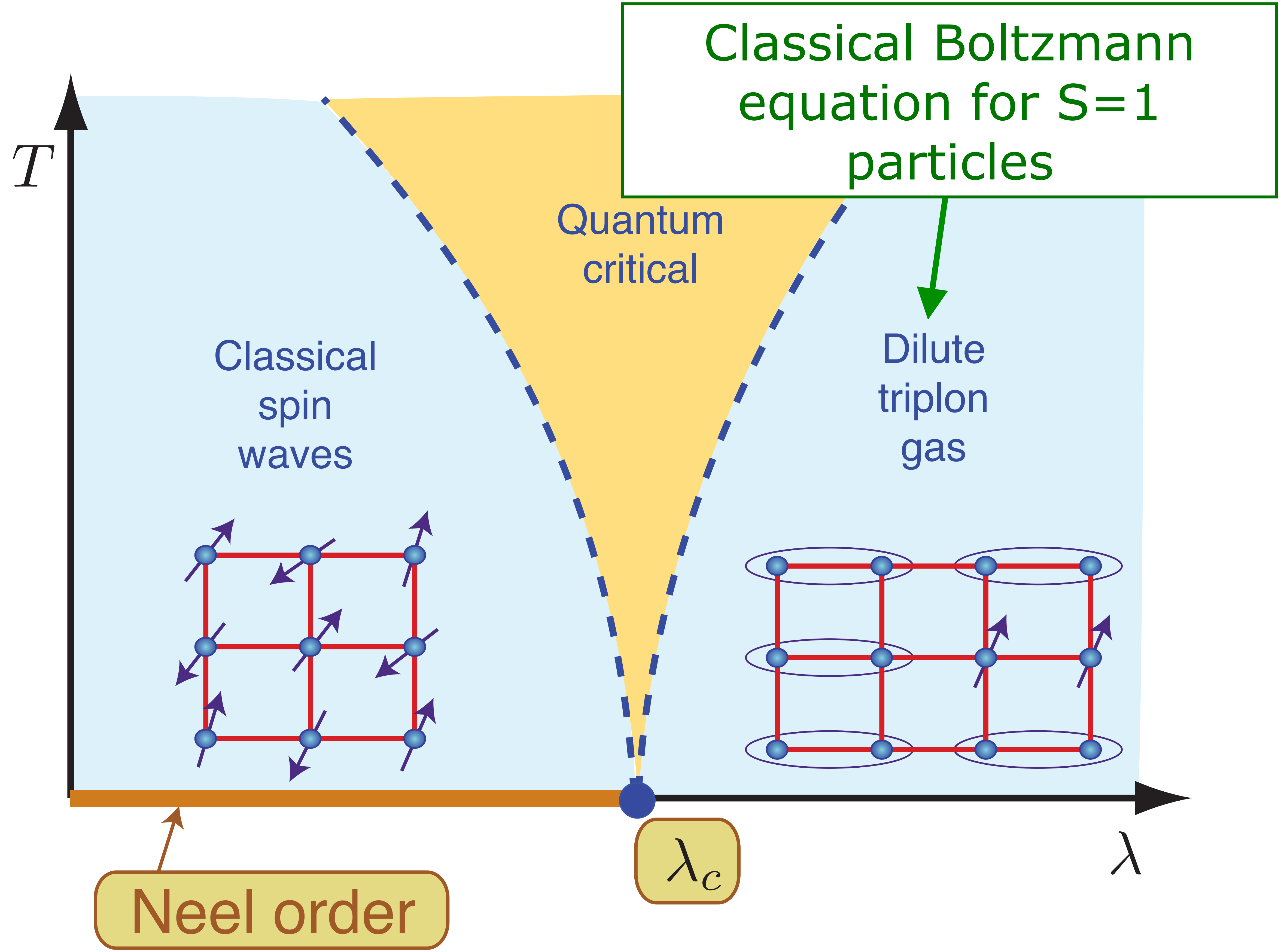
Classical Boltzmann equation for S=1 particles
T
Quantum critical
Classical spin waves
Dilute triplon gas
Neel order
λ_c
λ

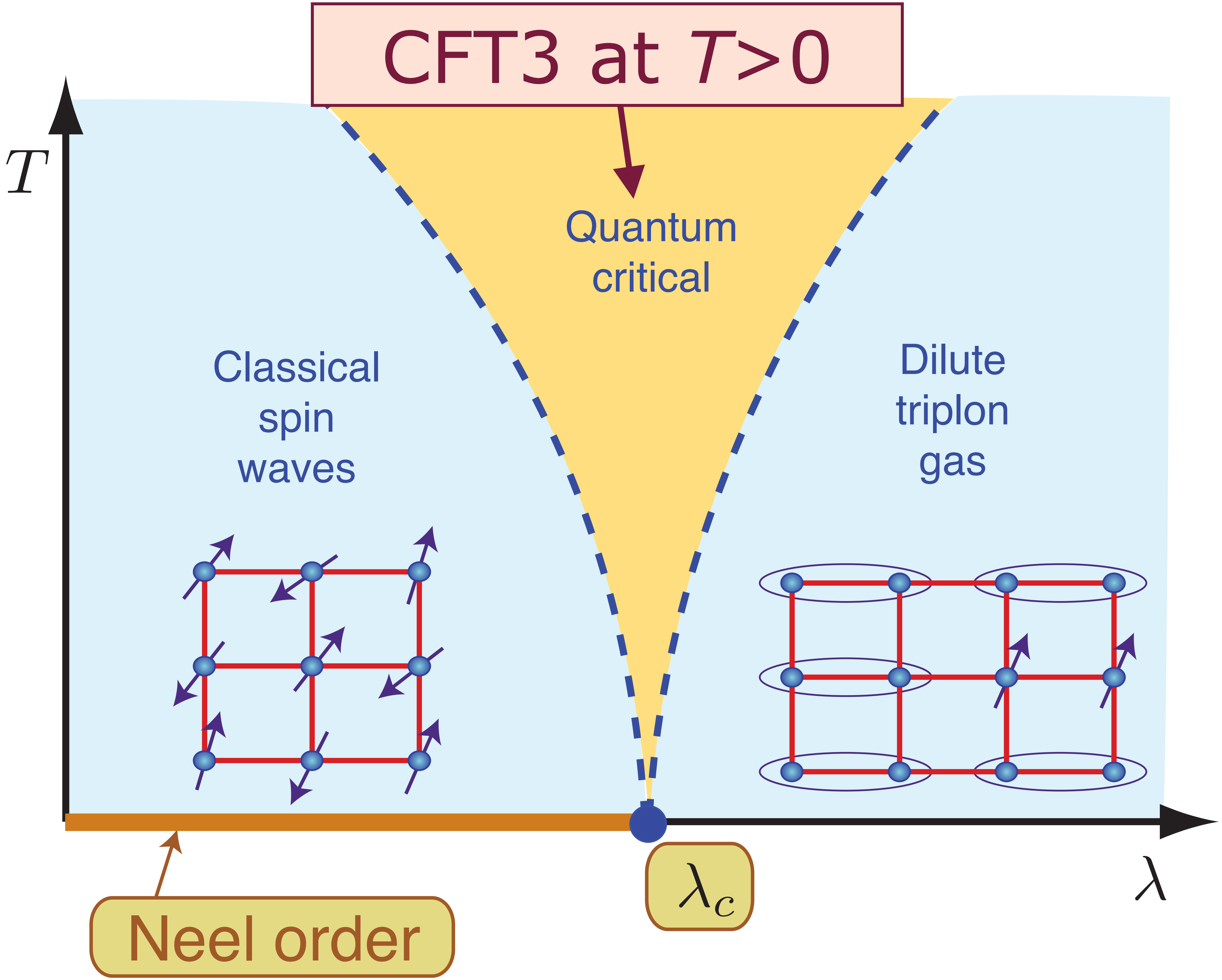
CFT3 at $T>0$
T
Quantum critical
Classical spin waves
Dilute triplon gas
λ
λ_c
Neel order

Outline

1. Coupled dimer antiferromagnets
   Order parameters and Landau-Ginzburg criticality

2. Graphene
   `Topological' Fermi surface transitions

3. Quantum criticality and black holes
   AdS_4 theory of compressible quantum liquids

4. Quantum criticality in the cuprates
   Global phase diagram and the spin density wave transition in metals

Outline

1. Coupled dimer antiferromagnets
   Order parameters and Landau-Ginzburg criticality

2. Graphene
   `Topological' Fermi surface transitions

3. Quantum criticality and black holes
   AdS_4 theory of compressible quantum liquids

4. Quantum criticality in the cuprates
   Global phase diagram and the spin density wave transition in metals

Graphene

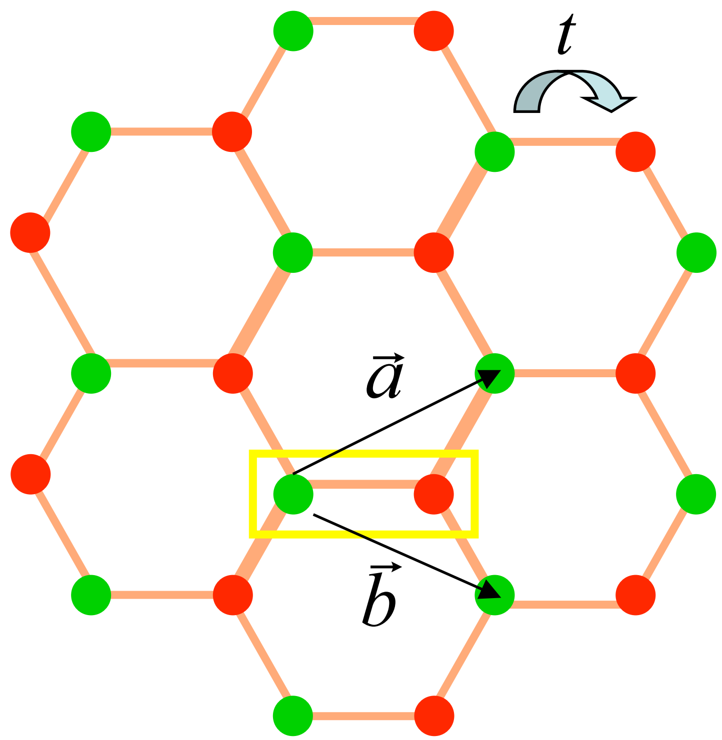

Graphene

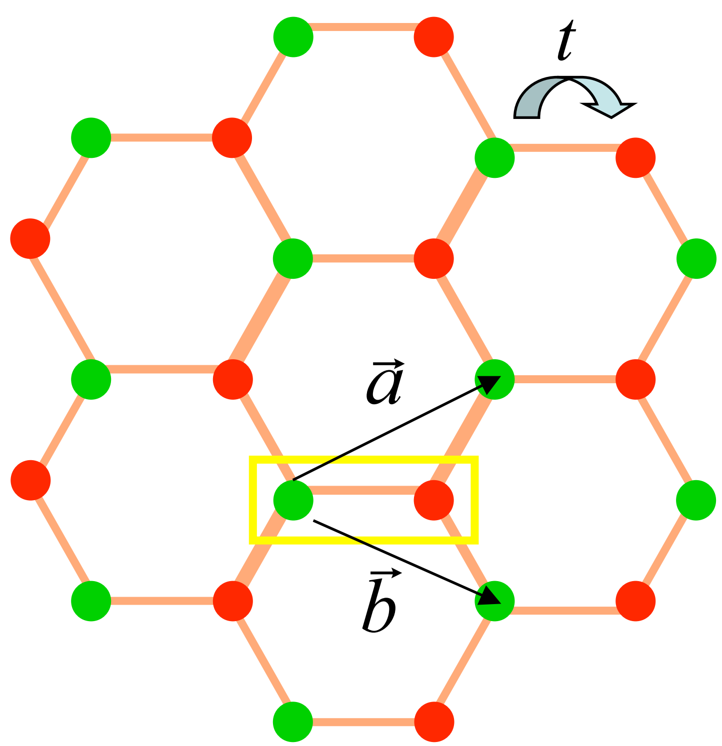

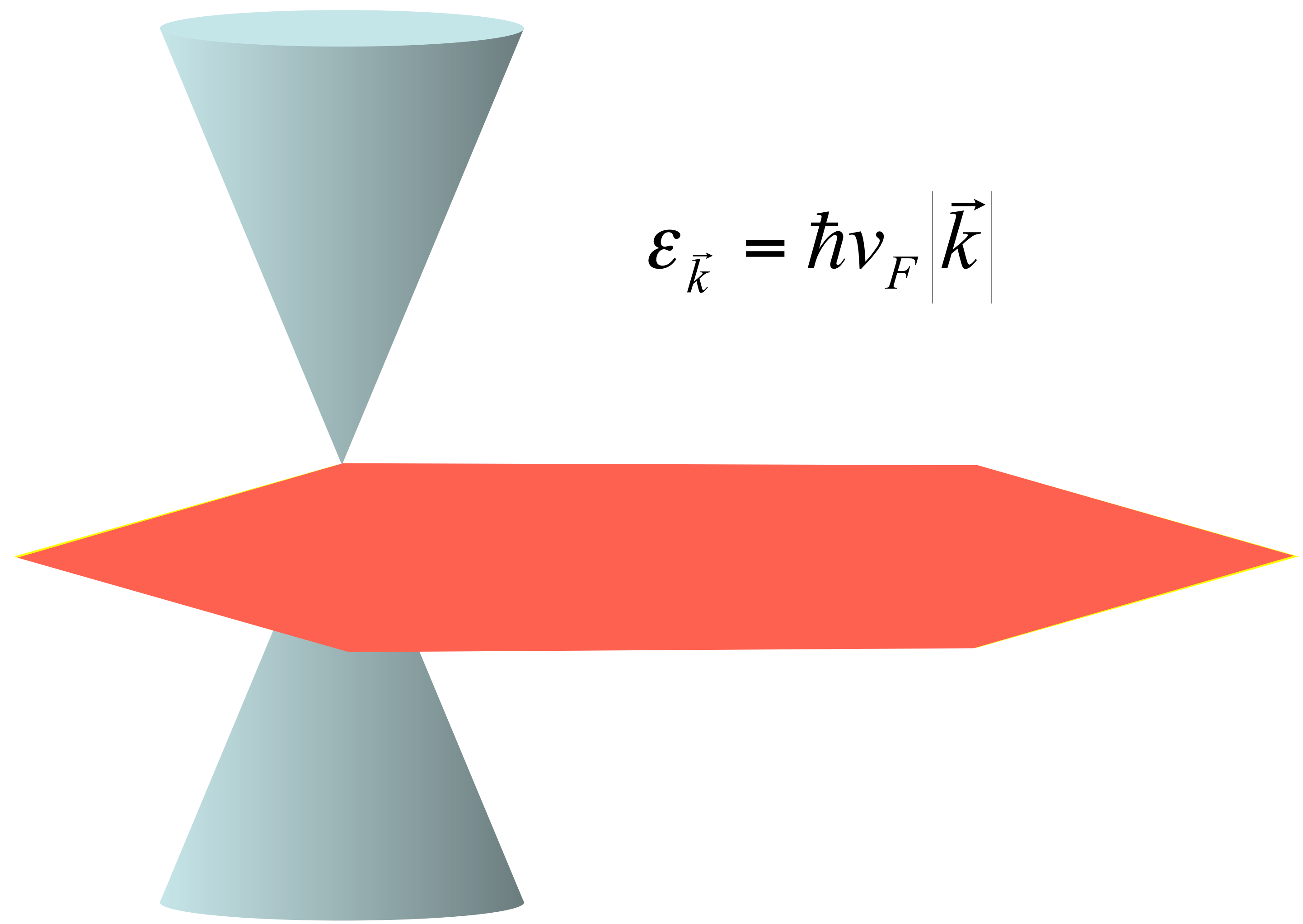

$$\varepsilon_{\vec{k}} = \hbar v_F \left|\vec{k}\right|$$

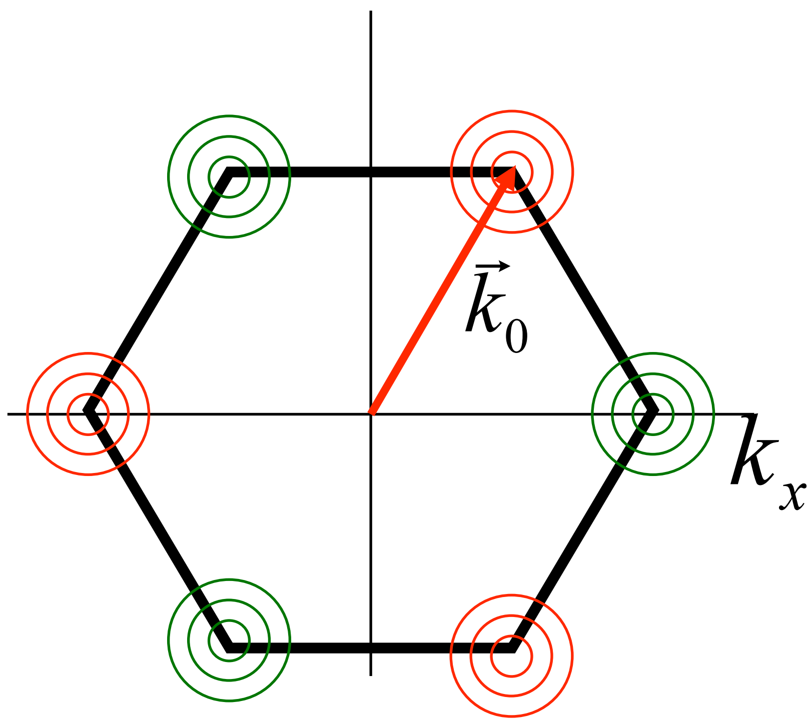

Conical Dirac dispersion

Quantum phase transition in graphene tuned by a gate voltage

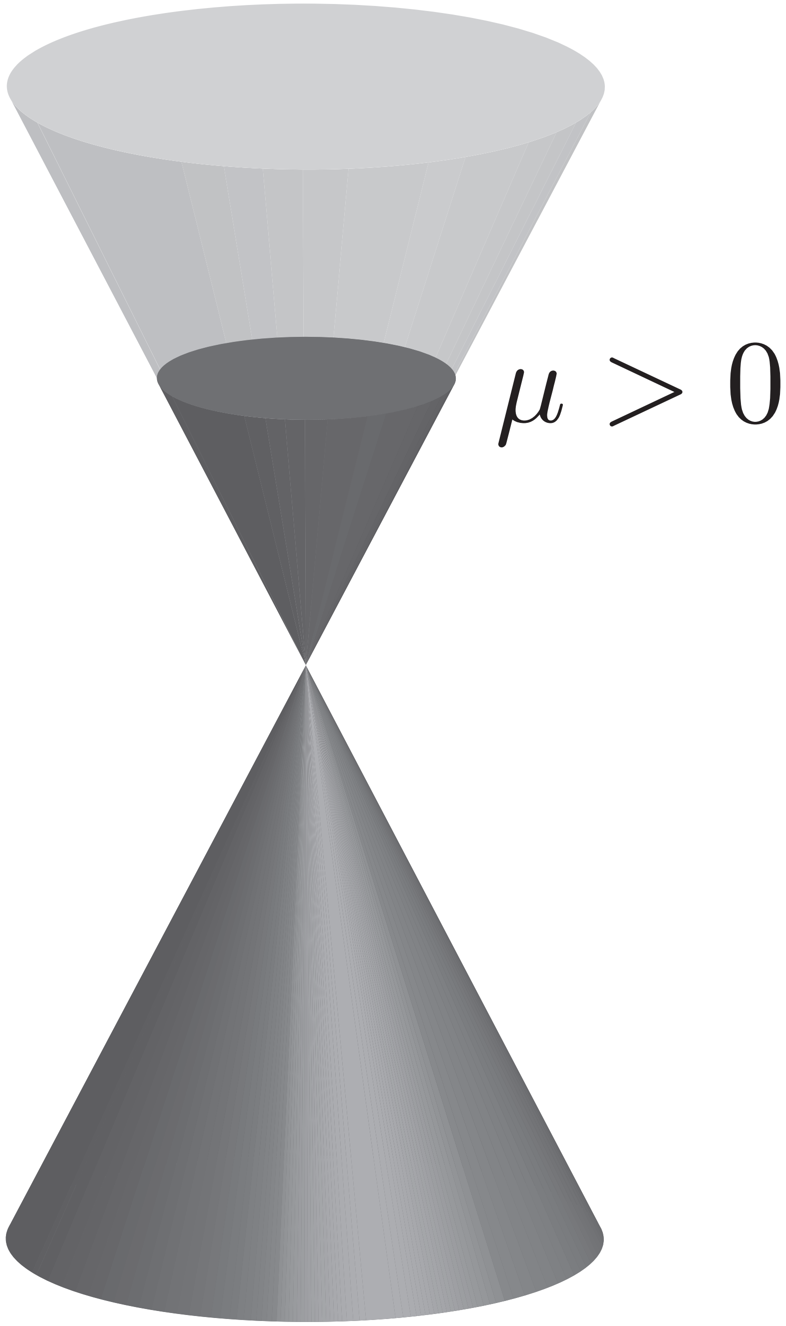

Electron
Fermi surface

Quantum phase transition in graphene tuned by a gate voltage

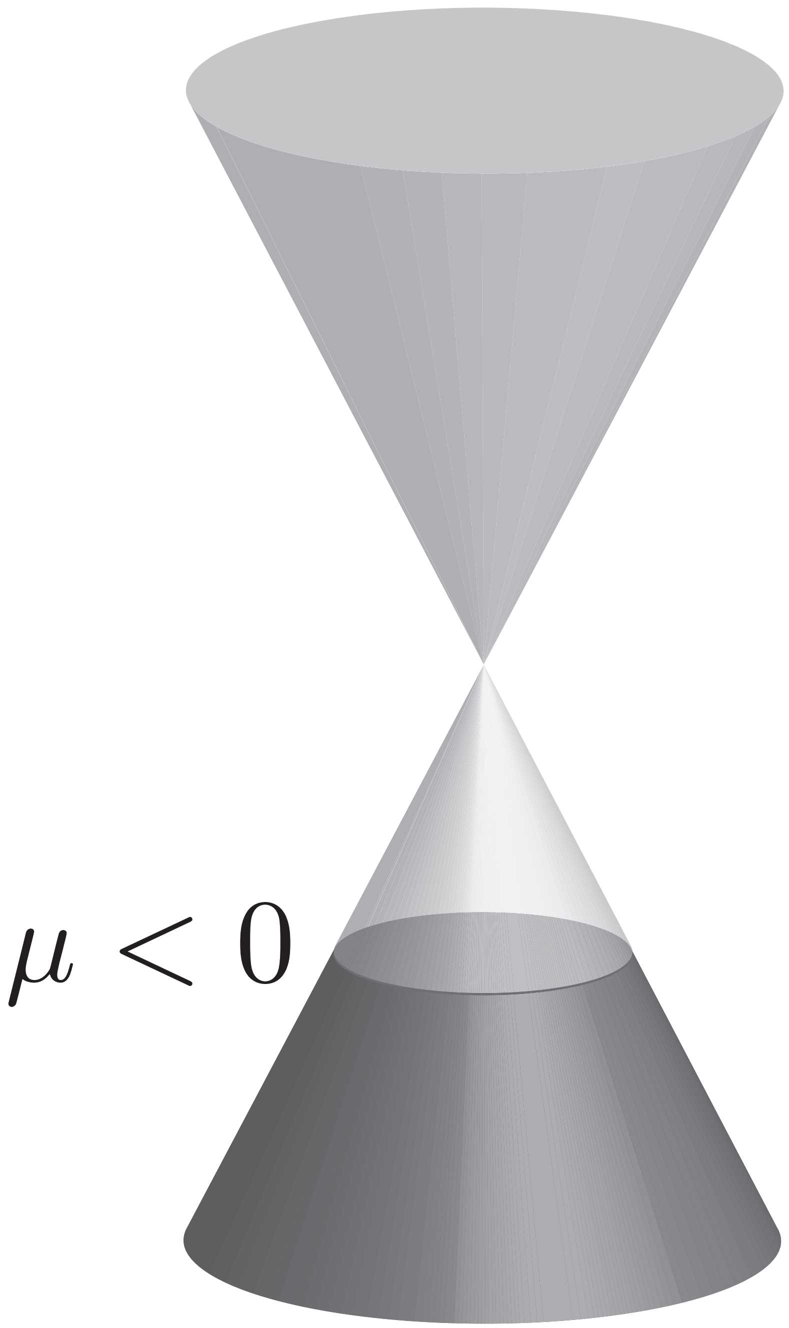

Hole
Fermi surface

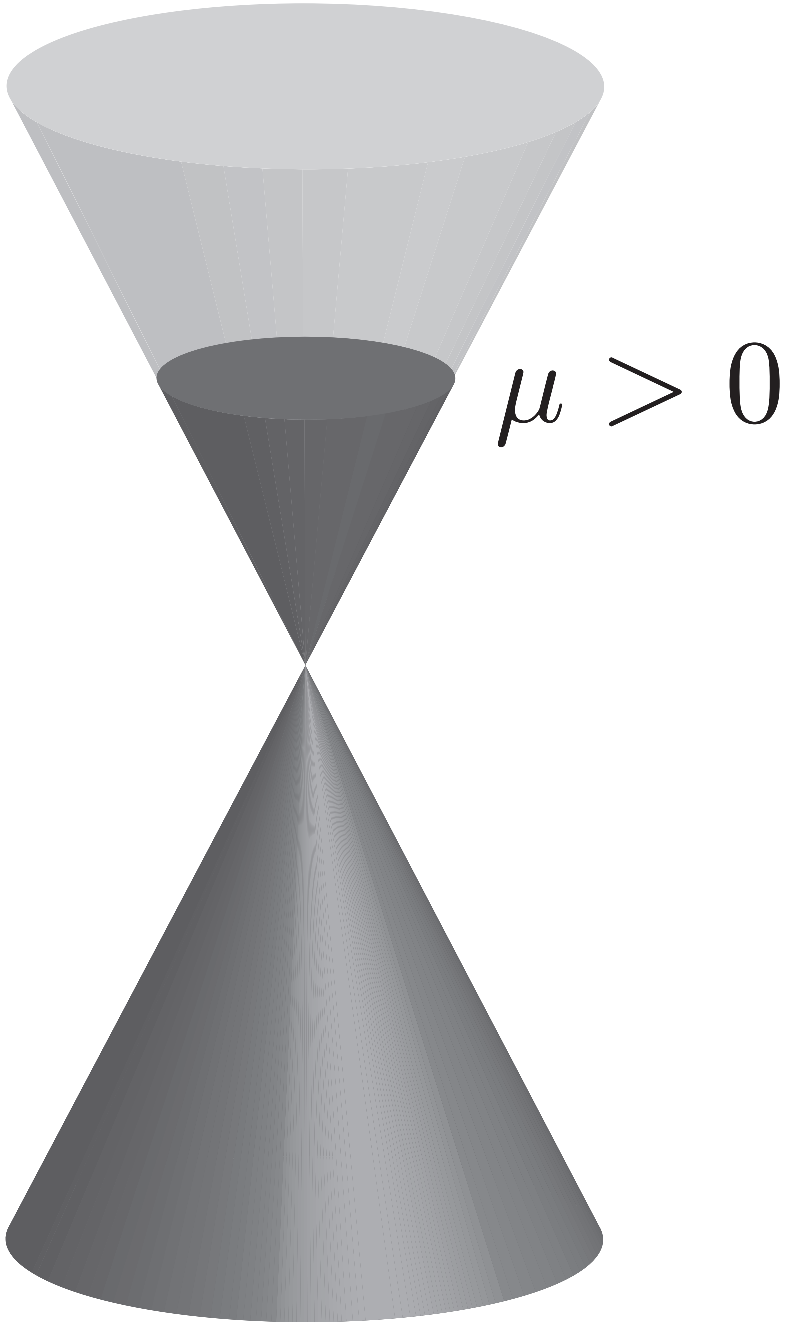

Electron
Fermi surface

Quantum phase transition in graphene tuned by a gate voltage

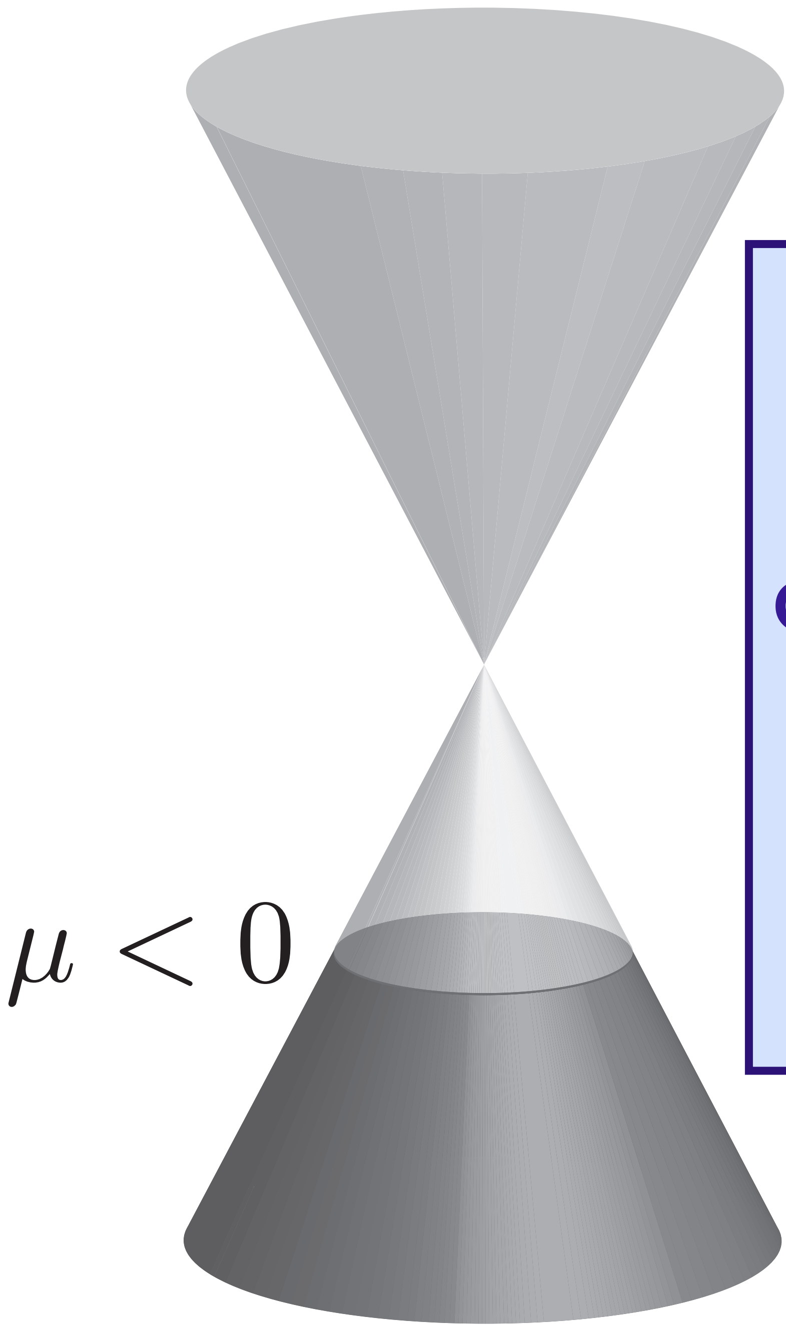

Hole
Fermi surface

There must be an intermediate quantum critical point where the Fermi surfaces reduce to a Dirac point

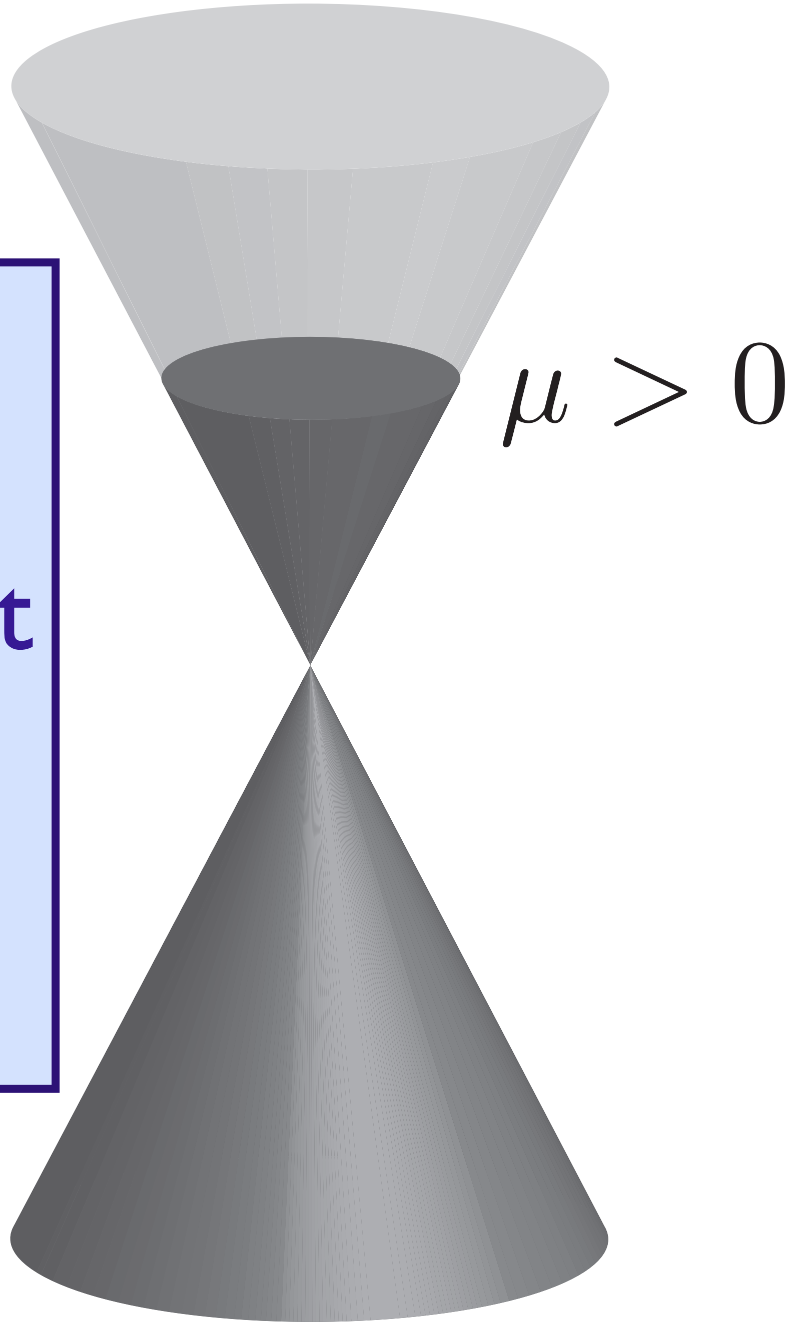

Electron
Fermi surface

Quantum critical graphene

Low energy theory has 4 two-component Dirac fermions, ψ_σ, $\sigma = 1 \ldots 4$, interacting with a $1/r$ Coulomb interaction

$$\mathcal{S} = \int d^2 r d\tau \psi_\sigma^\dagger \left(\partial_\tau - i v_F \vec{\sigma} \cdot \vec{\nabla} \right) \psi_\sigma + \frac{e^2}{2} \int d^2 r d^2 r' d\tau \psi_\sigma^\dagger \psi_\sigma(r) \frac{1}{|r - r'|} \psi_{\sigma'}^\dagger \psi_{\sigma'}(r')$$

Quantum critical graphene

Low energy theory has 4 two-component Dirac fermions, ψ_σ, $\sigma = 1 \ldots 4$, interacting with a $1/r$ Coulomb interaction

$$\mathcal{S} = \int d^2 r d\tau \psi_\sigma^\dagger \left(\partial_\tau - i v_F \vec{\sigma} \cdot \vec{\nabla} \right) \psi_\sigma + \frac{e^2}{2} \int d^2 r d^2 r' d\tau \psi_\sigma^\dagger \psi_\sigma(r) \frac{1}{|r - r'|} \psi_{\sigma'}^\dagger \psi_{\sigma'}(r')$$

Dimensionless "fine-structure" constant $\alpha = e^2/(\hbar v_F)$.
RG flow of α:

$$\frac{d\alpha}{d\ell} = -\alpha^2 + \ldots$$

Behavior is similar to a conformal field theory (CFT) in 2+1 dimensions with $\alpha \sim 1/\ln(\text{scale})$

Quantum phase transition in graphene

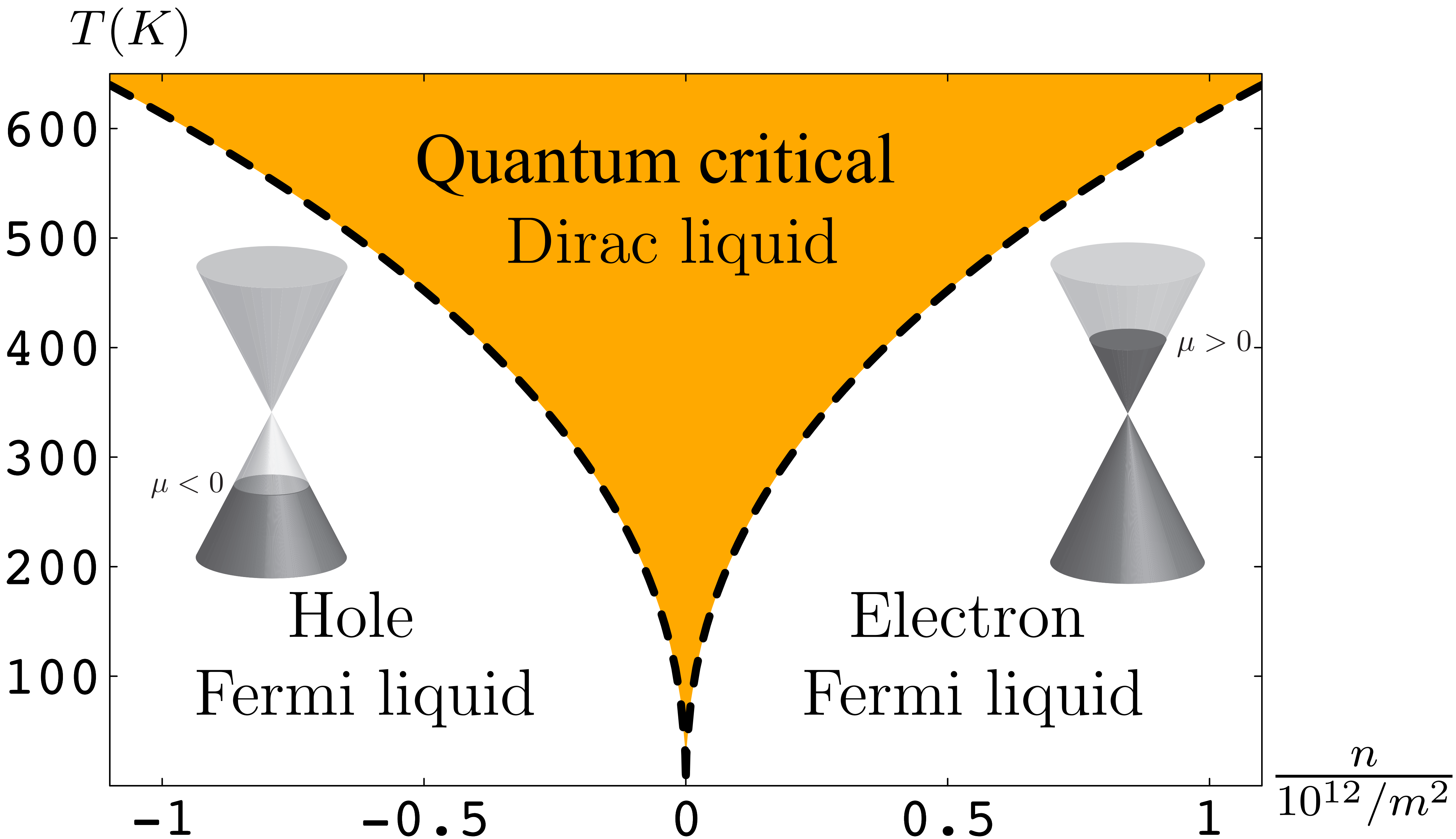

Quantum critical transport

Quantum *"perfect fluid"*
with shortest possible
relaxation time, τ_R

$$\tau_R \gtrsim \frac{\hbar}{k_B T}$$

S. Sachdev, *Quantum Phase Transitions,* Cambridge (1999).

Quantum critical transport

Transport co-oefficients not determined by collision rate, but by universal constants of nature

Electrical conductivity

$$\sigma = \frac{e^2}{h} \times [\text{Universal constant } \mathcal{O}(1)\ ]$$

K. Damle and S. Sachdev, *Phys. Rev. B* **56**, 8714 (1997).

Quantum critical transport

Transport co-oefficients not determined by collision rate, but by universal constants of nature

Momentum transport

$$\frac{\eta}{s} \equiv \frac{\text{viscosity}}{\text{entropy density}}$$

$$= \frac{\hbar}{k_B} \times [\text{Universal constant } \mathcal{O}(1) \,]$$

P. Kovtun, D. T. Son, and A. Starinets, *Phys. Rev. Lett.* **94,** 11601 (2005)

Quantum critical transport in graphene

$$\sigma(\omega) = \begin{cases} \dfrac{e^2}{h}\left[\dfrac{\pi}{2} + \mathcal{O}\left(\dfrac{1}{\ln(\Lambda/\omega)}\right)\right] & , \quad \hbar\omega \gg k_B T \\ \dfrac{e^2}{h\alpha^2(T)}\left[0.760 + \mathcal{O}\left(\dfrac{1}{|\ln(\alpha(T))|}\right)\right] & , \quad \hbar\omega \ll k_B T \alpha^2(T) \end{cases}$$

$$\frac{\eta}{s} = \frac{\hbar}{k_B \alpha^2(T)} \times 0.130$$

where the "fine structure constant" is

$$\alpha(T) = \frac{\alpha}{1 + (\alpha/4)\ln(\Lambda/T)} \overset{T\to 0}{\sim} \frac{4}{\ln(\Lambda/T)}$$

L. Fritz, J. Schmalian, M. Müller and S. Sachdev, *Physical Review B* **78**, 085416 (2008)
M. Müller, J. Schmalian, and L. Fritz, *Physical Review Letters* **103**, 025301 (2009)

Outline

1. Coupled dimer antiferromagnets

   Order parameters and Landau-Ginzburg criticality

2. Graphene

   `Topological' Fermi surface transitions

3. Quantum criticality and black holes

   AdS_4 theory of compressible quantum liquids

4. Quantum criticality in the cuprates

   Global phase diagram and the spin density wave transition in metals

Outline

1. Coupled dimer antiferromagnets
Order parameters and Landau-Ginzburg criticality

2. Graphene
`Topological' Fermi surface transitions

3. Quantum criticality and black holes
AdS_4 theory of compressible quantum liquids

4. Quantum criticality in the cuprates
Global phase diagram and the spin density wave transition in metals

AdS/CFT correspondence

The quantum theory of a black hole in a 3+1-dimensional negatively curved AdS universe is holographically represented by a CFT (the theory of a quantum critical point) in 2+1 dimensions

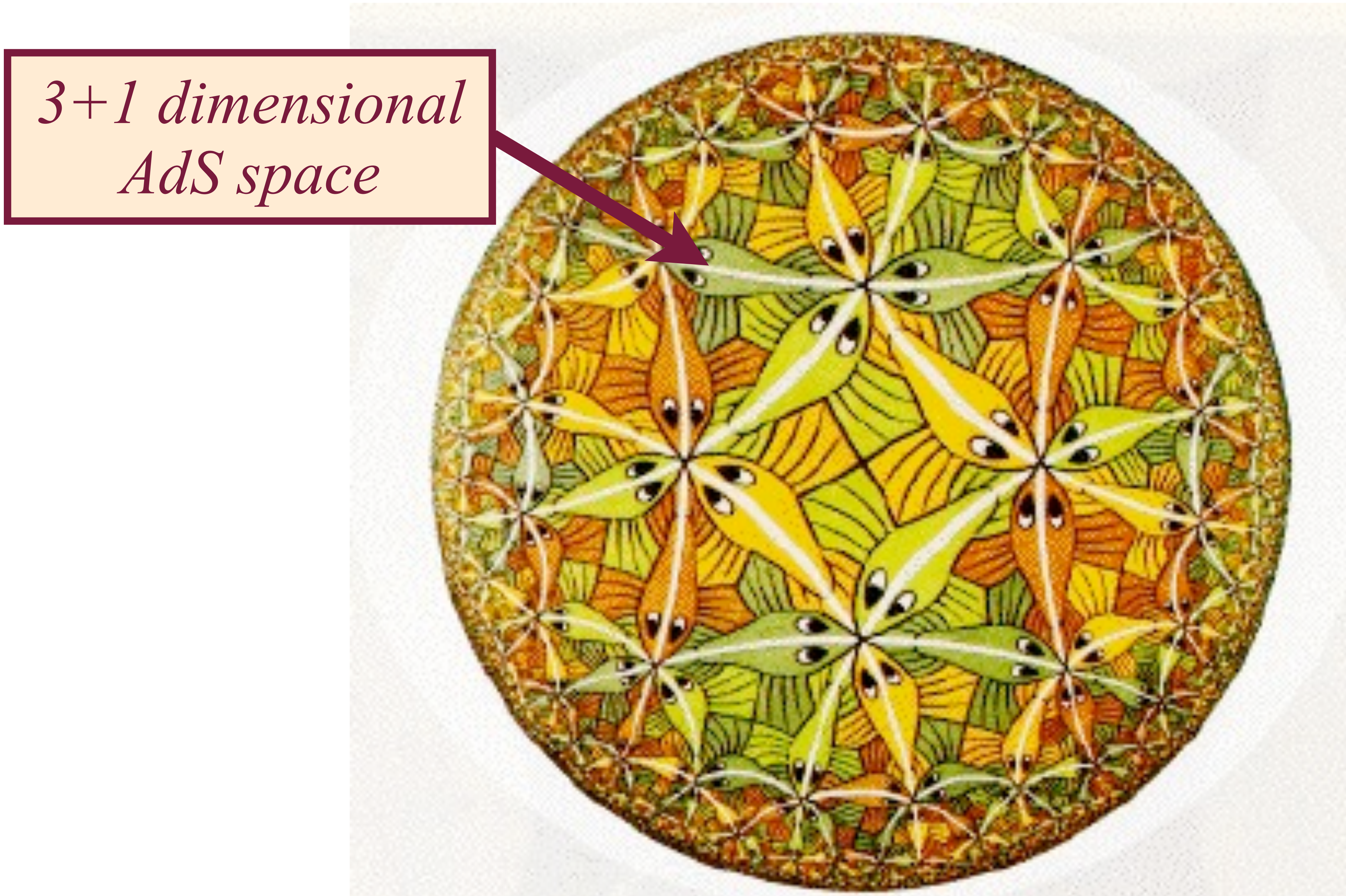

Maldacena, Gubser, Klebanov, Polyakov, Witten

AdS/CFT correspondence

The quantum theory of a black hole in a 3+1-dimensional negatively curved AdS universe is holographically represented by a CFT (the theory of a quantum critical point) in 2+1 dimensions

3+1 dimensional AdS space

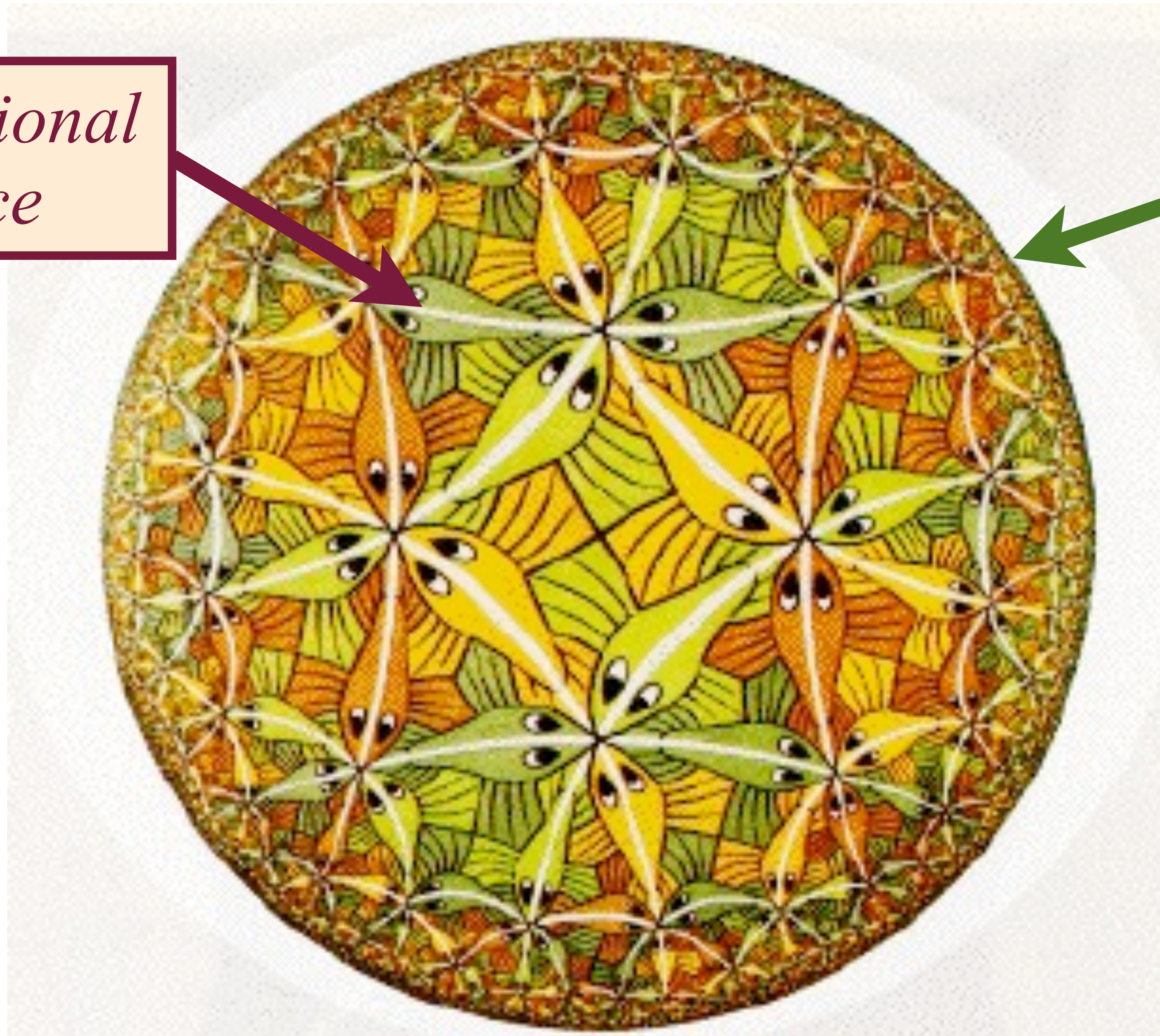

A 2+1 dimensional system at its quantum critical point

Maldacena, Gubser, Klebanov, Polyakov, Witten

AdS/CFT correspondence

The quantum theory of a black hole in a 3+1-dimensional negatively curved AdS universe is holographically represented by a CFT (the theory of a quantum critical point) in 2+1 dimensions

3+1 dimensional AdS space

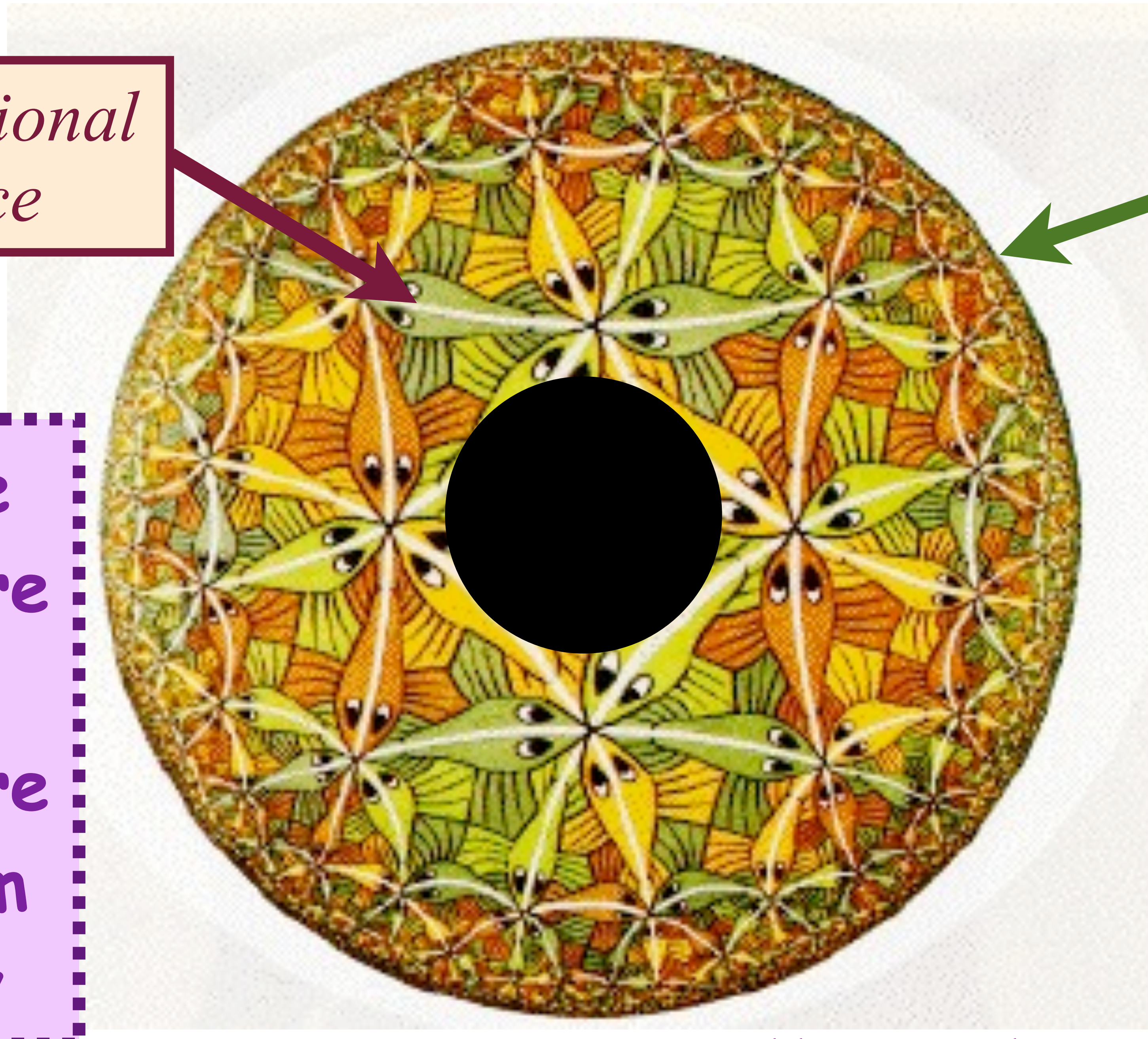

Quantum criticality in 2+1 dimensions

Black hole temperature = temperature of quantum criticality

Maldacena, Gubser, Klebanov, Polyakov, Witten

AdS/CFT correspondence

The quantum theory of a black hole in a 3+1-dimensional negatively curved AdS universe is holographically represented by a CFT (the theory of a quantum critical point) in 2+1 dimensions

3+1 dimensional AdS space

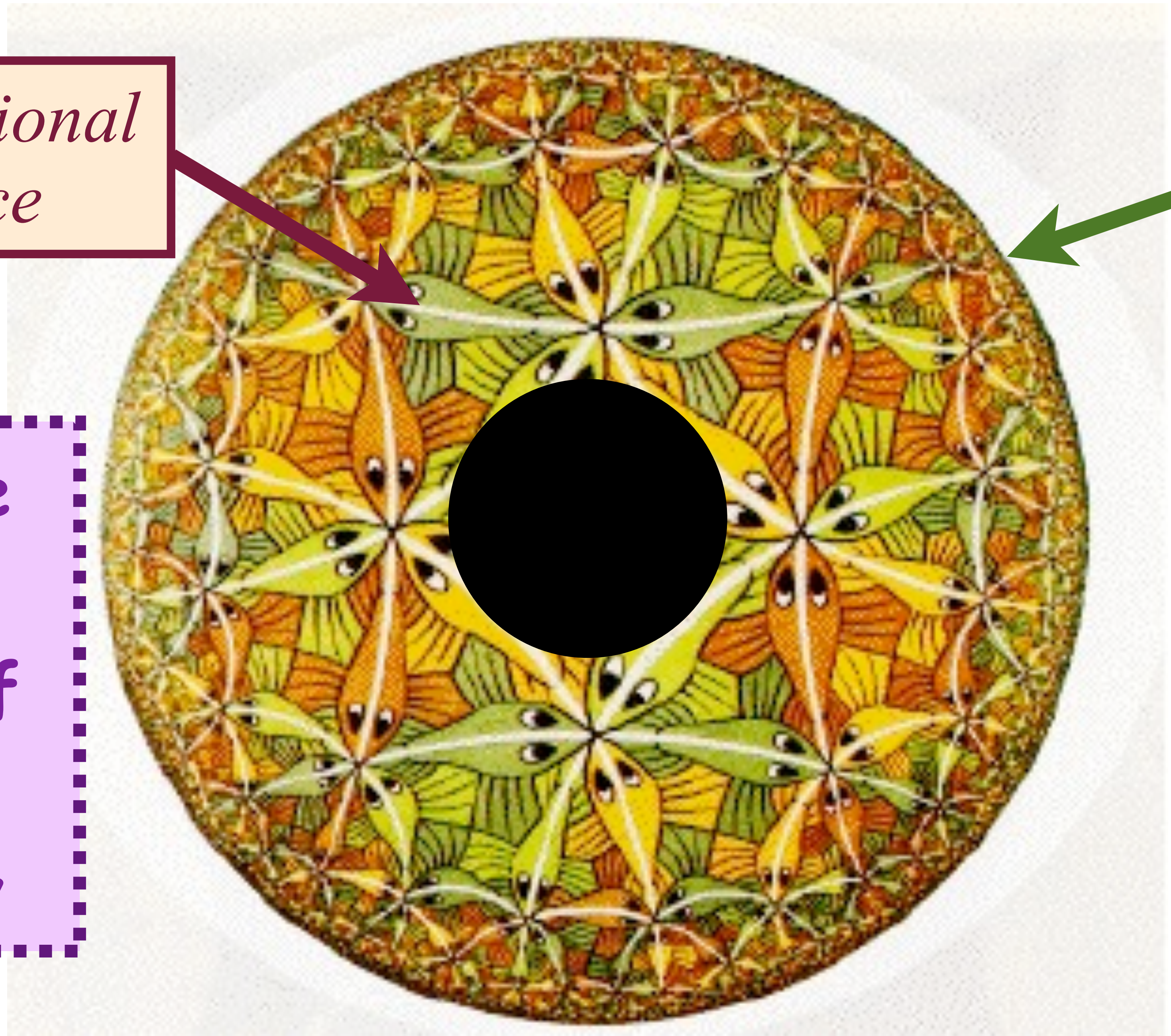

Quantum criticality in 2+1 dimensions

Black hole entropy = entropy of quantum criticality

Strominger, Vafa

AdS/CFT correspondence

The quantum theory of a black hole in a 3+1-dimensional negatively curved AdS universe is holographically represented by a CFT (the theory of a quantum critical point) in 2+1 dimensions

3+1 dimensional AdS space

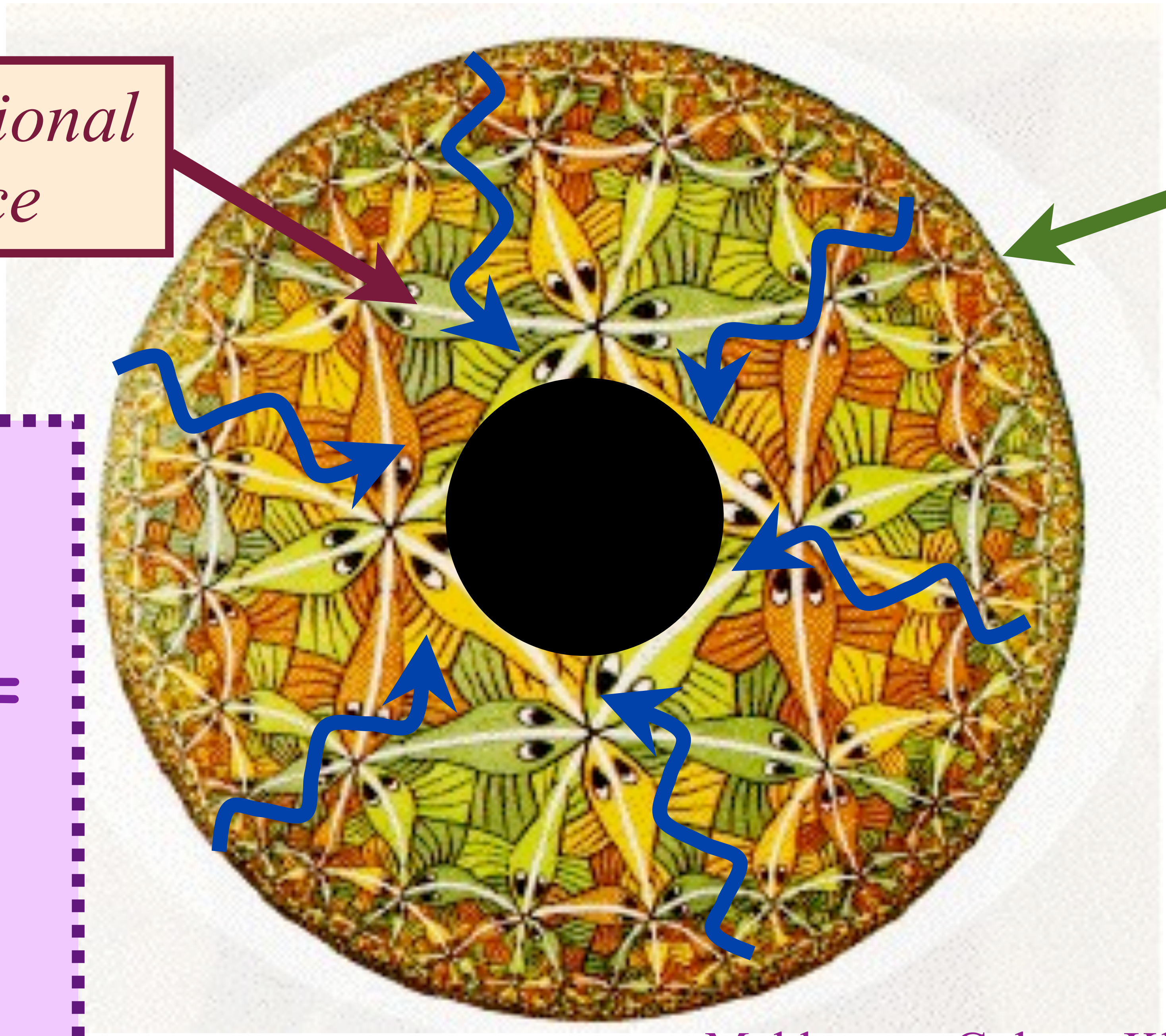

Quantum criticality in 2+1 dimensions

Quantum critical dynamics = waves in curved space

Maldacena, Gubser, Klebanov, Polyakov, Witten

AdS/CFT correspondence

The quantum theory of a black hole in a 3+1-dimensional negatively curved AdS universe is holographically represented by a CFT (the theory of a quantum critical point) in 2+1 dimensions

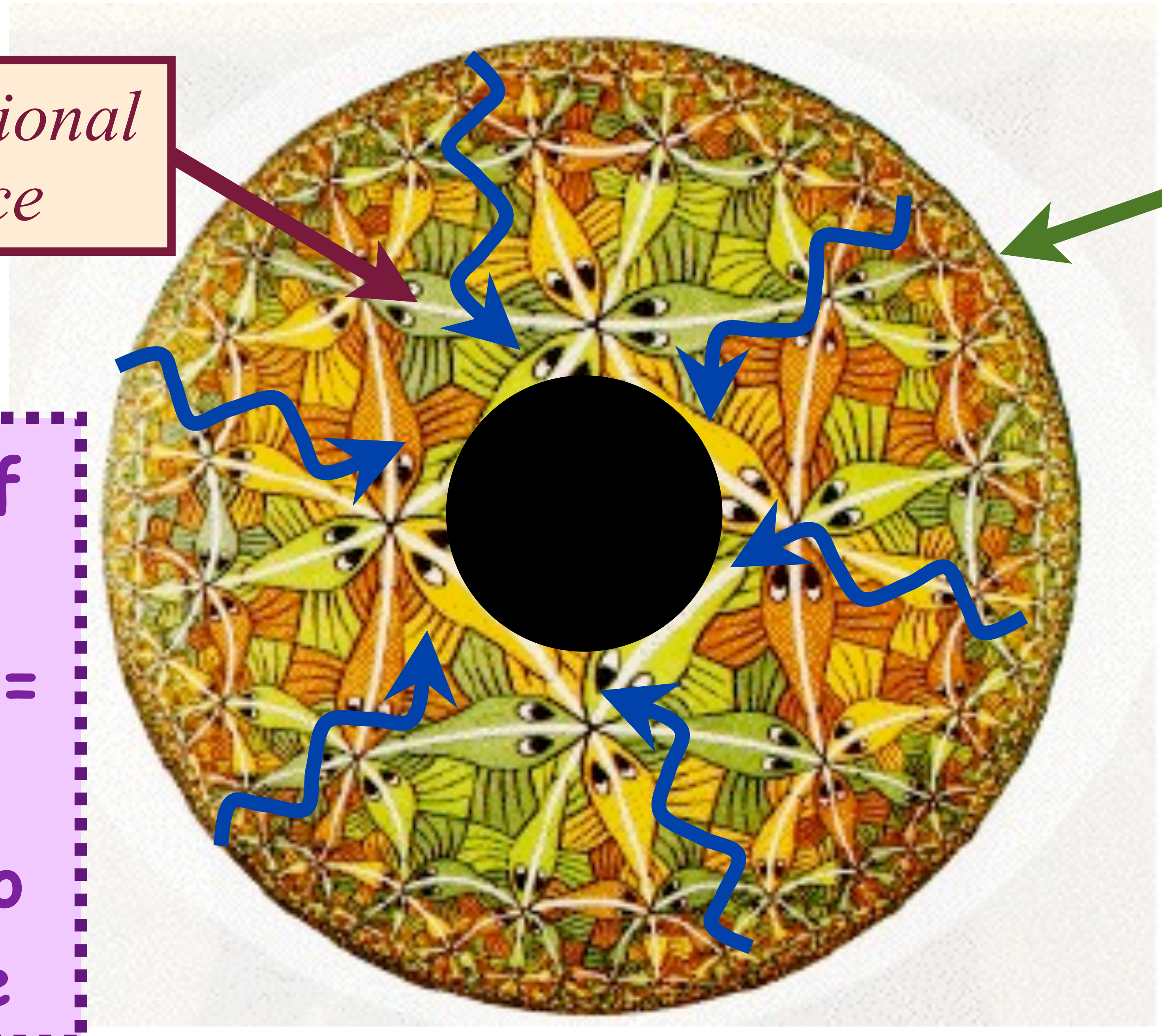

Kovtun, Policastro, Son

Conformal field theory
in 2+1 dimensions at $T = 0$

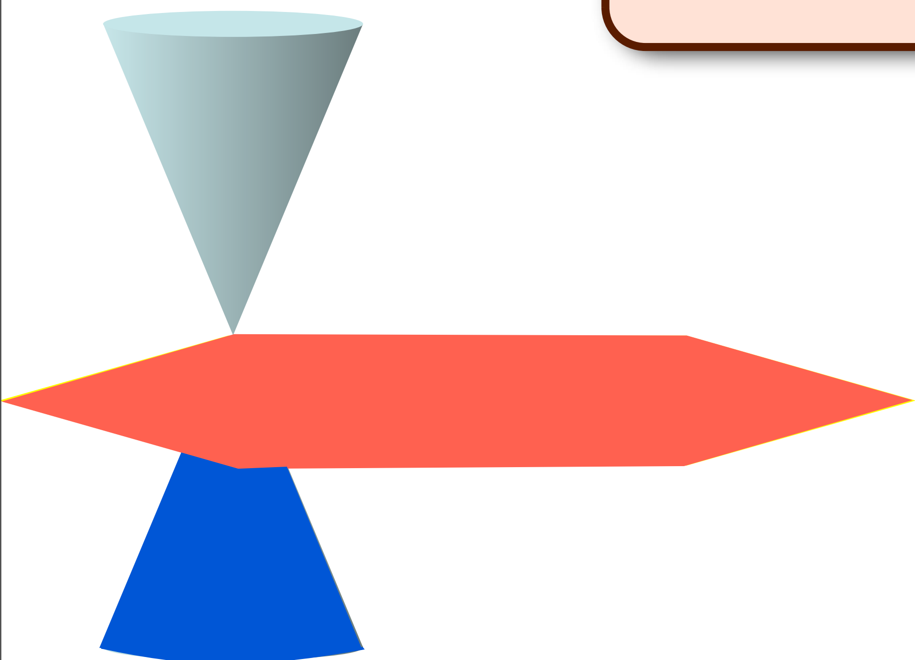

Einstein gravity
on AdS_4

Conformal field theory in 2+1 dimensions at $T > 0$

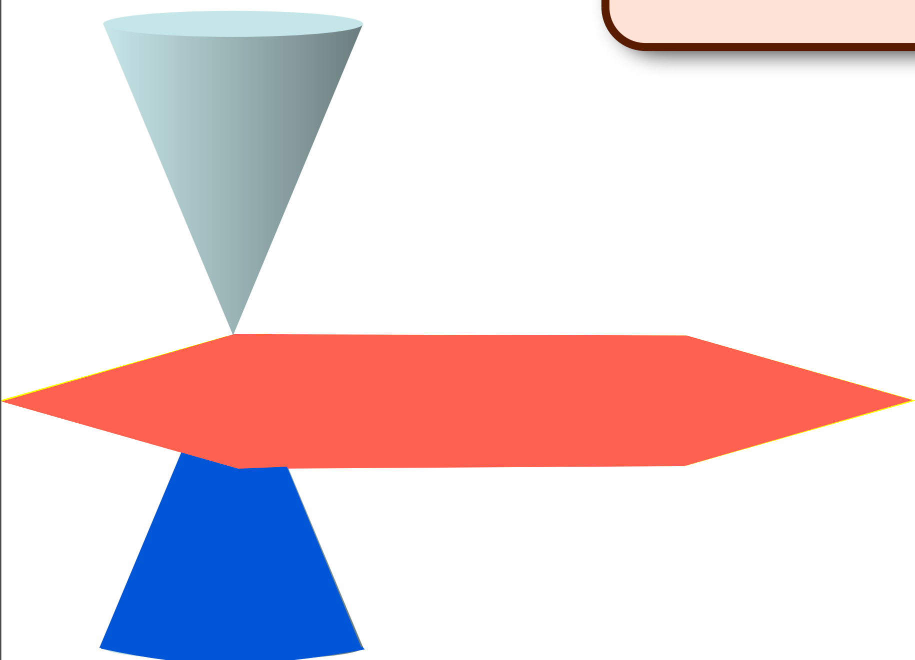

Einstein gravity on AdS_4 with a Schwarzschild black hole

Conformal field theory
in 2+1 dimensions at $T > 0$,
with a non-zero chemical potential, μ
and applied magnetic field, B

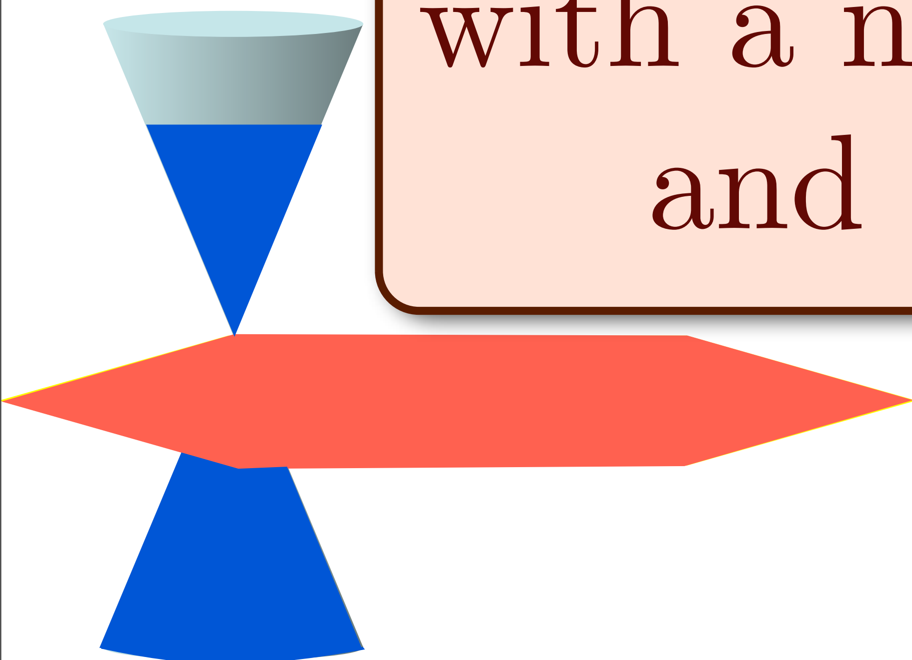

$\Updownarrow$

Einstein gravity on AdS_4
with a Reissner-Nordstrom
black hole carrying electric
and magnetic charges

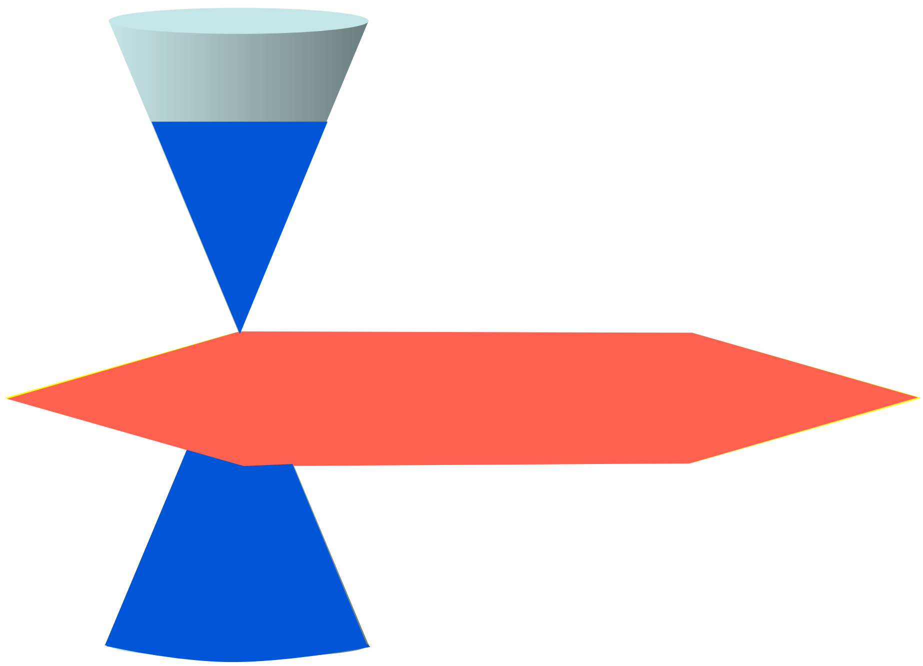

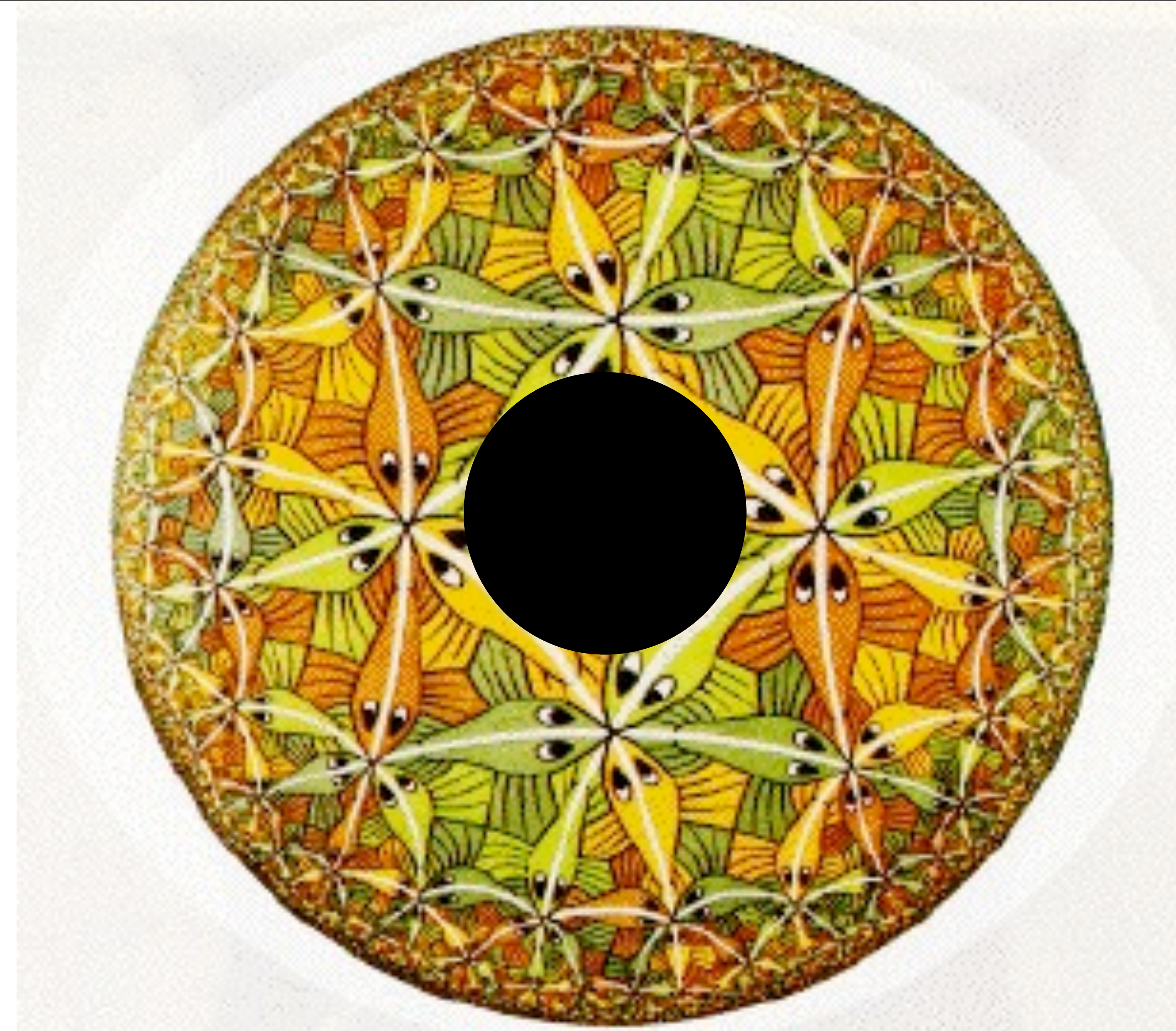

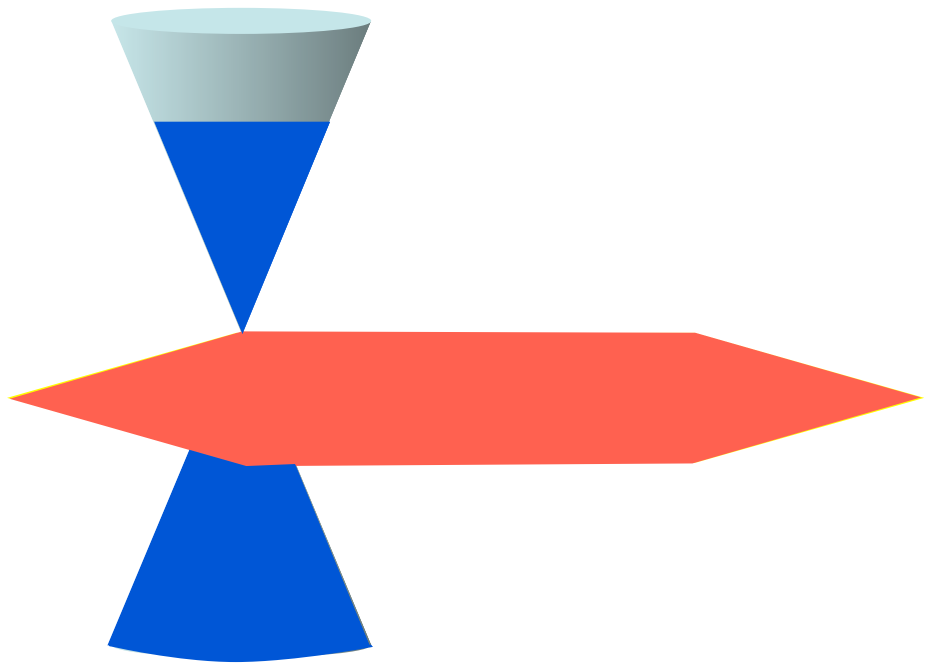

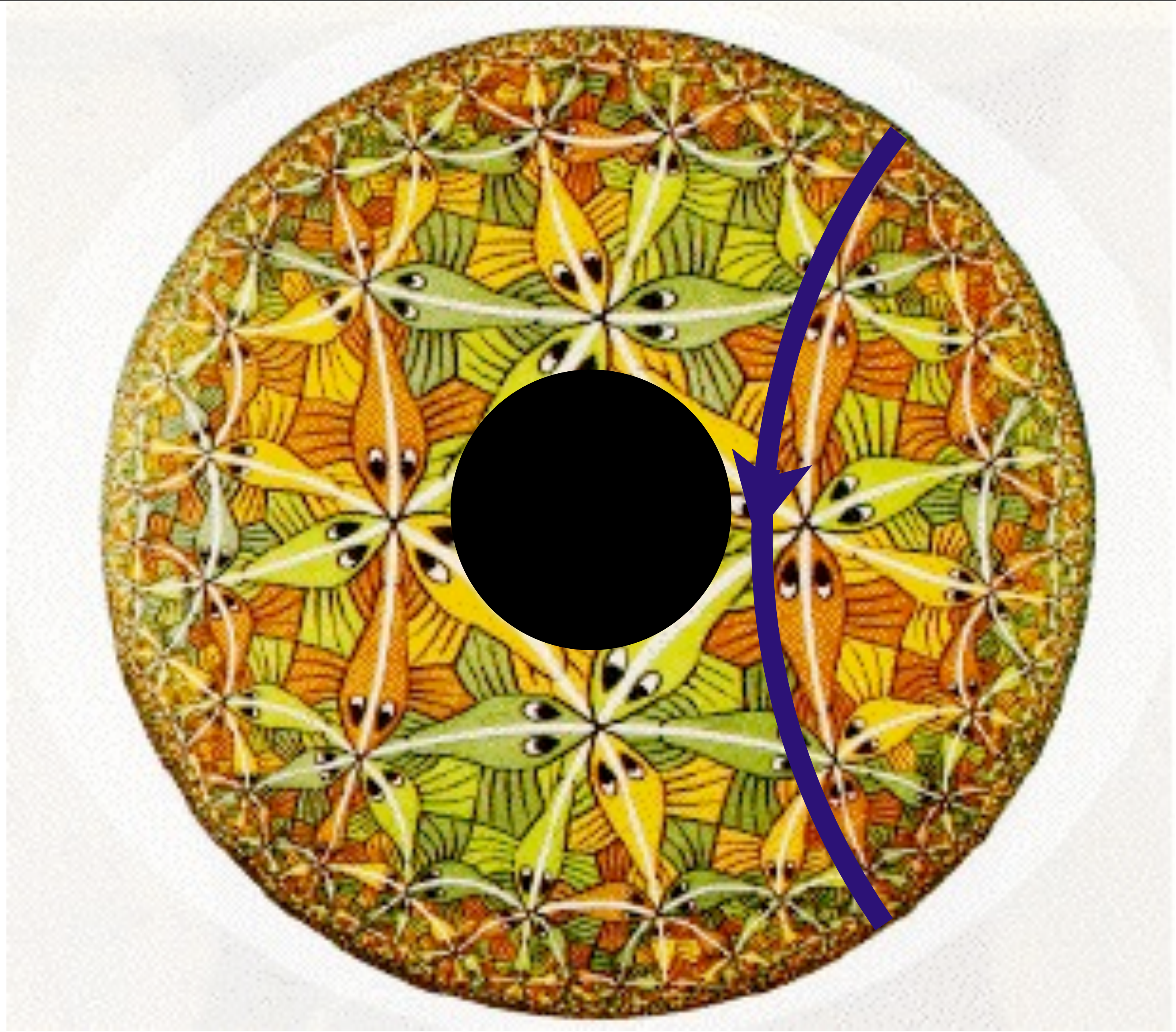

Examine free energy and Green's function
of a probe particle

T. Faulkner, H. Liu, J. McGreevy, and D. Vegh, arXiv:0907.2694
F. Denef, S. Hartnoll, and S. Sachdev, to appear

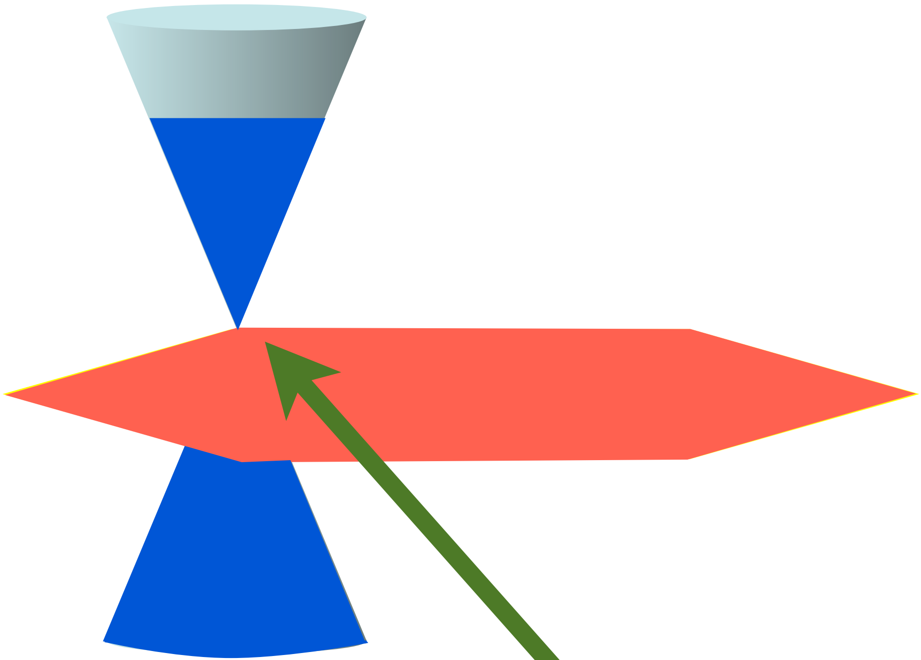

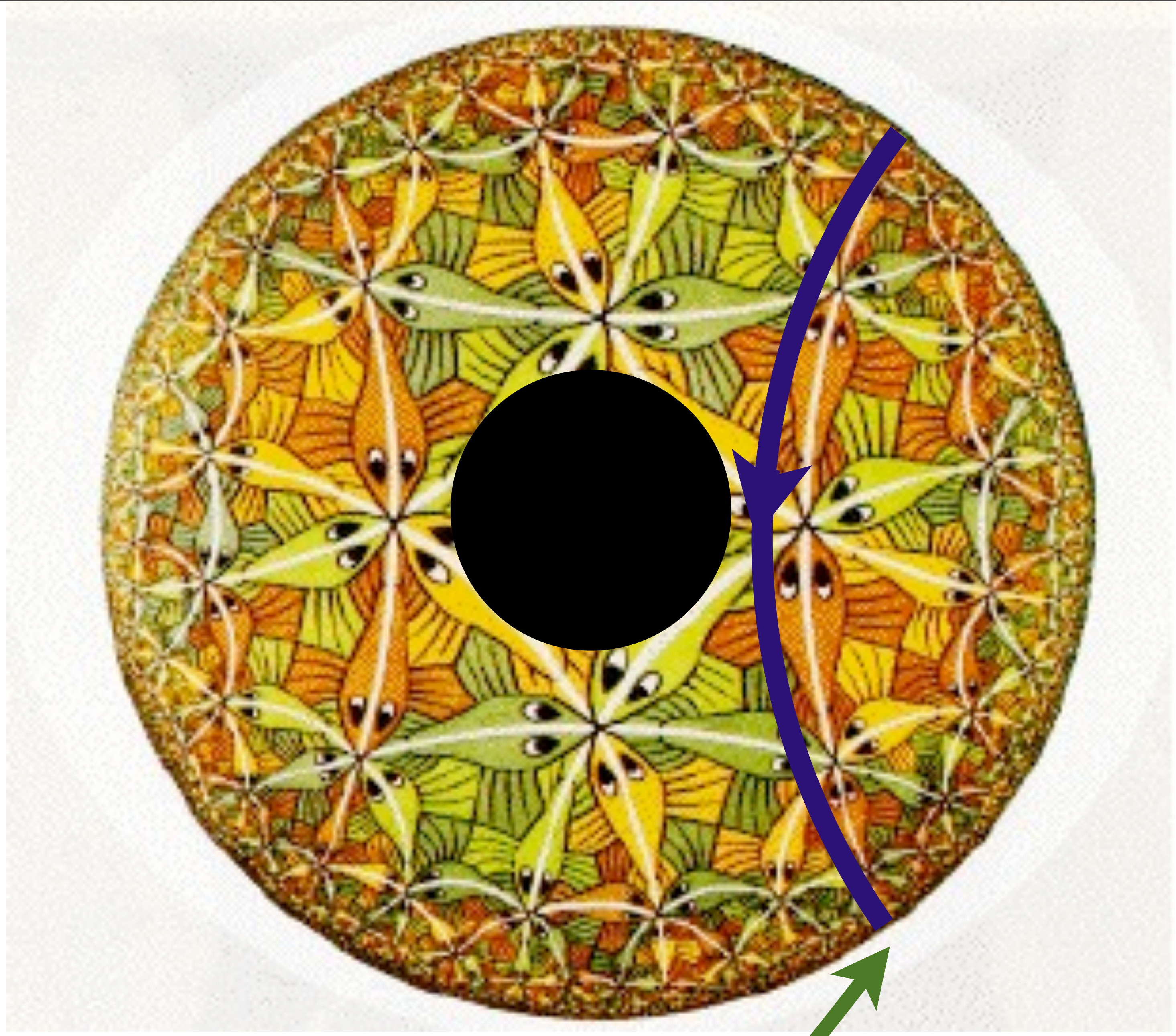

Short time behavior depends upon conformal AdS_4 geometry near boundary

T. Faulkner, H. Liu, J. McGreevy, and D. Vegh, arXiv:0907.2694
F. Denef, S. Hartnoll, and S. Sachdev, to appear

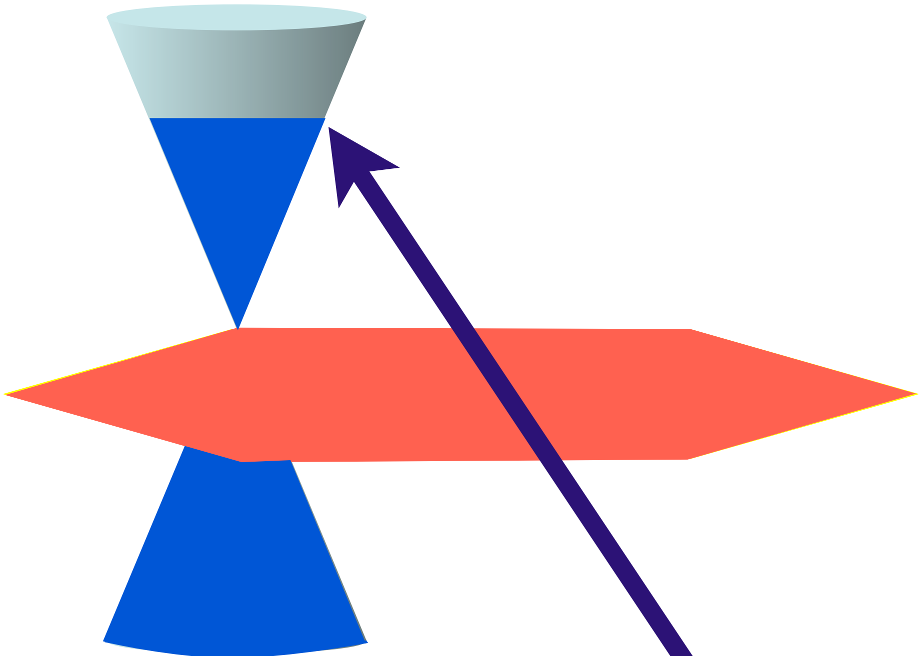

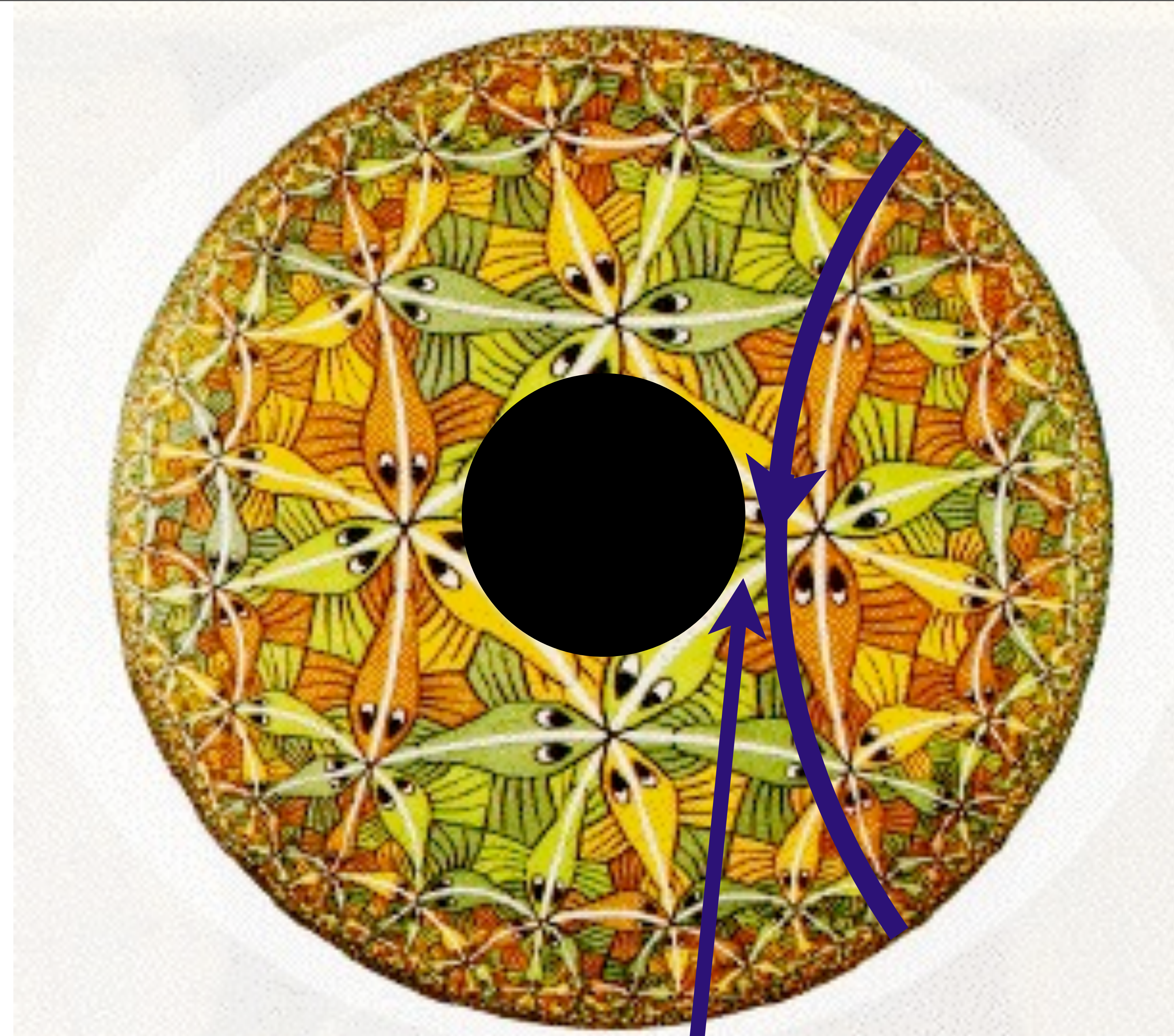

Long time behavior depends upon near-horizon geometry of black hole

T. Faulkner, H. Liu, J. McGreevy, and D. Vegh, arXiv:0907.2694
F. Denef, S. Hartnoll, and S. Sachdev, to appear

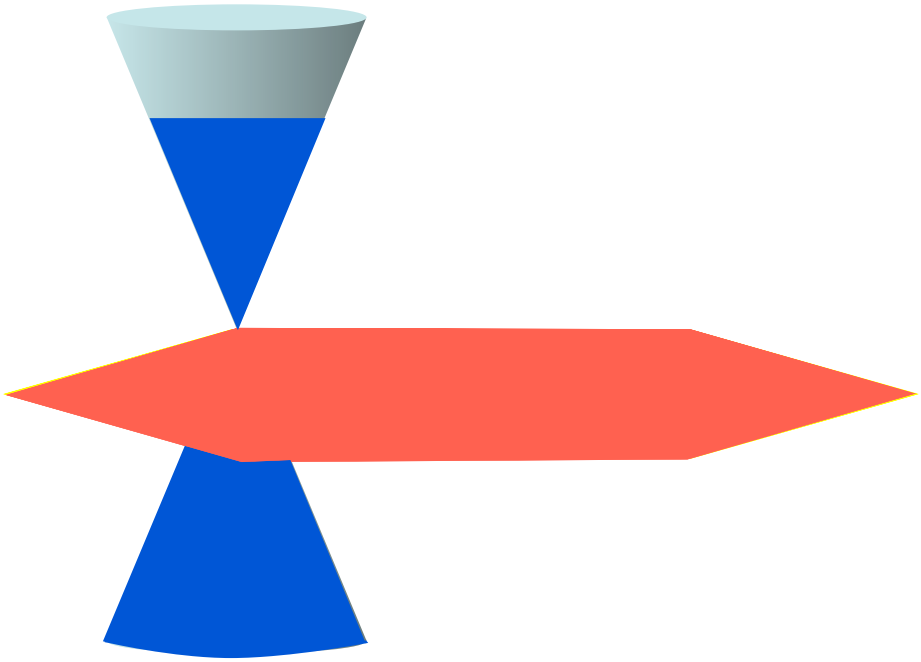

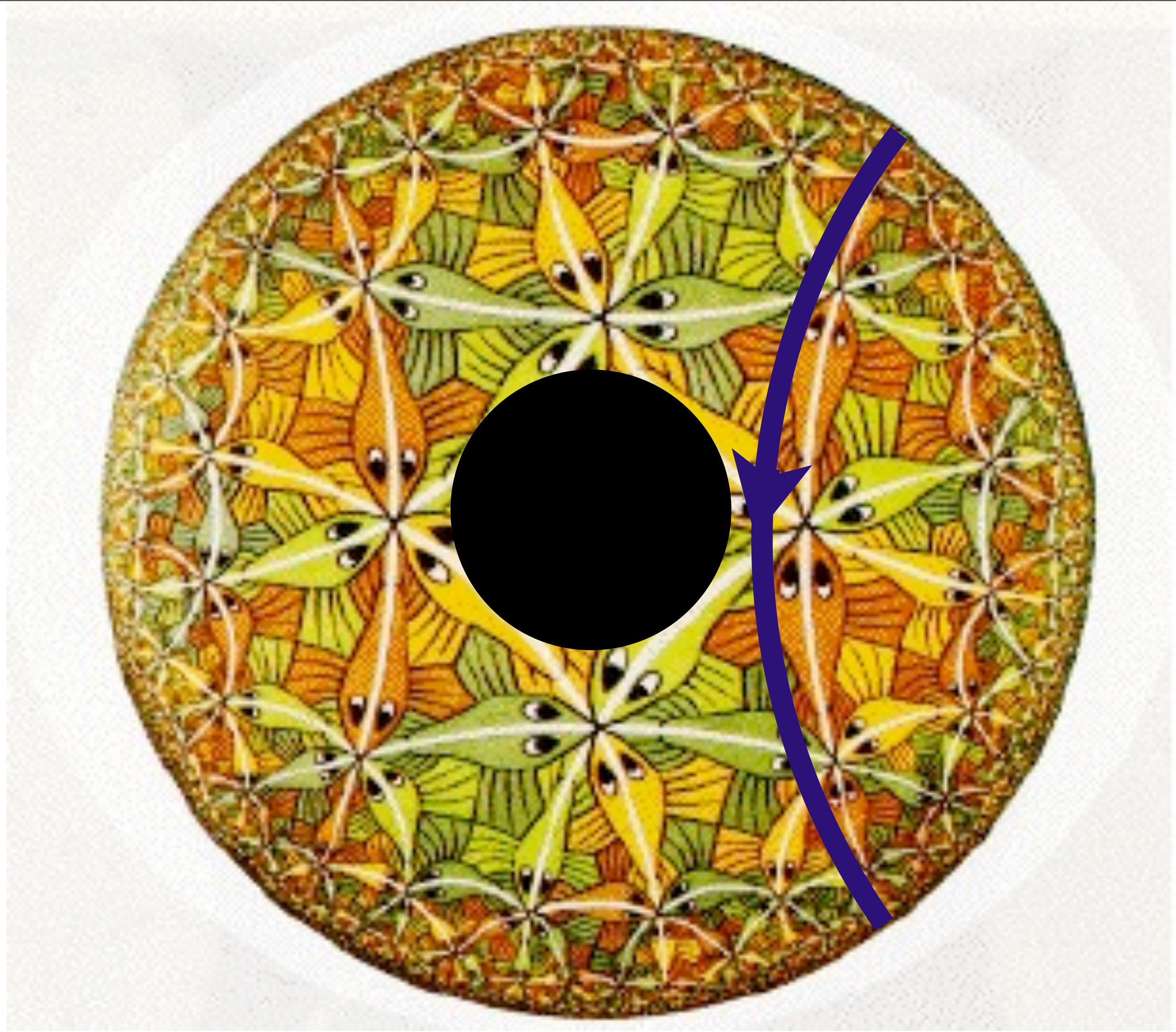

Radial direction of gravity theory is measure of energy scale in CFT

T. Faulkner, H. Liu, J. McGreevy, and D. Vegh, arXiv:0907.2694
F. Denef, S. Hartnoll, and S. Sachdev, to appear

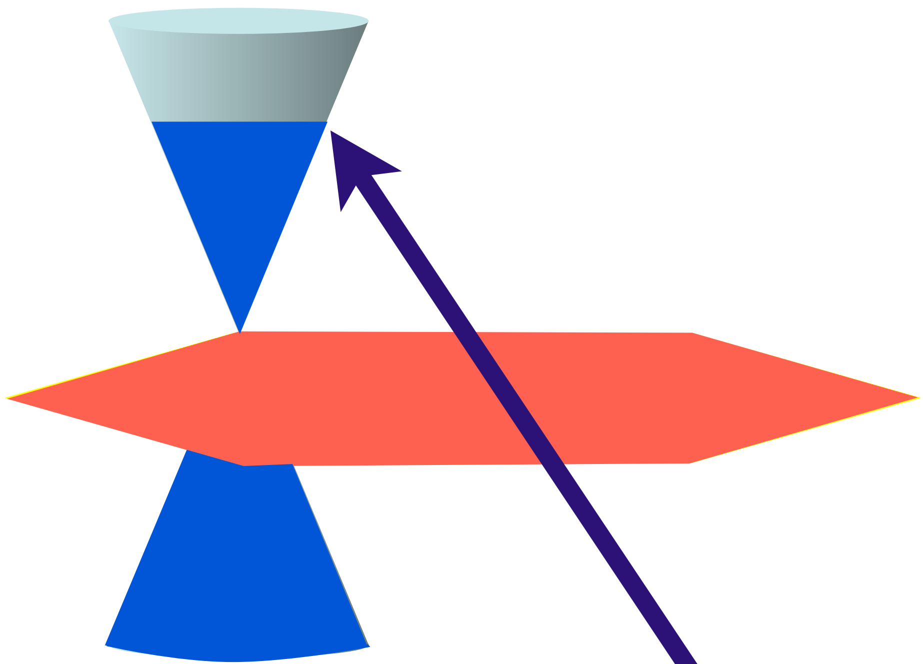

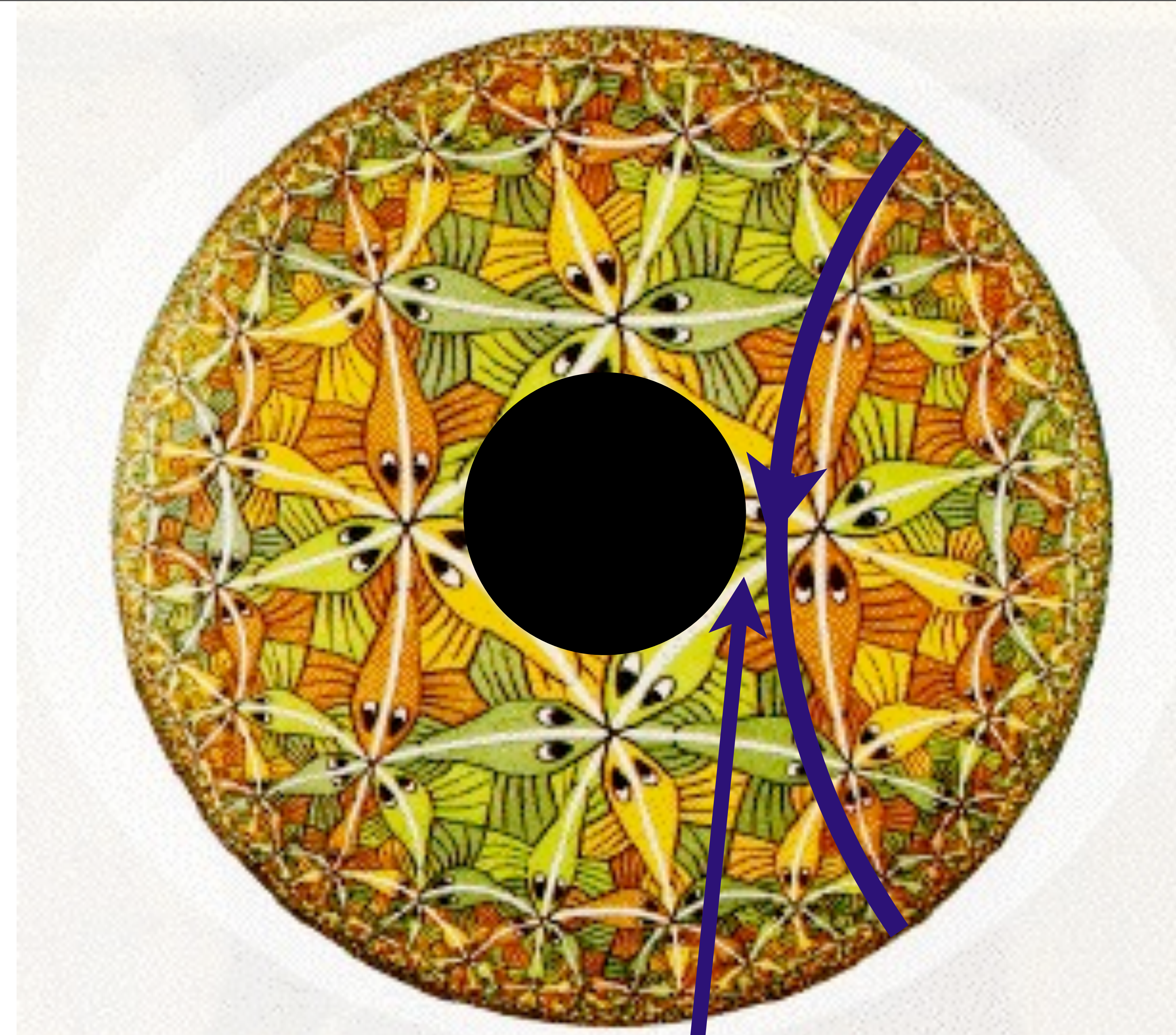

Infrared physics of Fermi surface is linked to the near horizon AdS_2 geometry of Reissner-Nordstrom black hole

T. Faulkner, H. Liu, J. McGreevy, and D. Vegh, arXiv:0907.2694

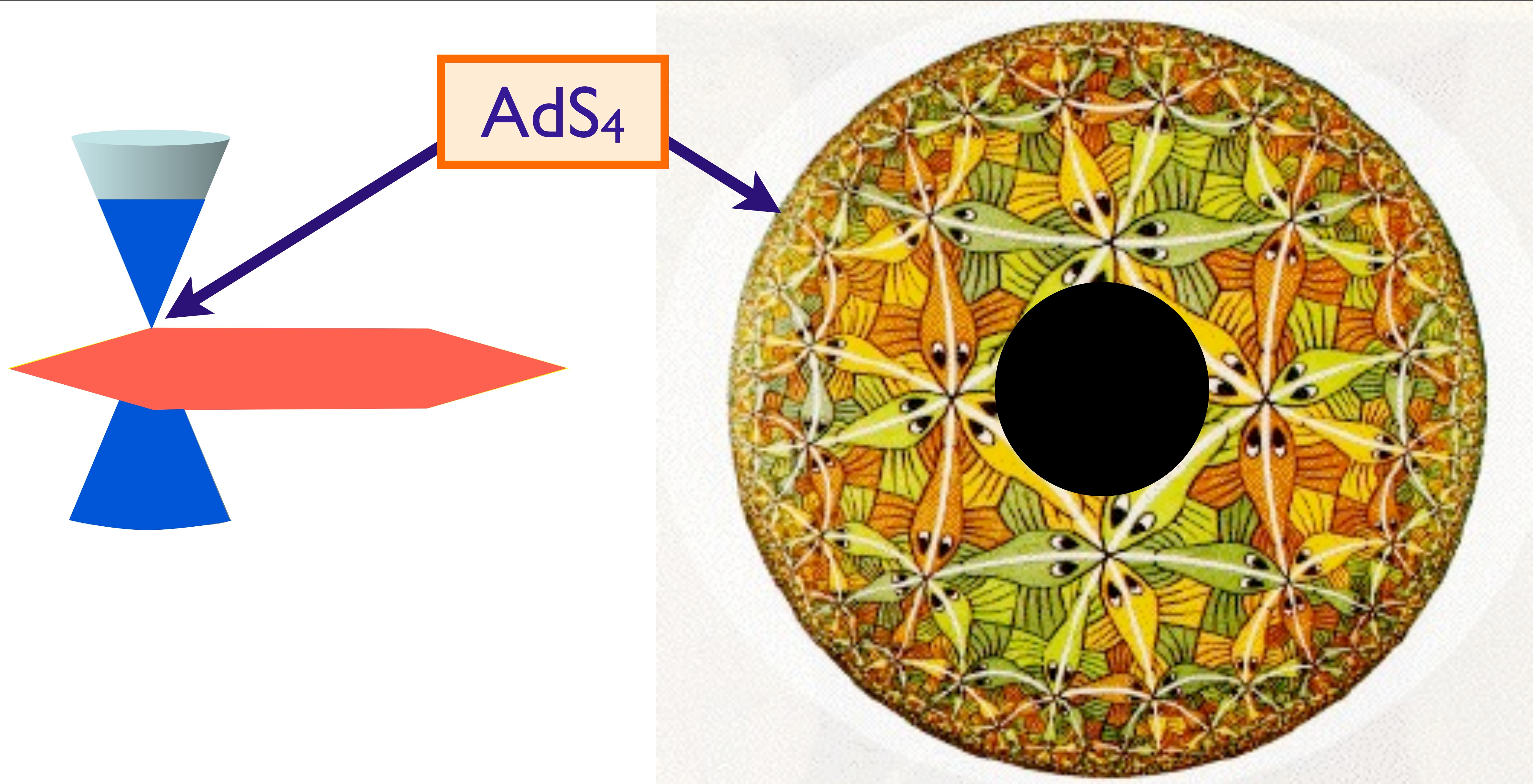

Geometric interpretation of RG flow

T. Faulkner, H. Liu, J. McGreevy, and D. Vegh, arXiv:0907.2694

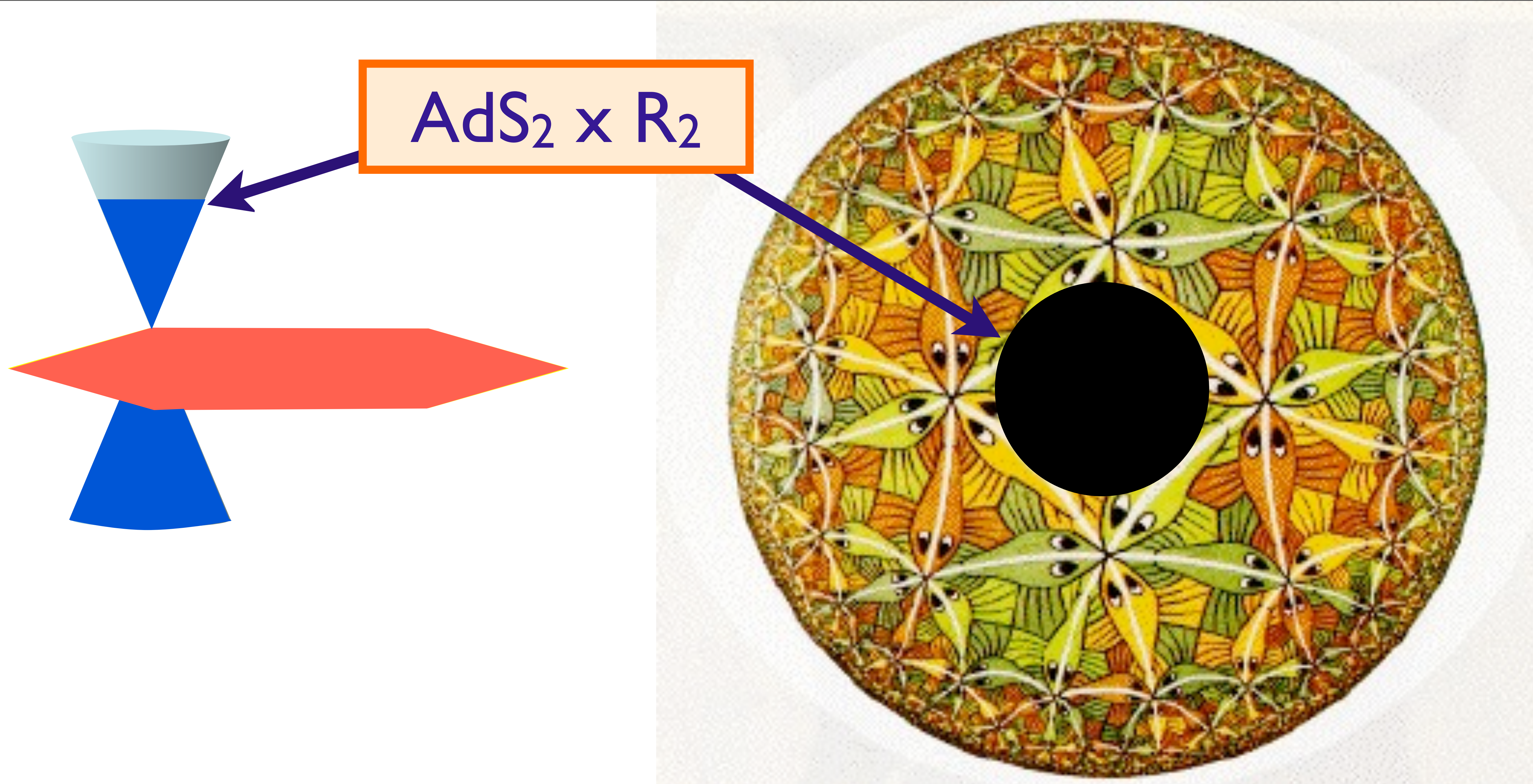

Geometric interpretation of RG flow

T. Faulkner, H. Liu, J. McGreevy, and D. Vegh, arXiv:0907.2694

Magnetohydrodynamics of quantum criticality

We used the AdS/CFT connection to derive many new relations between thermoelectric transport co-efficients in the quantum critical regime.

S.A. Hartnoll, P.K. Kovtun, M. Müller, and S. Sachdev, *Phys. Rev.* B **76** 144502 (2007)

Magnetohydrodynamics of quantum criticality

We used the AdS/CFT connection to derive many new relations between thermoelectric transport co-efficients in the quantum critical regime.

The **same** results were later obtained from the equations of generalized relativistic magnetohydrodynamics.

So the results apply to experiments on graphene, *and* to the dynamics of black holes.

S.A. Hartnoll, P.K. Kovtun, M. Müller, and S. Sachdev, *Phys. Rev.* B **76** 144502 (2007)

Magnetohydrodynamics of quantum criticality

We used the AdS/CFT connection to derive many new relations between thermoelectric transport co-efficients in the quantum critical regime.

As a simple example, in zero magnetic field, we can write the electrical conductivity as

$$\sigma = \sigma_Q + \frac{e^{*2}\rho^2 v^2}{\varepsilon + P}\pi\delta(\omega)$$

where σ_Q is the universal conductivity of the CFT, ρ is the charge density, ε is the energy density and P is the pressure.

The same quantities also determine the thermal conductivity, κ:

$$\kappa = \sigma_Q \left(\frac{k_B^2 T}{e^{*2}}\right)\left(\frac{\varepsilon + P}{k_B T \rho}\right)^2$$

Magnetohydrodynamics of quantum criticality

We used the AdS/CFT connection to derive many new relations between thermoelectric transport co-efficients in the quantum critical regime.

A second example: In an applied magnetic field B, the dynamic transport co-efficients exhibit a **hydrodynamic cyclotron resonance** at a frequency ω_c

$$\omega_c = \frac{e^* B \rho v^2}{c(\varepsilon + P)}$$

and damping constant γ

$$\gamma = \sigma_Q \frac{B^2 v^2}{c^2(\varepsilon + P)}.$$

The same constants determine the **quasinormal frequency** of the Reissner-Nordstrom black hole.

Green's function of a fermion

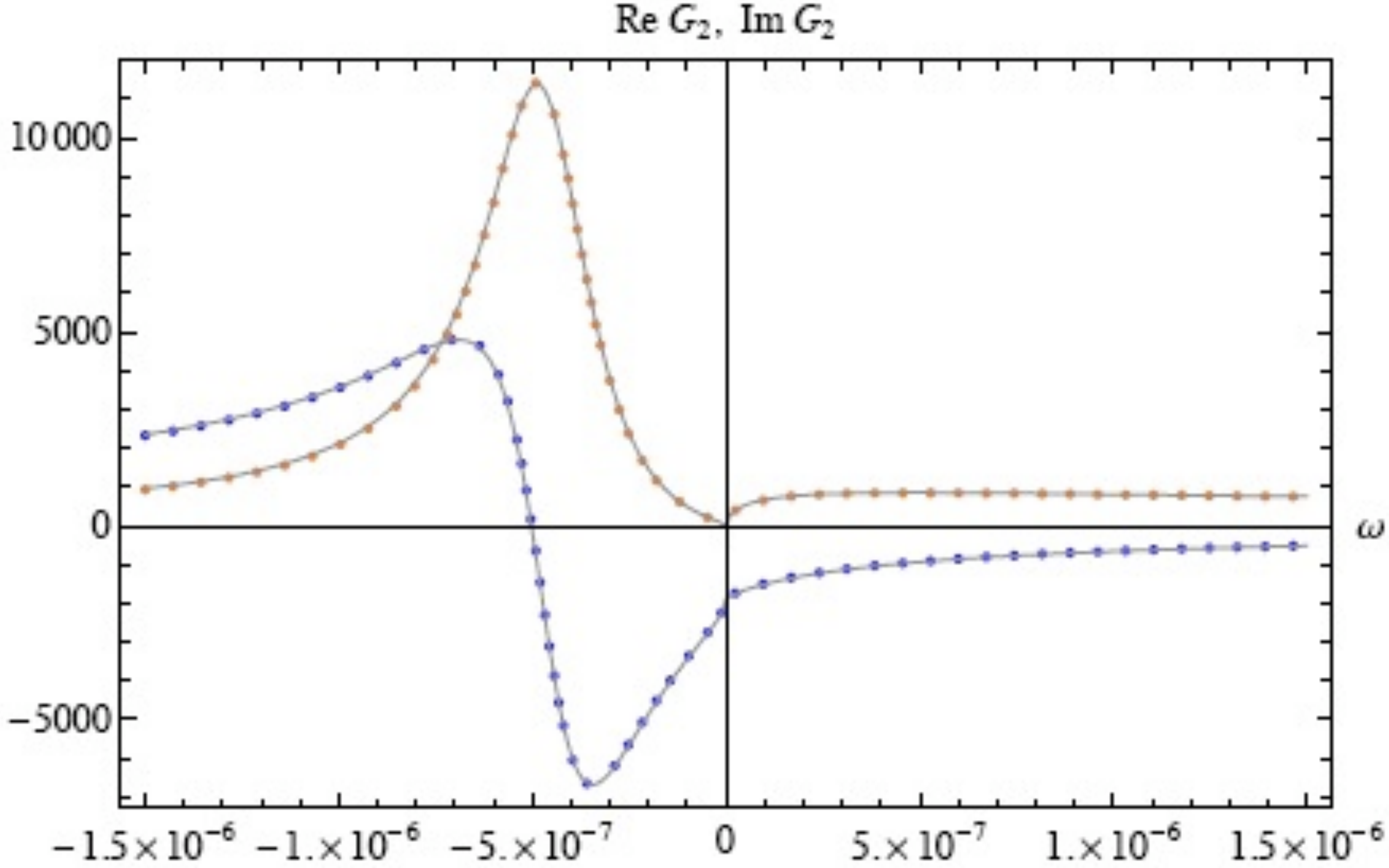

T. Faulkner, H. Liu, J. McGreevy, and D. Vegh, arXiv:0907.2694

$$G(k,\omega) \approx \frac{1}{\omega - v_F(k-k_F) - i\omega^{\theta(k)}}$$

Green's function of a fermion

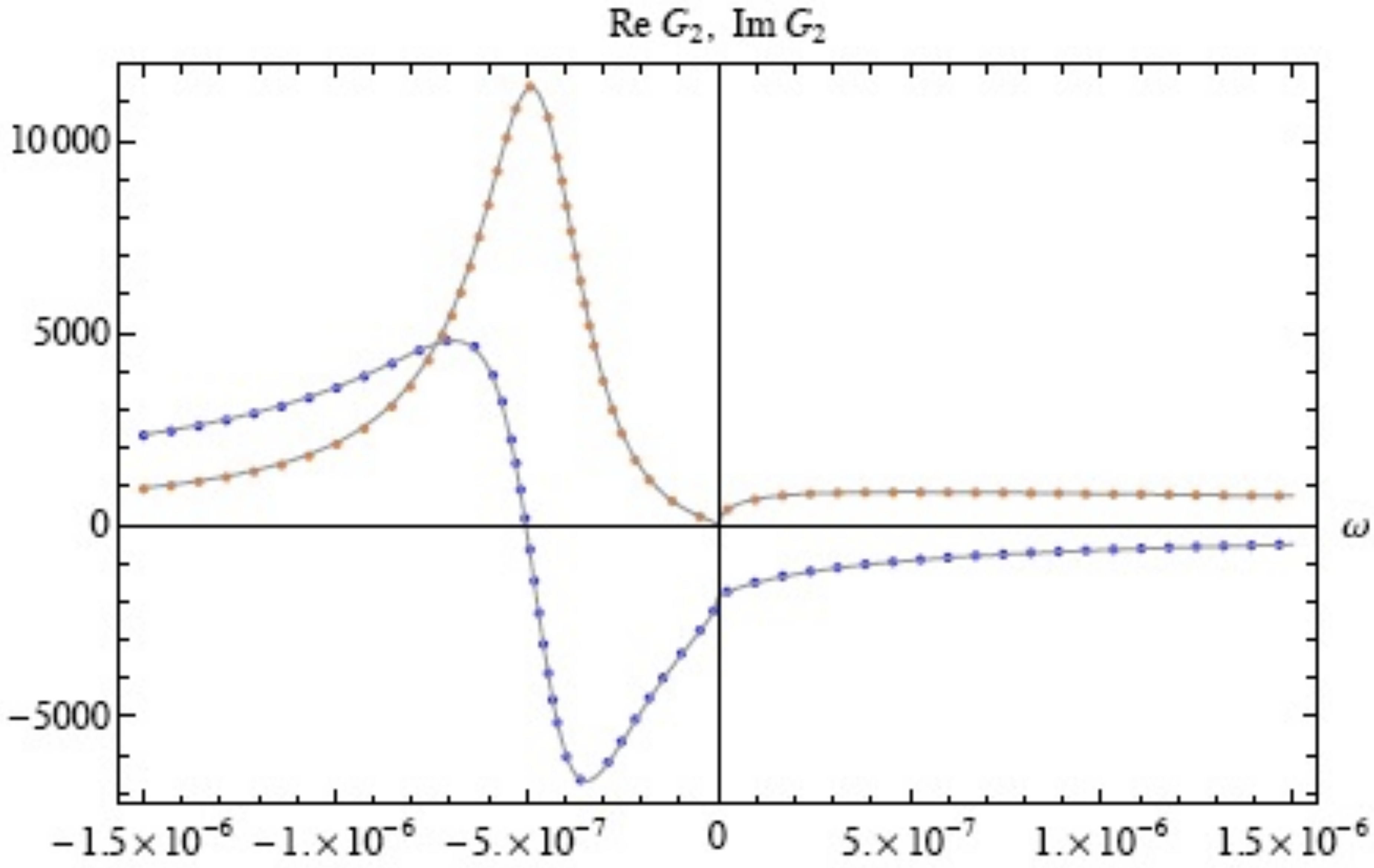

T. Faulkner, H. Liu, J. McGreevy, and D. Vegh, arXiv:0907.2694

$$G(k,\omega) \approx \frac{1}{\omega - v_F(k-k_F) - i\omega^{\theta(k)}}$$

Similar to non-Fermi liquid theories of Fermi surfaces coupled to gauge fields, and at quantum critical points

Free energy from gravity theory

The free energy is expressed as a sum over the "quasinormal frequencies", z_ℓ, of the black hole. Here ℓ represents any set of quantum numbers:

$$\mathcal{F}_{\text{boson}} = -T \sum_{\ell} \ln \left(\frac{|z_\ell|}{2\pi T} \left| \Gamma \left(\frac{i z_\ell}{2\pi T} \right) \right|^2 \right)$$

$$\mathcal{F}_{\text{fermion}} = T \sum_{\ell} \ln \left(\left| \Gamma \left(\frac{i z_\ell}{2\pi T} + \frac{1}{2} \right) \right|^2 \right)$$

Application of this formula shows that the fermions exhibit the dHvA quantum oscillations with expected period ($2\pi/$(Fermi surface ares)) in $1/B$, but with an amplitude corrected from the Fermi liquid formula of Lifshitz-Kosevich.

F. Denef, S. Hartnoll, and S. Sachdev, arXiv:0908.1788

Outline

1. Coupled dimer antiferromagnets

    Order parameters and Landau-Ginzburg criticality

2. Graphene

    `Topological' Fermi surface transitions

3. Quantum criticality and black holes

    AdS_4 theory of compressible quantum liquids

4. Quantum criticality in the cuprates

    Global phase diagram and the spin density wave transition in metals

Outline

1. Coupled dimer antiferromagnets
   Order parameters and Landau-Ginzburg criticality

2. Graphene
   `Topological' Fermi surface transitions

3. Quantum criticality and black holes
   AdS_4 theory of compressible quantum liquids

4. Quantum criticality in the cuprates
   Global phase diagram and the spin density wave transition in metals

Central ingredients in cuprate phase diagram: antiferromagnetism, superconductivity, and topological change in Fermi surface

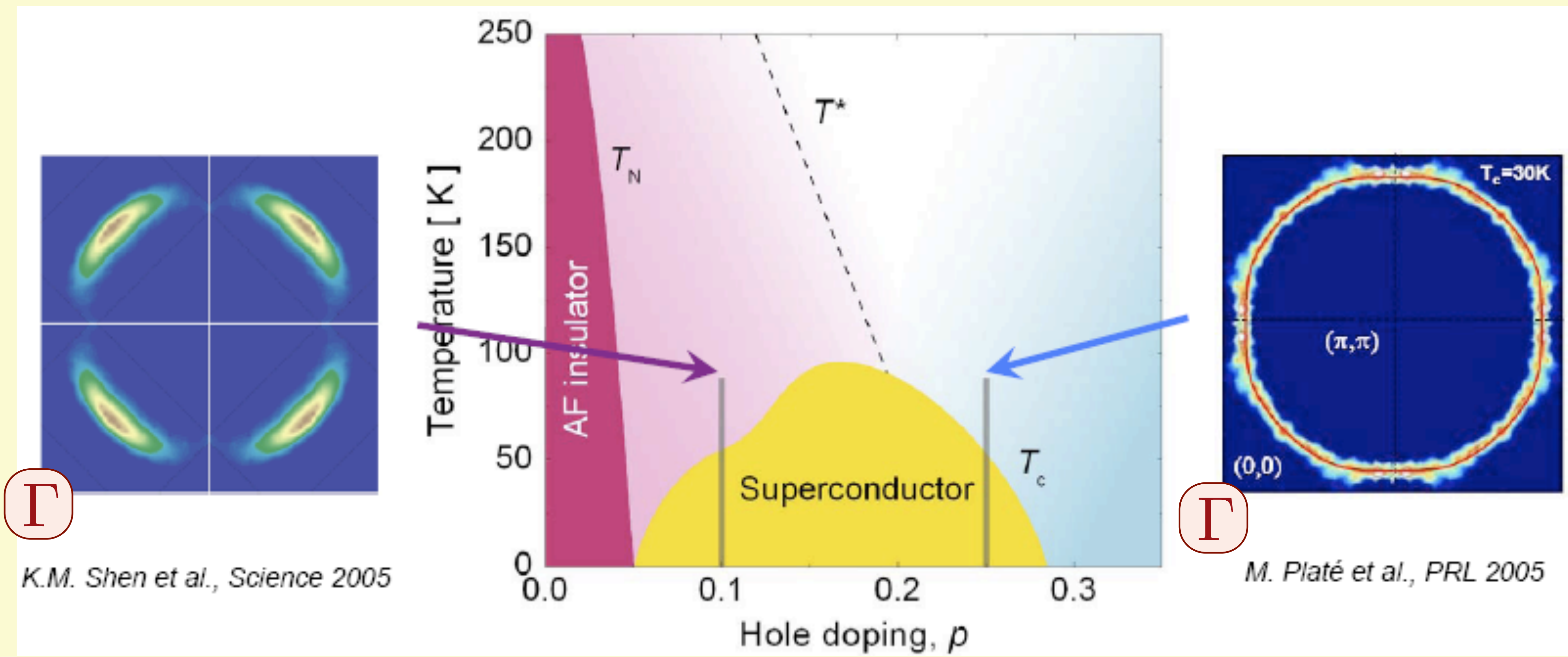

Smaller hole Fermi-pockets

Large hole Fermi surface

Crossovers in transport properties of hole-doped cuprates

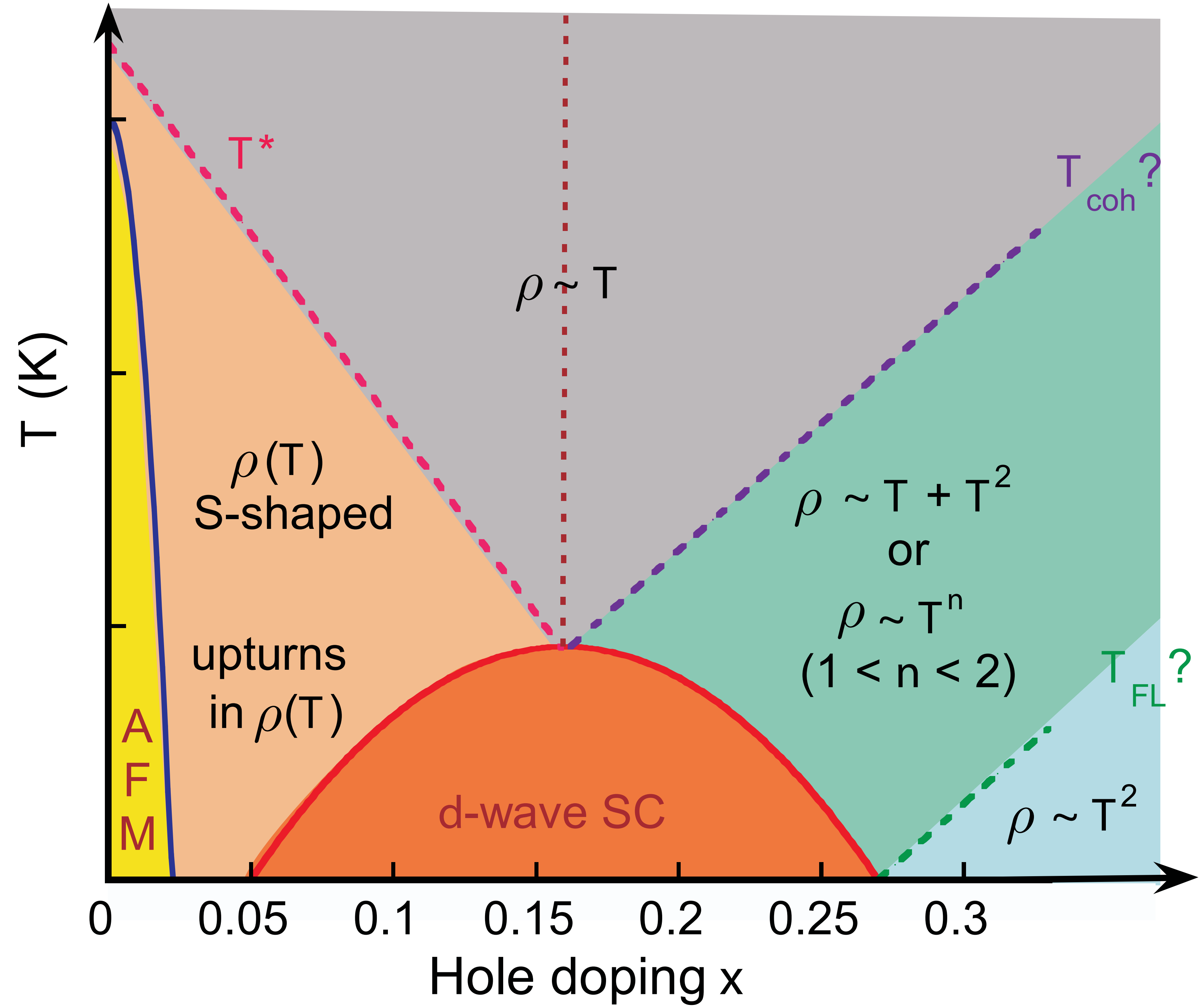

N. E. Hussey, *J. Phys: Condens. Matter* **20**, 123201 (2008)

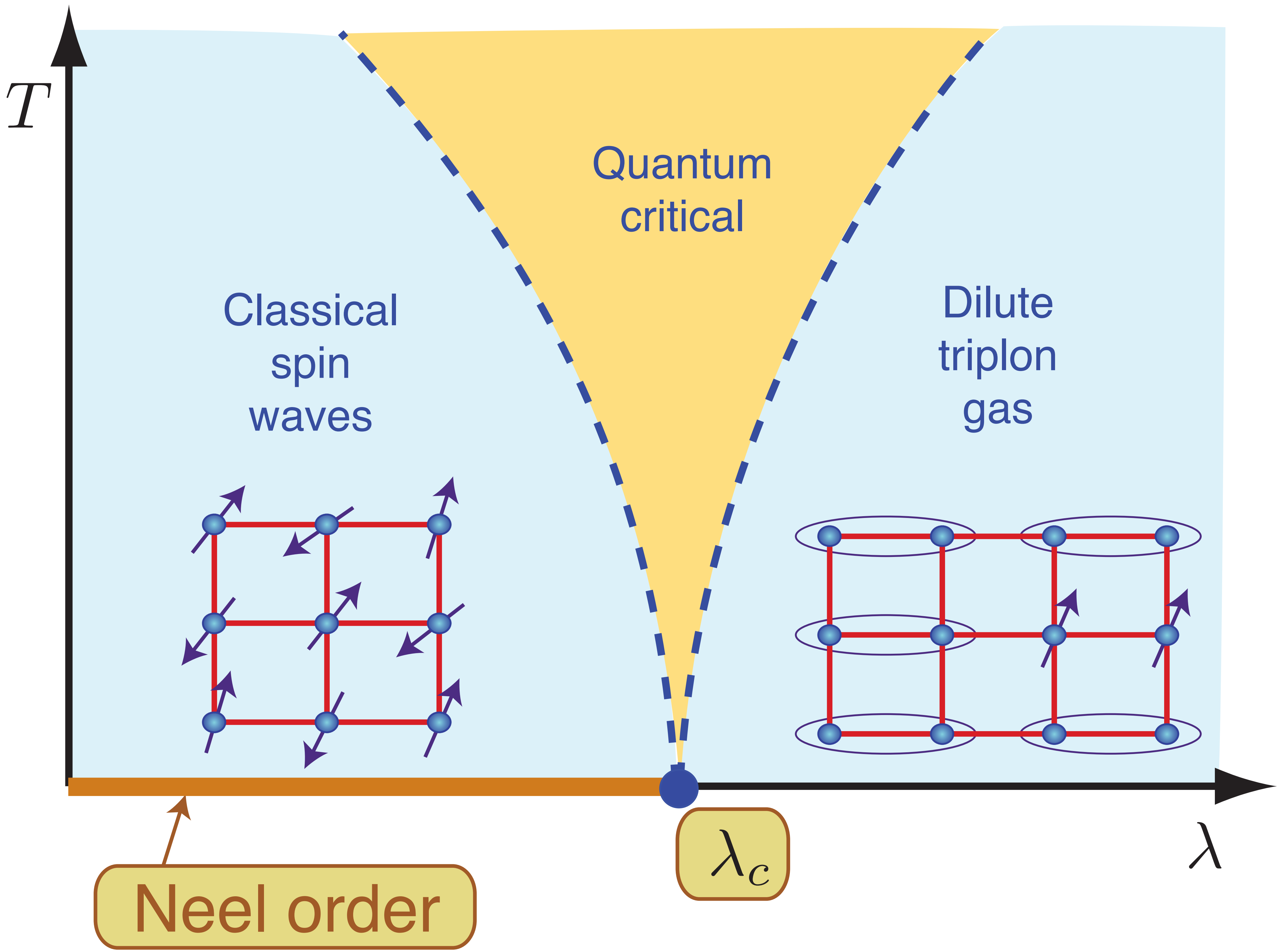

T
Quantum critical
Classical spin waves
Dilute triplon gas
λ
λ_c
Neel order

Crossovers in transport properties of hole-doped cuprates

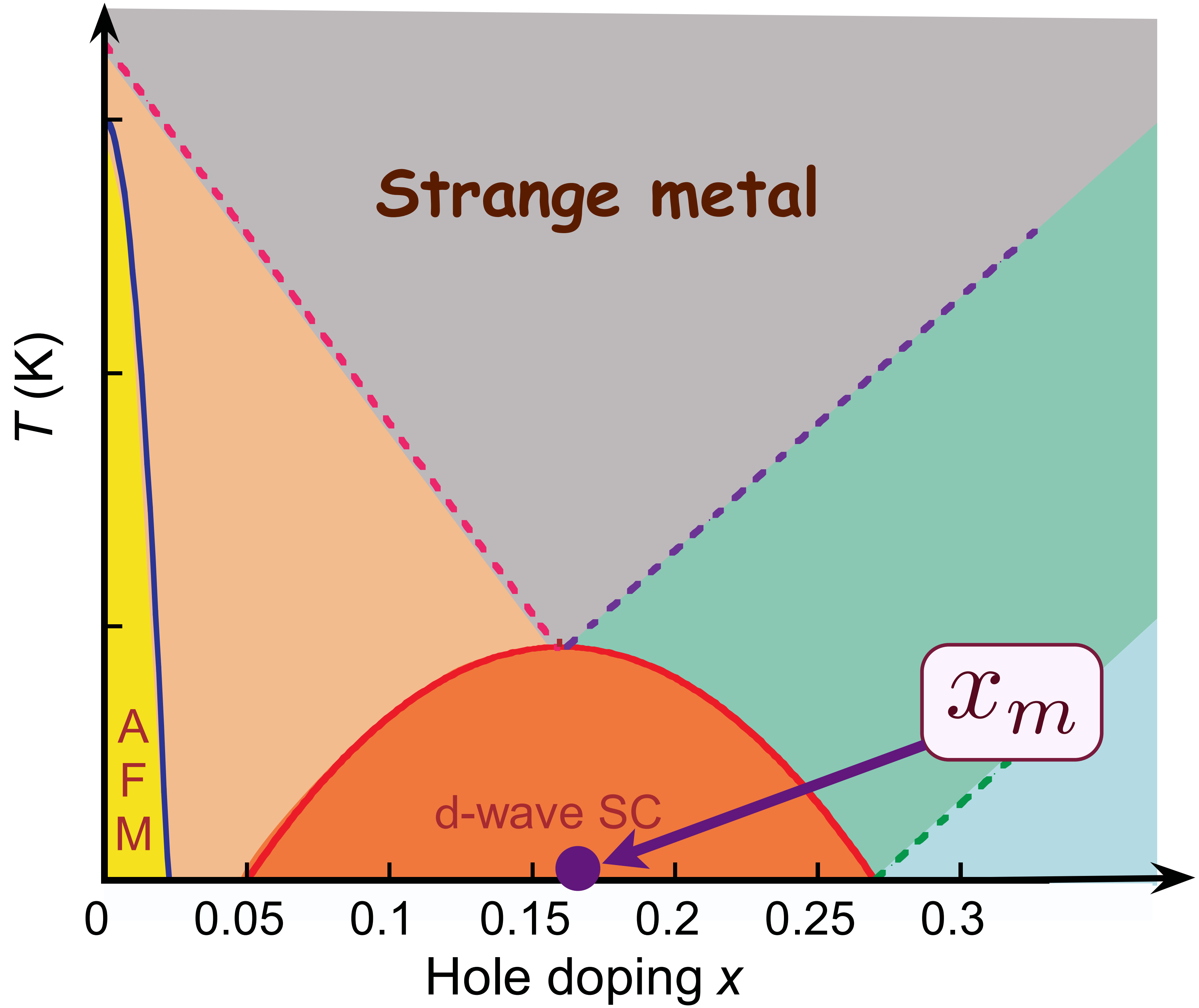

Strange metal: quantum criticality of optimal doping critical point at $x = x_m$?

Only candidate quantum critical point observed at low T

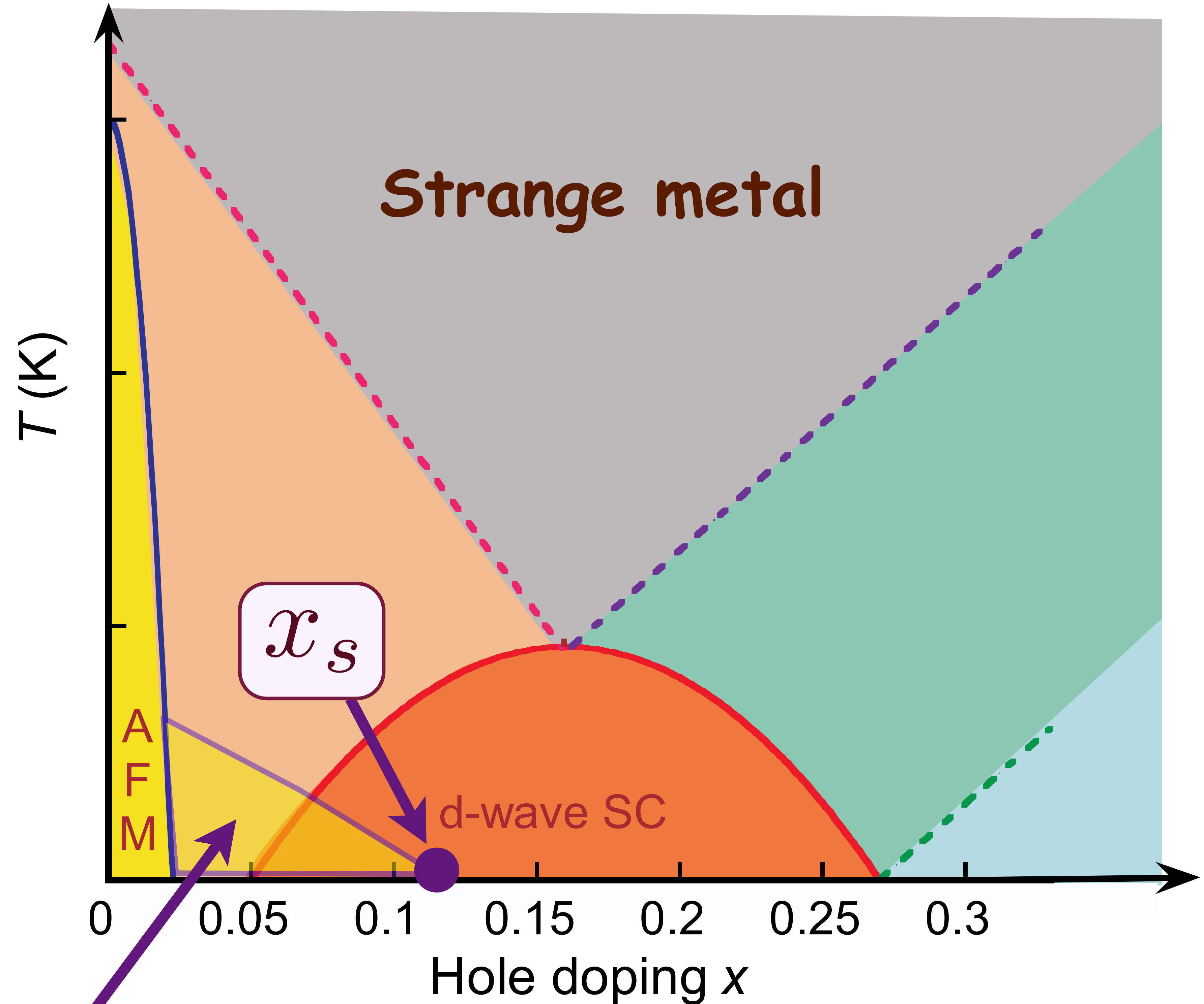

Spin density wave order present below a quantum critical point at $x = x_s$ with $x_s \approx 0.12$ in the La series of cuprates

Central ingredients in cuprate phase diagram: antiferromagnetism, superconductivity, and topological change in Fermi surface

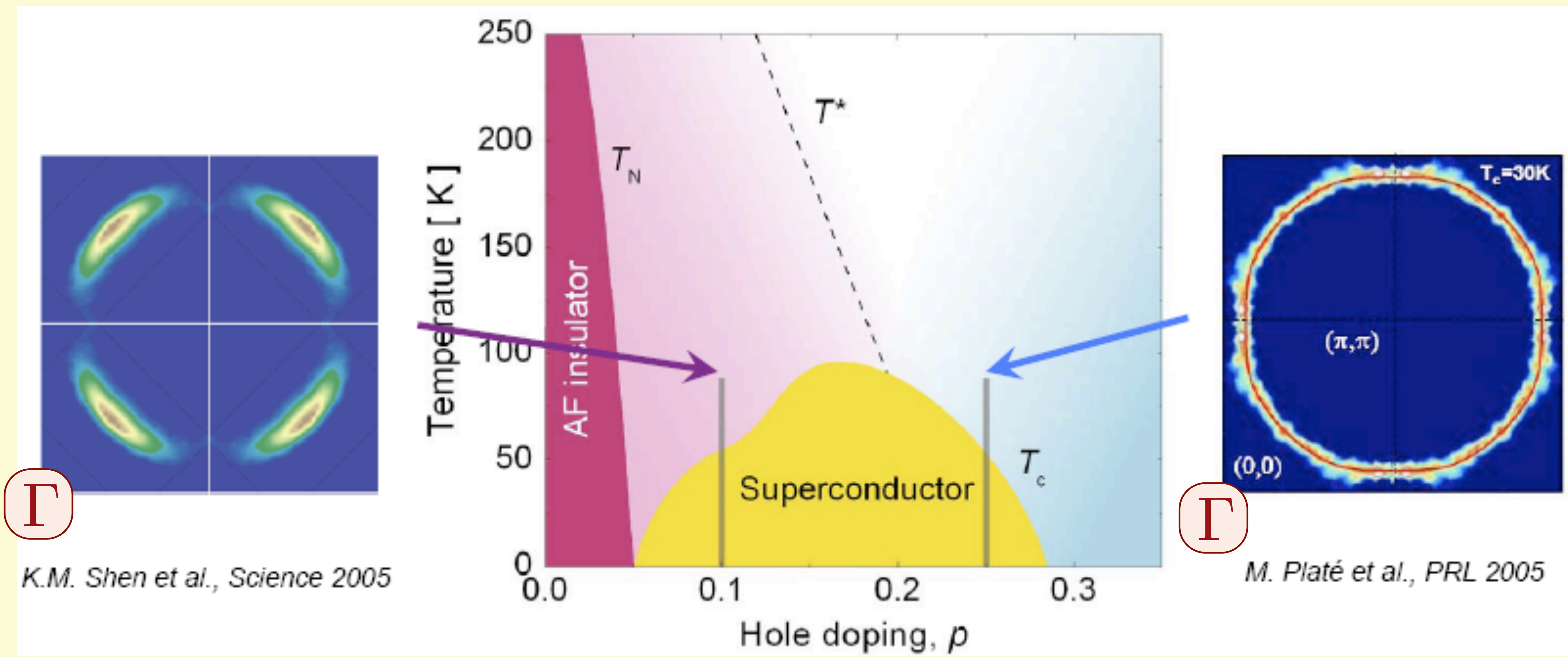

Smaller hole Fermi-pockets

Large hole Fermi surface

"Large" Fermi surfaces in cuprates

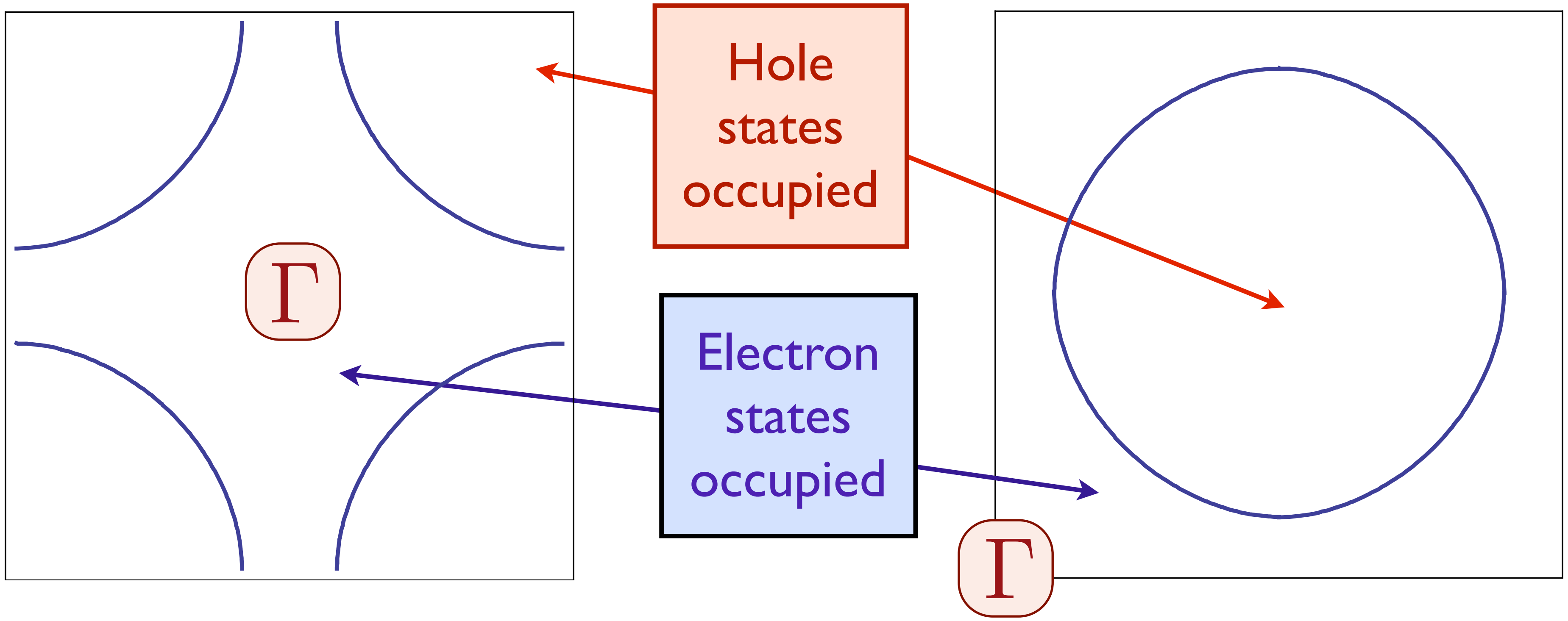

$$H_0 = -\sum_{i<j} t_{ij} c^{\dagger}_{i\alpha} c_{i\alpha} \equiv \sum_{\mathbf{k}} \varepsilon_{\mathbf{k}} c^{\dagger}_{\mathbf{k}\alpha} c_{\mathbf{k}\alpha}$$

The area of the occupied electron/hole states:

$$\mathcal{A}_e = \begin{cases} 2\pi^2(1-x) & \text{for hole-doping } x \\ 2\pi^2(1+p) & \text{for electron-doping } p \end{cases}$$

$$\mathcal{A}_h = 4\pi^2 - \mathcal{A}_e$$

Spin density wave theory

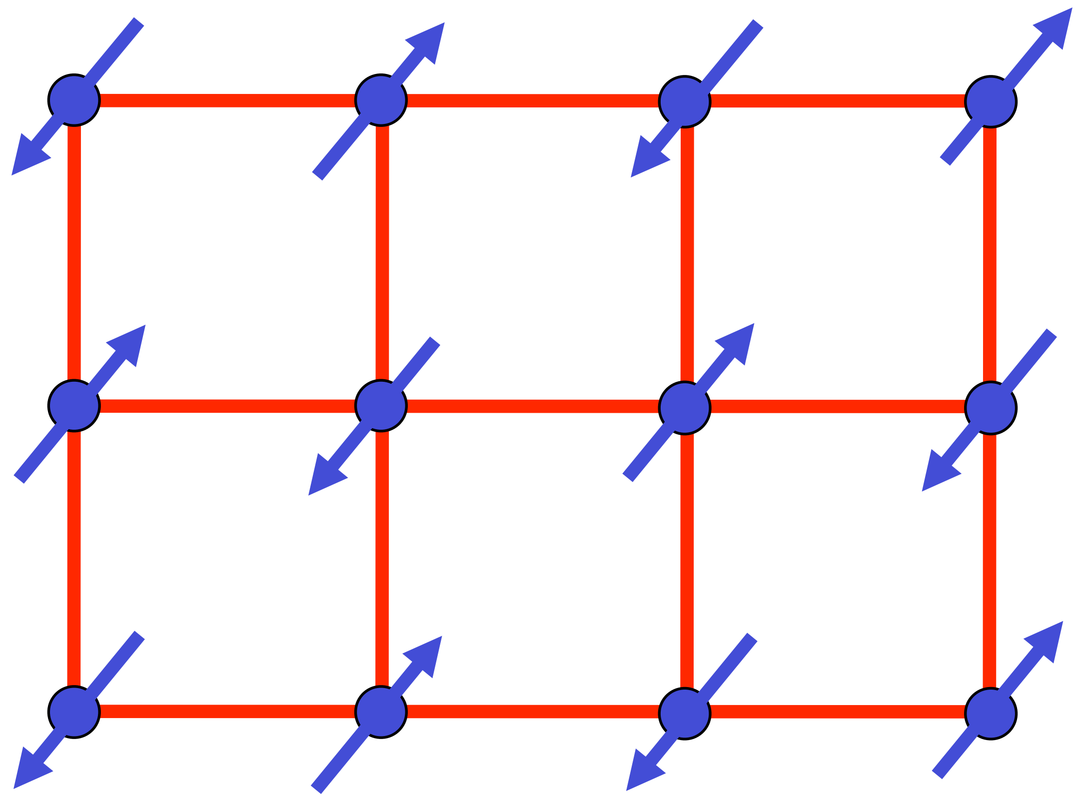

The electron spin polarization obeys

$$\left\langle \vec{S}(\mathbf{r},\tau) \right\rangle = \vec{\varphi}(\mathbf{r},\tau) e^{i\mathbf{K}\cdot\mathbf{r}}$$

where $\vec{\varphi}$ is the spin density wave (SDW) order parameter, and $\mathbf{K}$ is the ordering wavevector. For simplicity, we consider $\mathbf{K} = (\pi, \pi)$.

Spin density wave theory

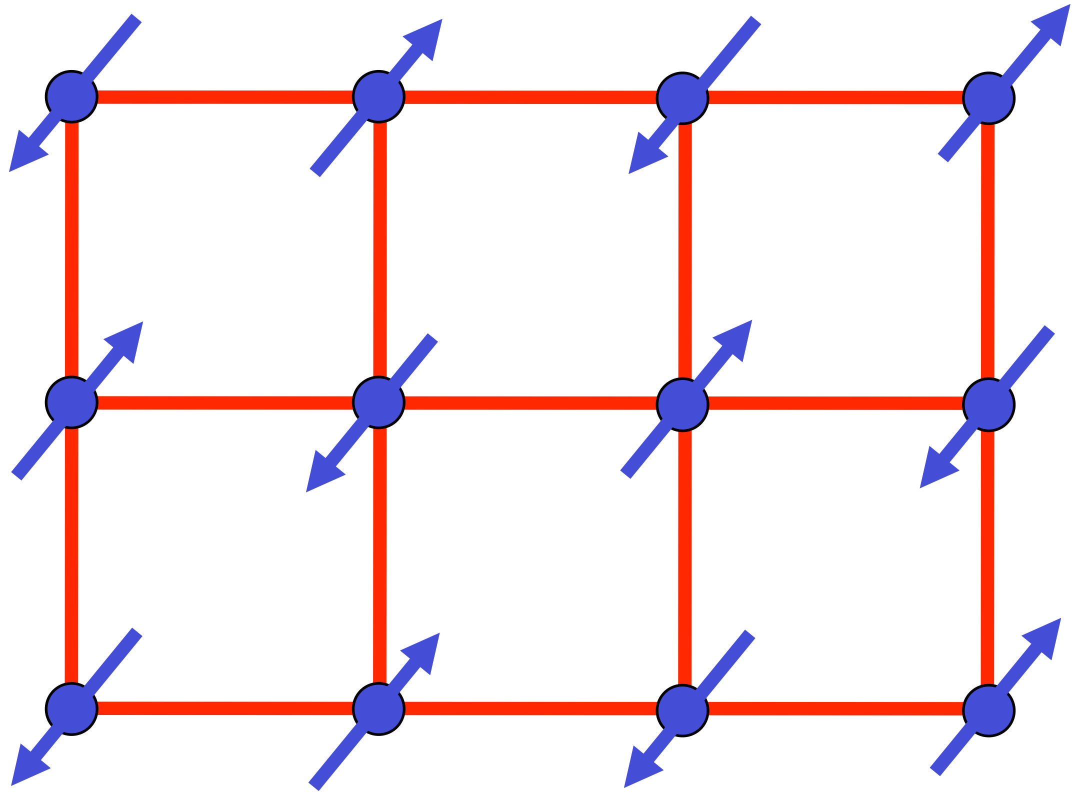

Spin density wave Hamiltonian

$$H_{\rm sdw} = \vec{\varphi} \cdot \sum_{\mathbf{k},\alpha,\beta} c^\dagger_{\mathbf{k},\alpha} \vec{\sigma}_{\alpha\beta} c_{\mathbf{k}+\mathbf{K},\beta}$$

Diagonalize $H_0 + H_{\rm sdw}$ for $\vec{\varphi} = (0, 0, \varphi)$

$$E_{\mathbf{k}\pm} = \frac{\varepsilon_{\mathbf{k}} + \varepsilon_{\mathbf{k}+\mathbf{K}}}{2} \pm \sqrt{\left(\frac{\varepsilon_{\mathbf{k}} - \varepsilon_{\mathbf{k}+\mathbf{K}}}{2}\right) + \varphi^2}$$

Spin density wave theory

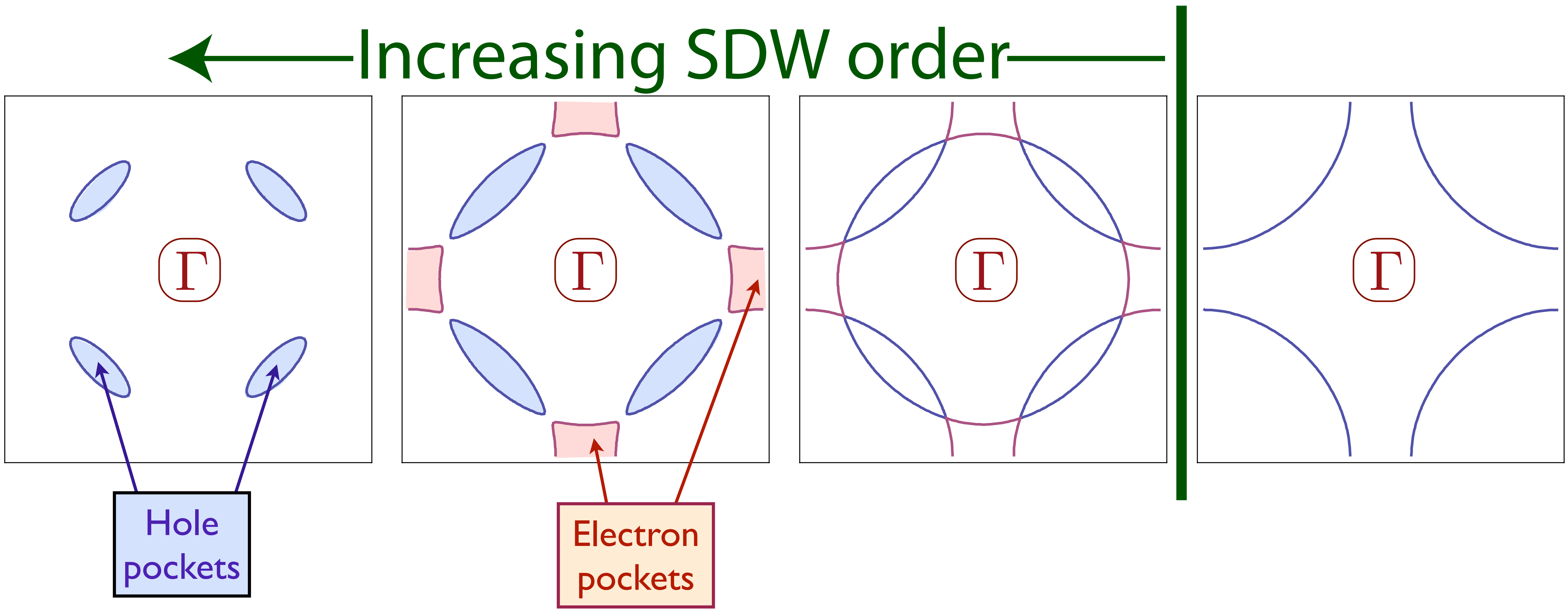

Large Fermi surface breaks up into electron and hole pockets

S. Sachdev, A. V. Chubukov, and A. Sokol, *Phys. Rev. B* **51**, 14874 (1995).
A. V. Chubukov and D. K. Morr, *Physics Reports* **288**, 355 (1997).
D. Senechal and A.-M. S. Tremblay, *Phys. Rev. Lett.* **92**, 126401 (2004)

Theory of quantum criticality in the cuprates

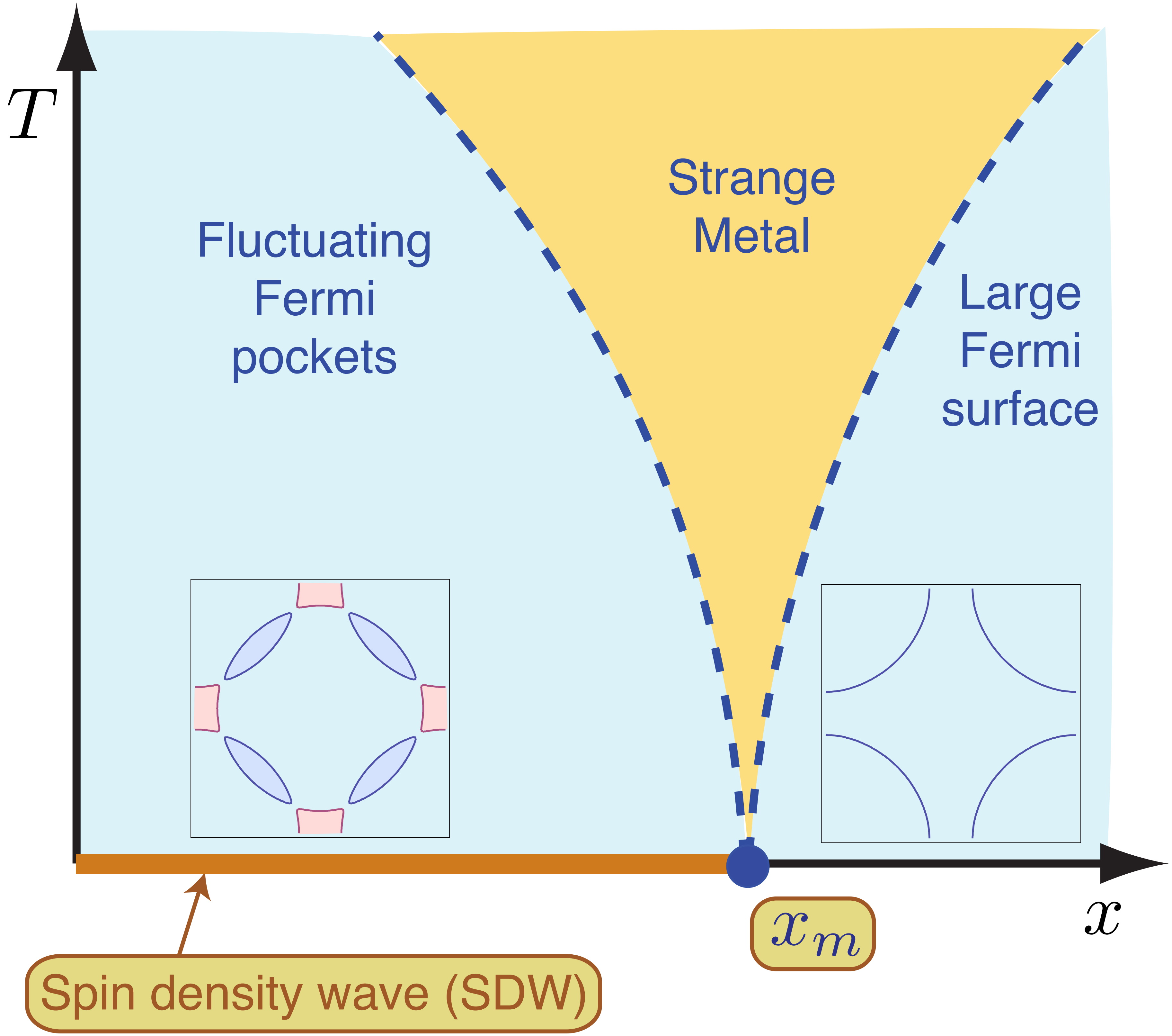

Underlying SDW ordering quantum critical point in **metal** at $x = x_m$

Theory of quantum criticality in the cuprates

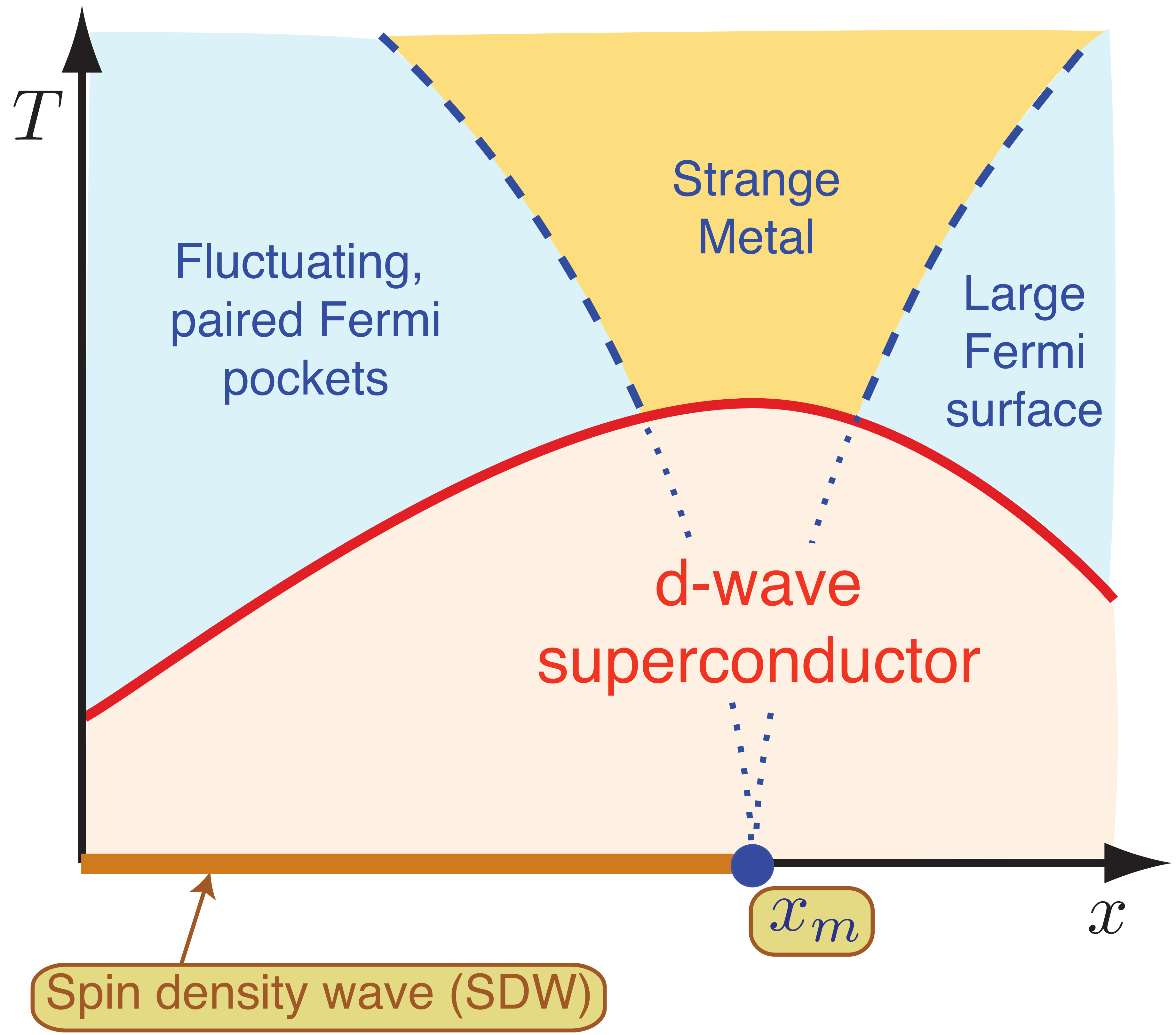

Onset of d-wave superconductivity hides the critical point $x = x_m$

Theory of quantum criticality in the cuprates

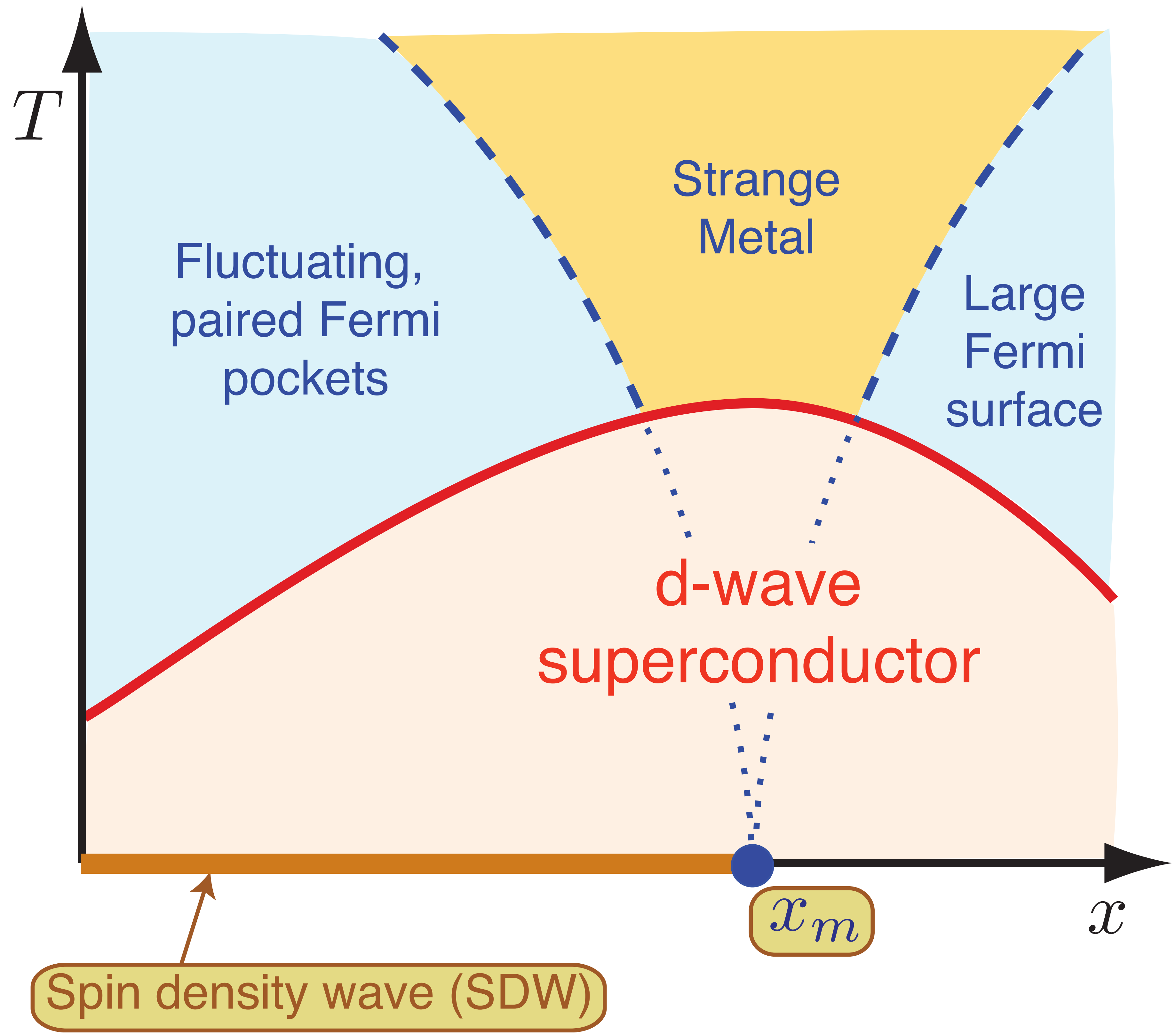

Competition between SDW order and superconductivity moves the actual quantum critical point to $x = x_s < x_m$.

Theory of quantum criticality in the cuprates

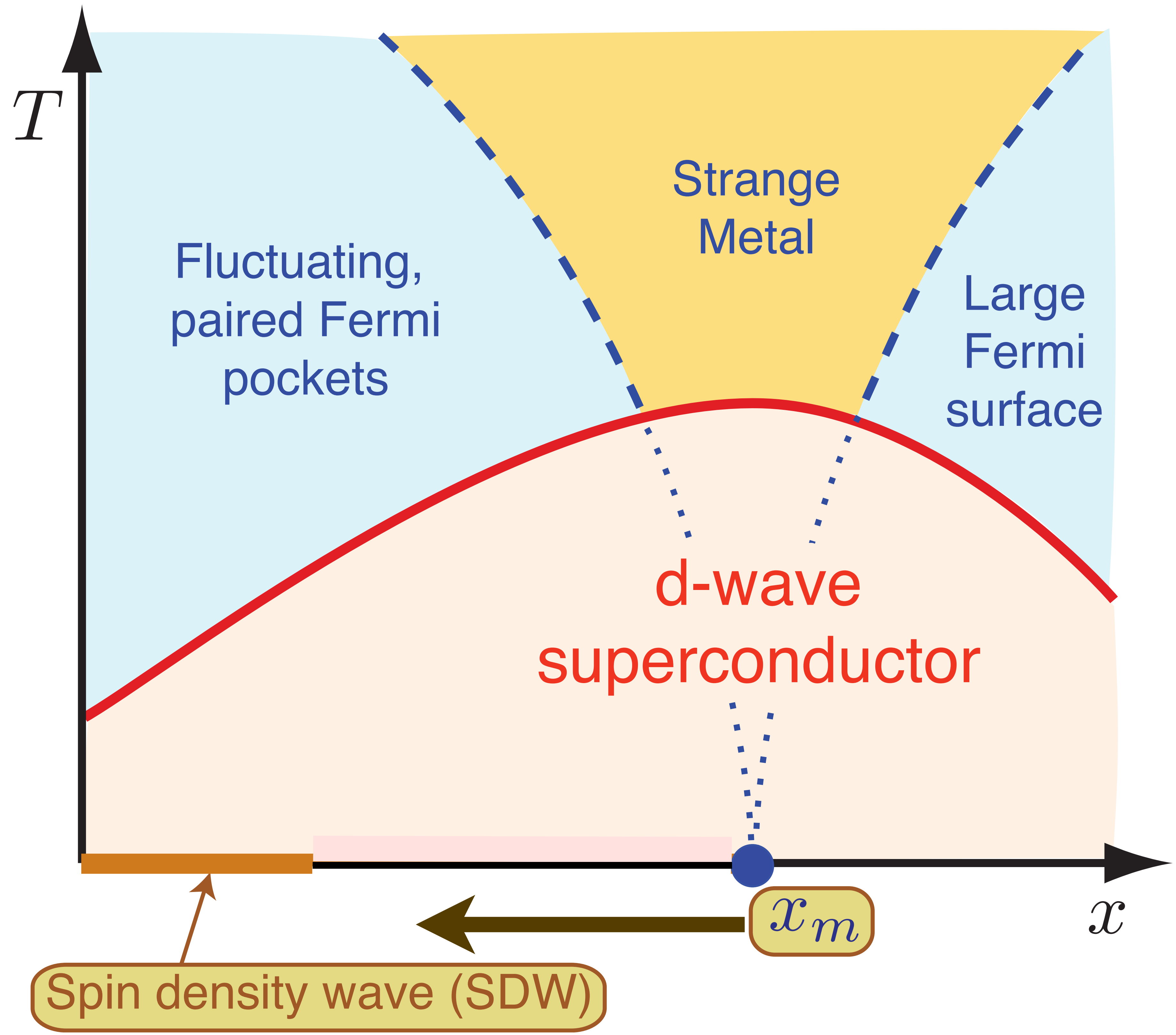

Competition between SDW order and superconductivity moves the actual quantum critical point to $x = x_s < x_m$.

Theory of quantum criticality in the cuprates

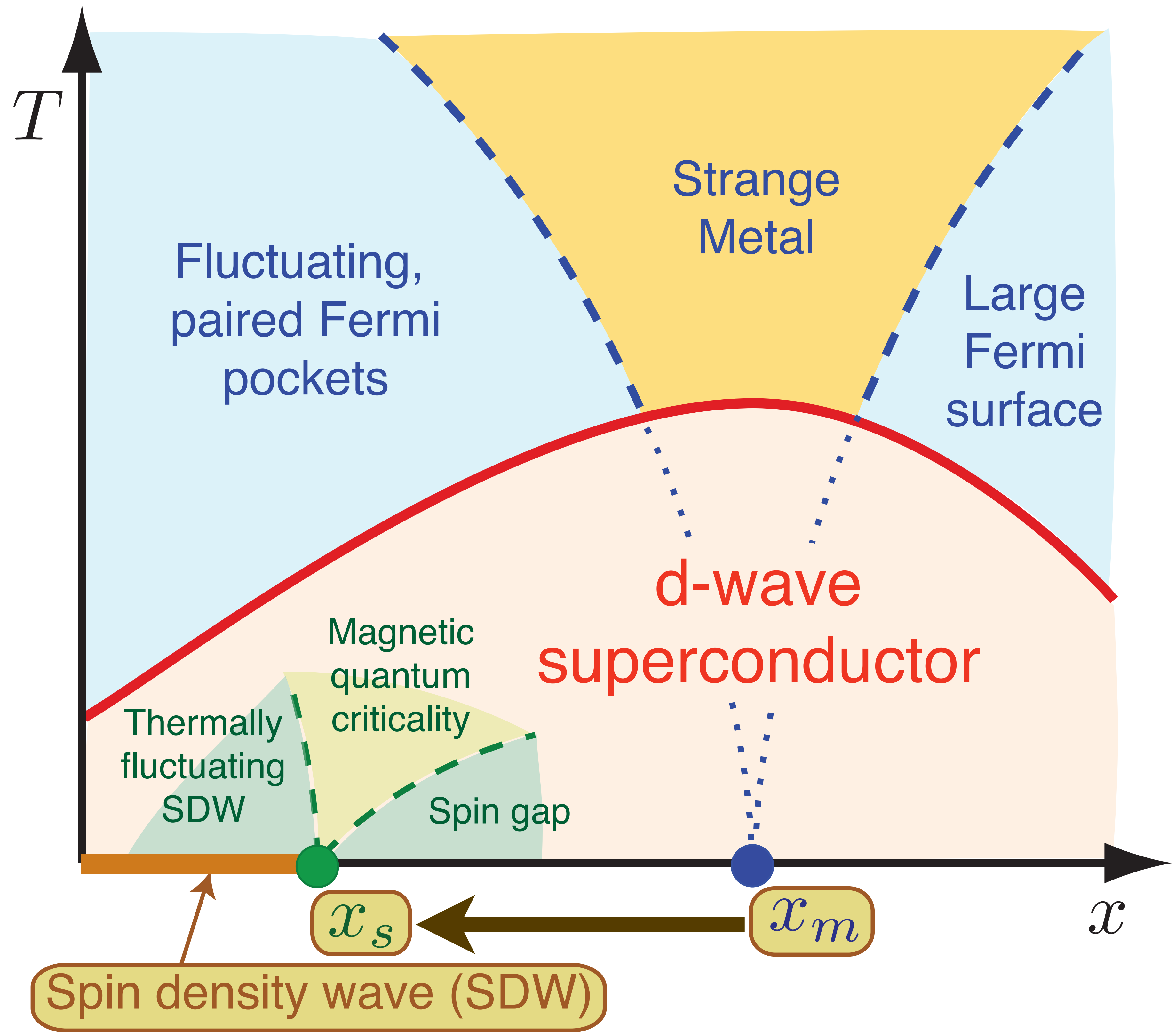

Competition between SDW order and superconductivity moves the actual quantum critical point to $x = x_s < x_m$.

Theory of quantum criticality in the cuprates

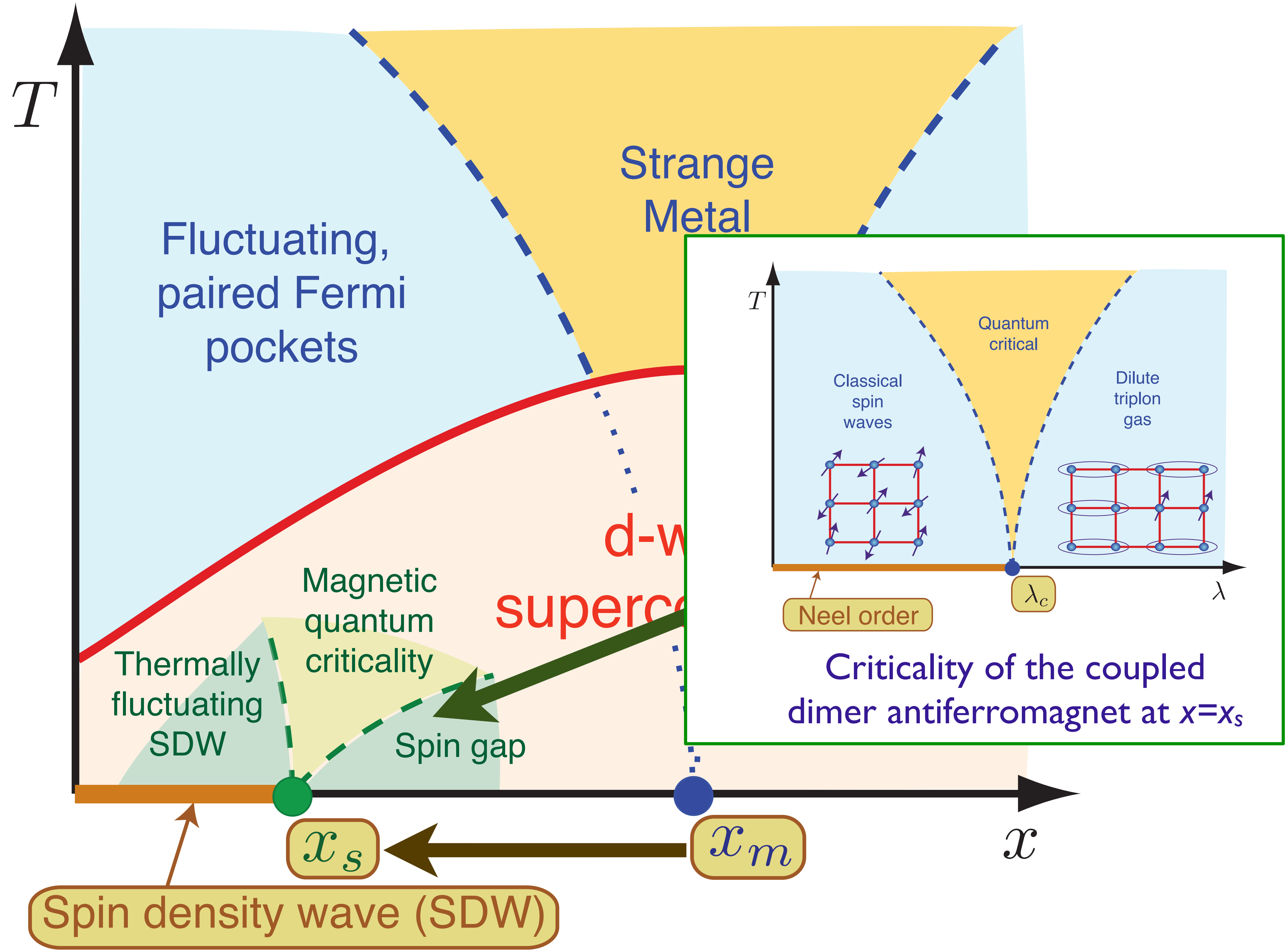

Competition between SDW order and superconductivity moves the actual quantum critical point to $x = x_s < x_m$.

Theory of quantum criticality in the cuprates

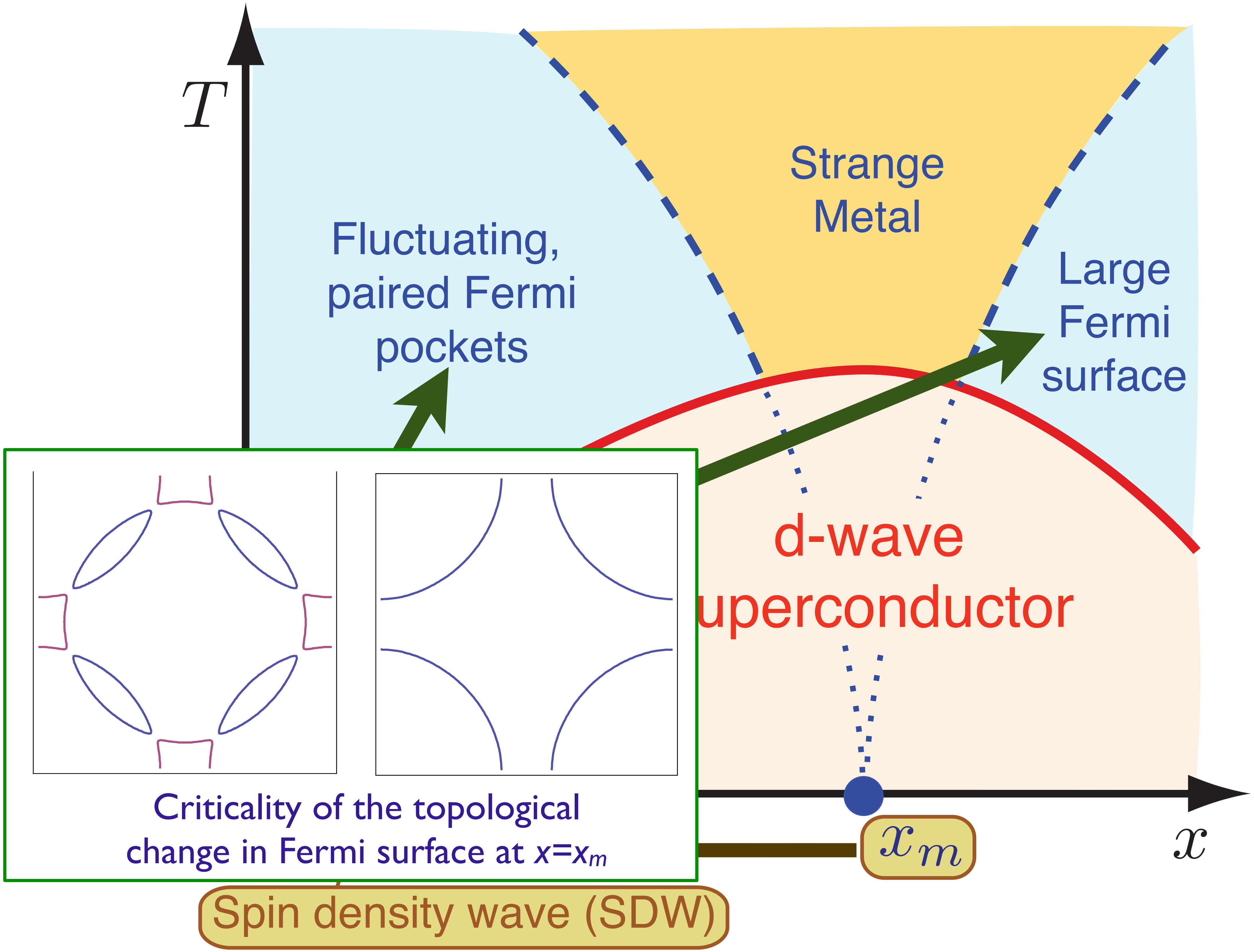

Competition between SDW order and superconductivity moves the actual quantum critical point to $x = x_s < x_m$.

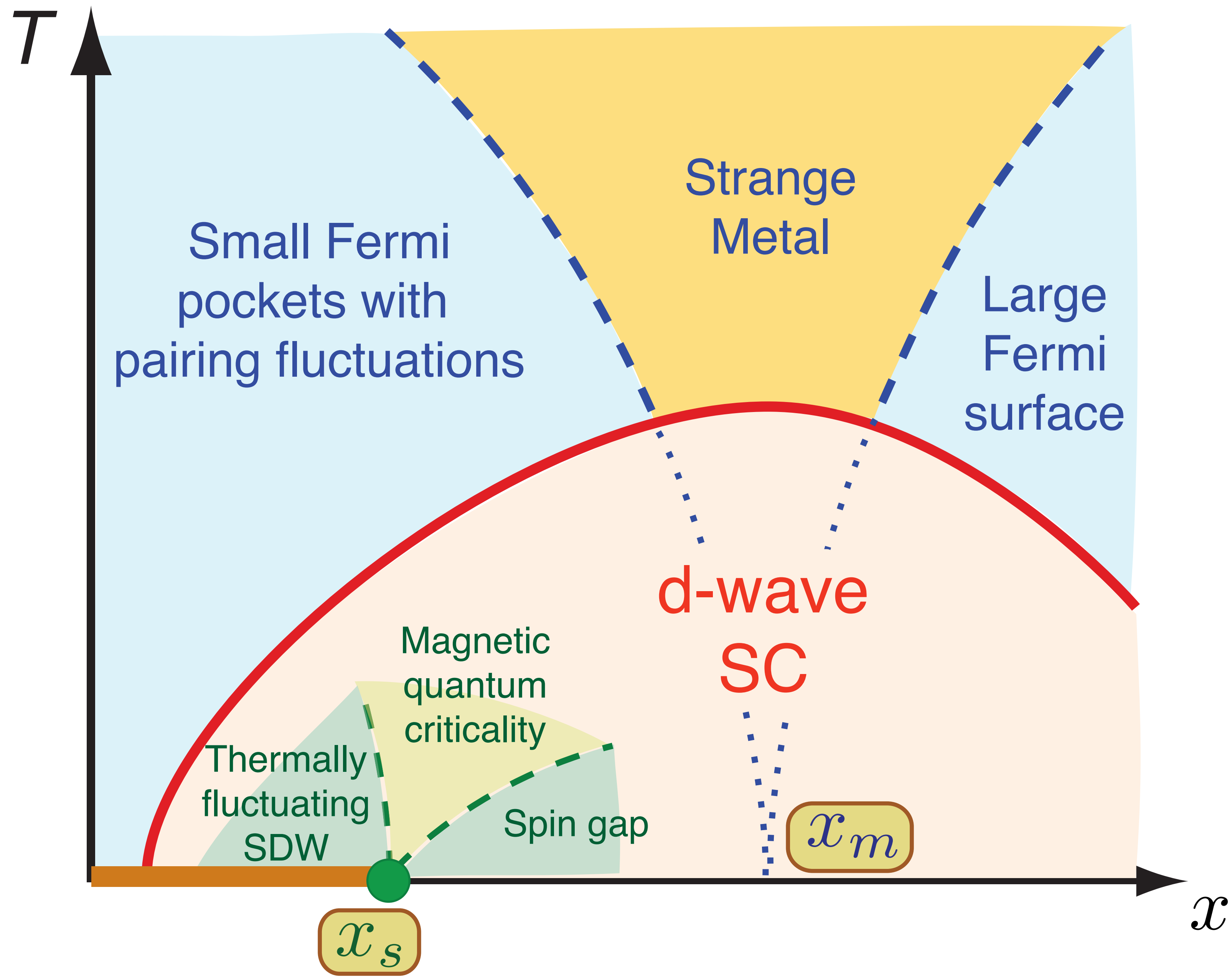
T
Small Fermi
pockets with
pairing fluctuations
Strange
Metal
Large
Fermi
surface
d-wave
SC
Magnetic
quantum
criticality
Thermally
fluctuating
SDW
Spin gap
x_m
x_s
x

Many recent neutron scattering and quantum oscillation experiments are consistent with phase diagram in the magnetic field-doping plane.

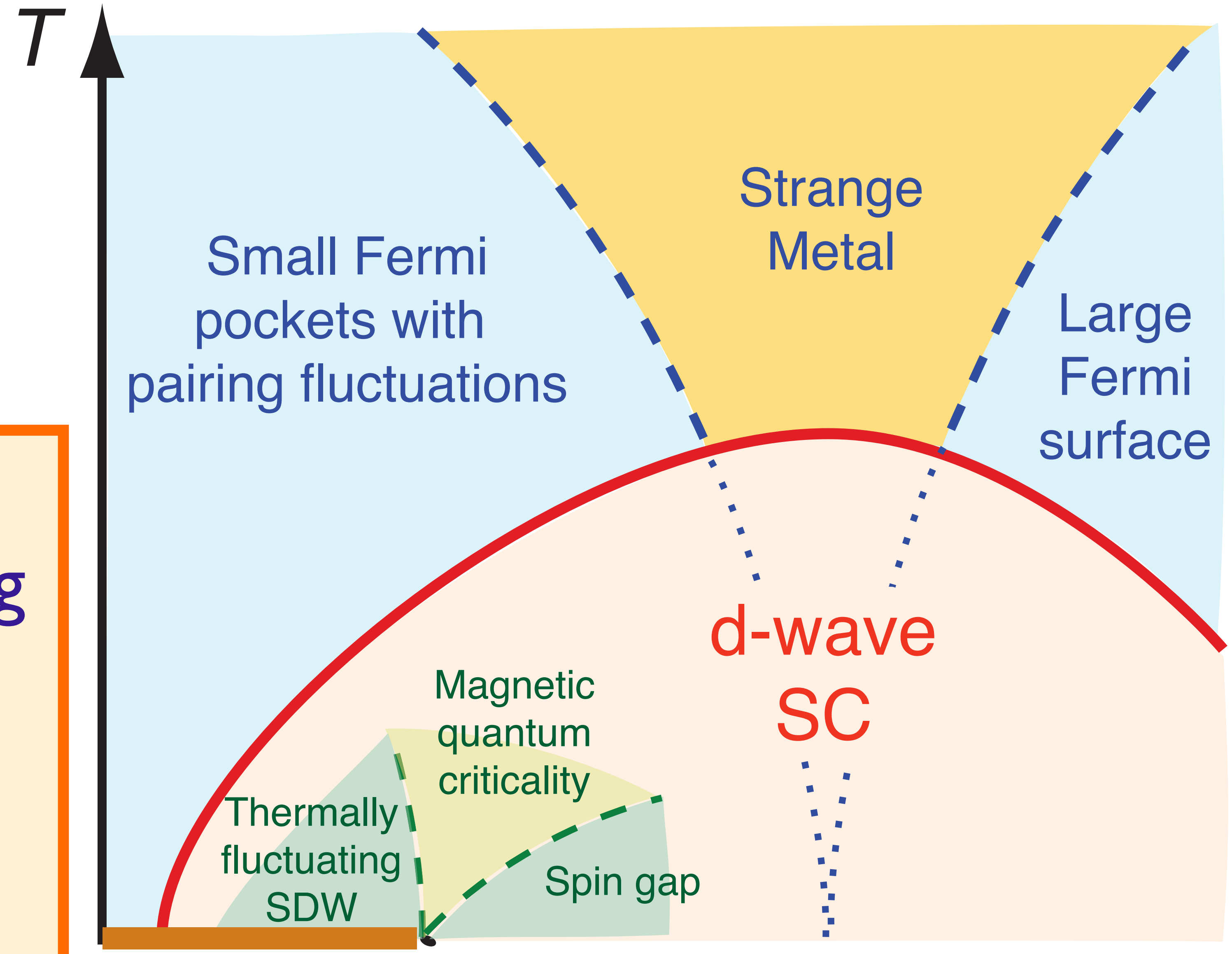

E. Demler, S. Sachdev and Y. Zhang, *Phys. Rev. Lett.* **87**, 067202 (2001).

Many recent neutron scattering and quantum oscillation experiments are consistent with phase diagram in the magnetic field-doping plane.

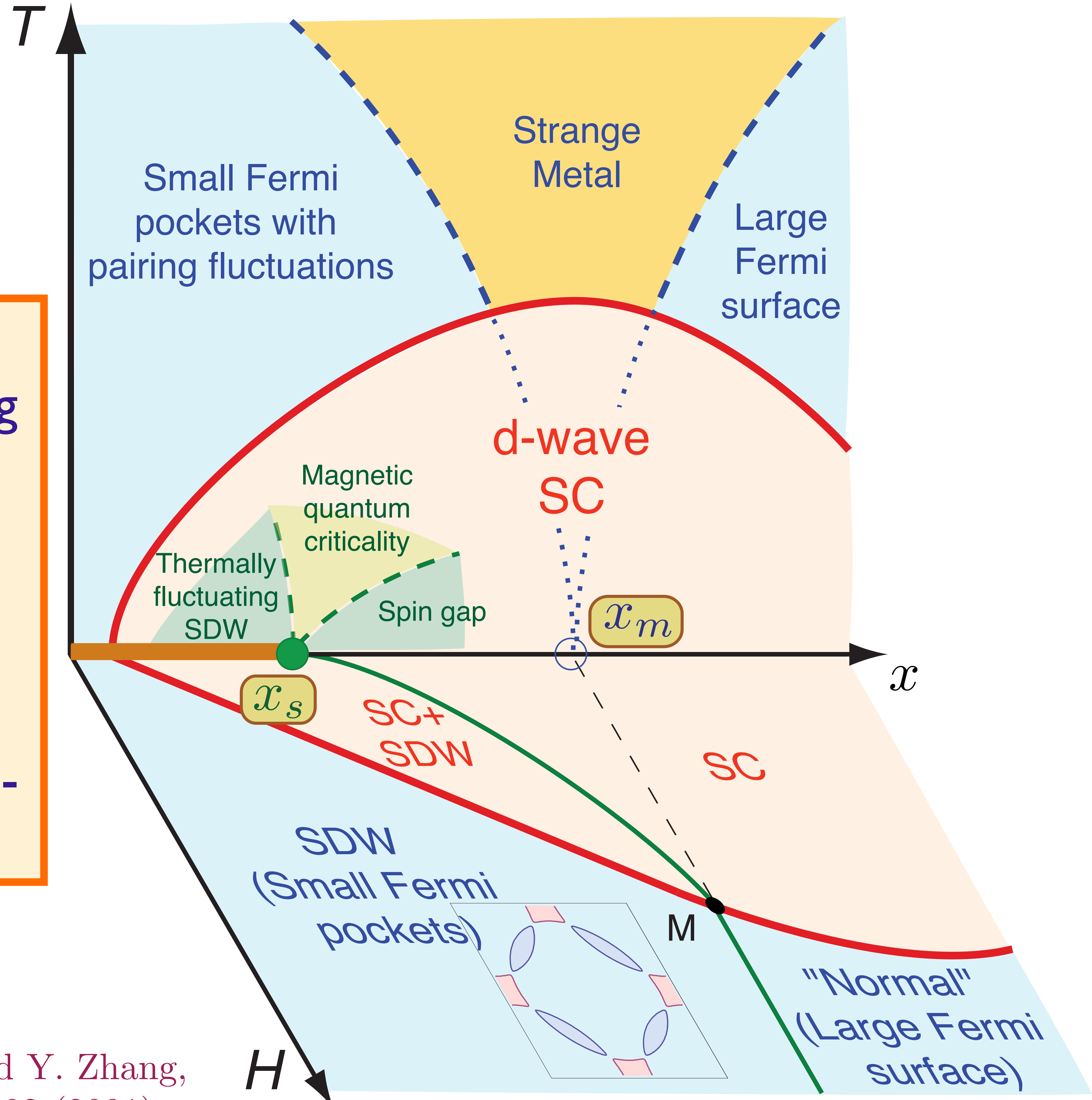

E. Demler, S. Sachdev and Y. Zhang, *Phys. Rev. Lett.* **87**, 067202 (2001).

Theory of quantum criticality in the cuprates

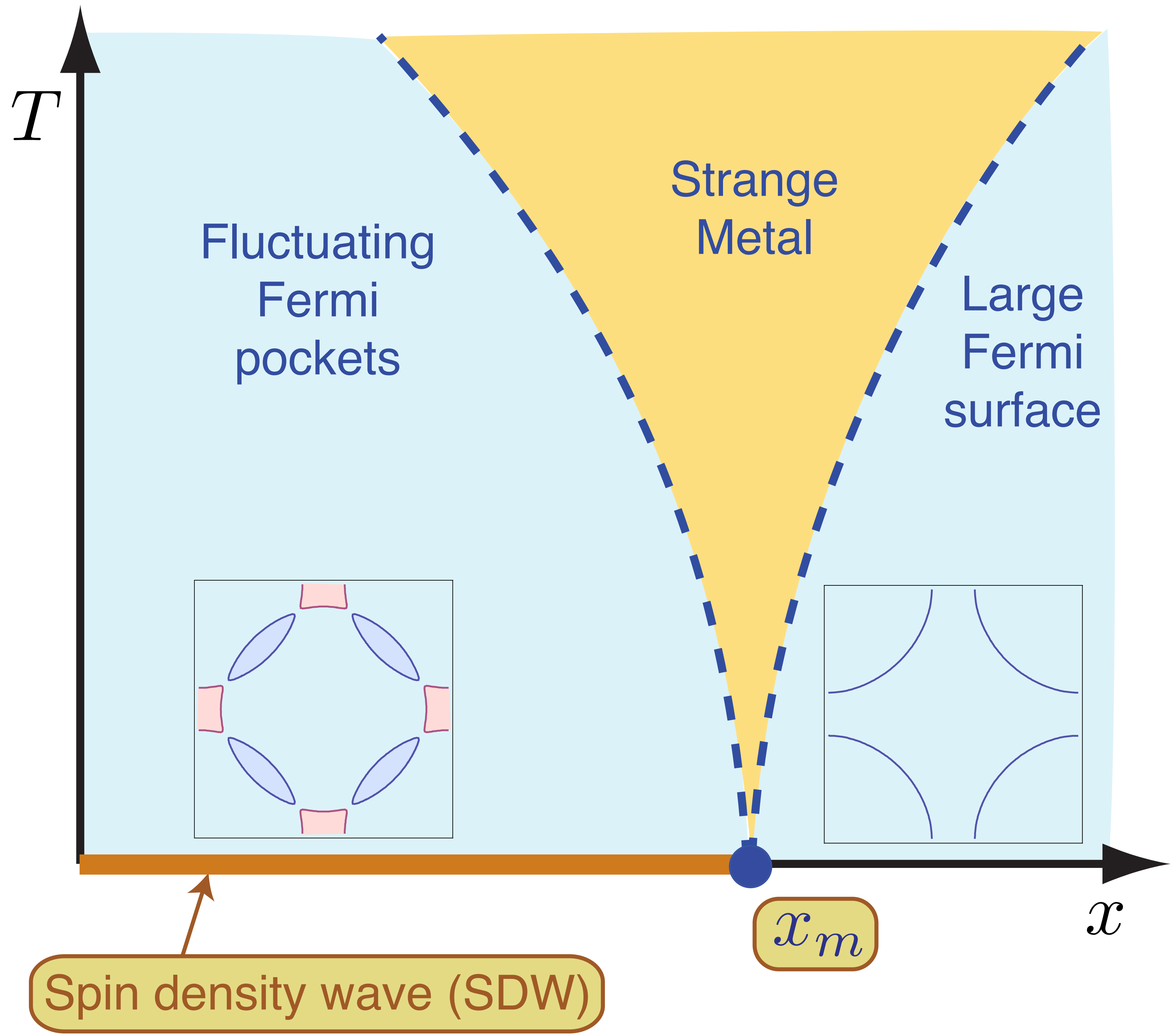

Underlying SDW ordering quantum critical point in **metal** at $x = x_m$

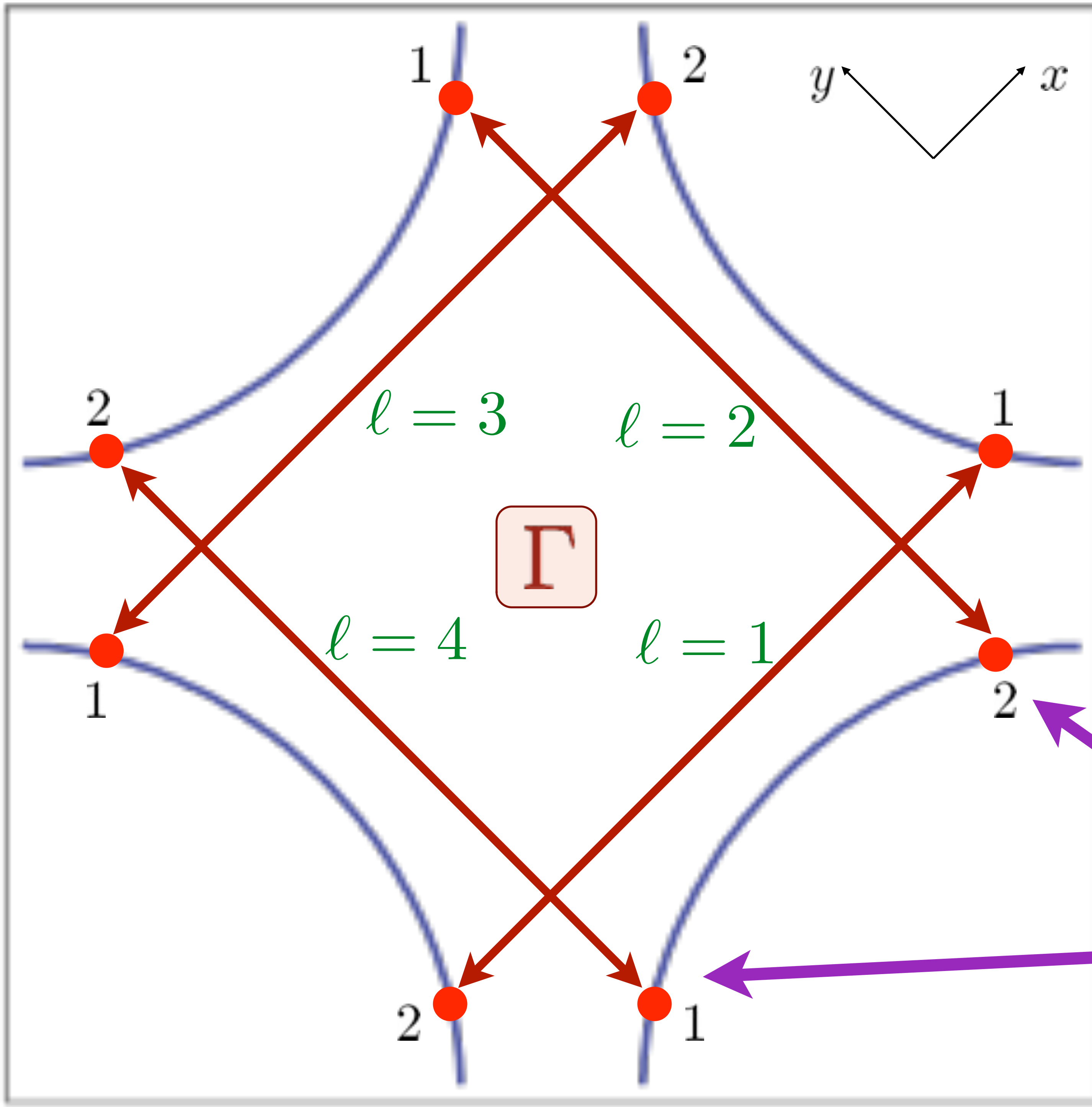

Low energy fermions
$\psi^{\ell}_{1\alpha},\ \psi^{\ell}_{2\alpha}$
$\ell = 1, \ldots, 4$

$$\mathcal{L}_f \;=\; \psi^{\ell\dagger}_{1\alpha}\left(\zeta\partial_\tau - i\mathbf{v}^{\ell}_1\cdot\boldsymbol{\nabla}_r\right)\psi^{\ell}_{1\alpha} + \psi^{\ell\dagger}_{2\alpha}\left(\zeta\partial_\tau - i\mathbf{v}^{\ell}_2\cdot\boldsymbol{\nabla}_r\right)\psi^{\ell}_{2\alpha}$$

$$\mathbf{v}^{\ell=1}_1 = (v_x, v_y),\ \mathbf{v}^{\ell=1}_2 = (-v_x, v_y)$$

$$\mathcal{L}_f = \psi_{1\alpha}^{\ell\dagger}\left(\zeta\partial_\tau - i\mathbf{v}_1^\ell\cdot\boldsymbol{\nabla}_r\right)\psi_{1\alpha}^\ell + \psi_{2\alpha}^{\ell\dagger}\left(\zeta\partial_\tau - i\mathbf{v}_2^\ell\cdot\boldsymbol{\nabla}_r\right)\psi_{2\alpha}^\ell$$

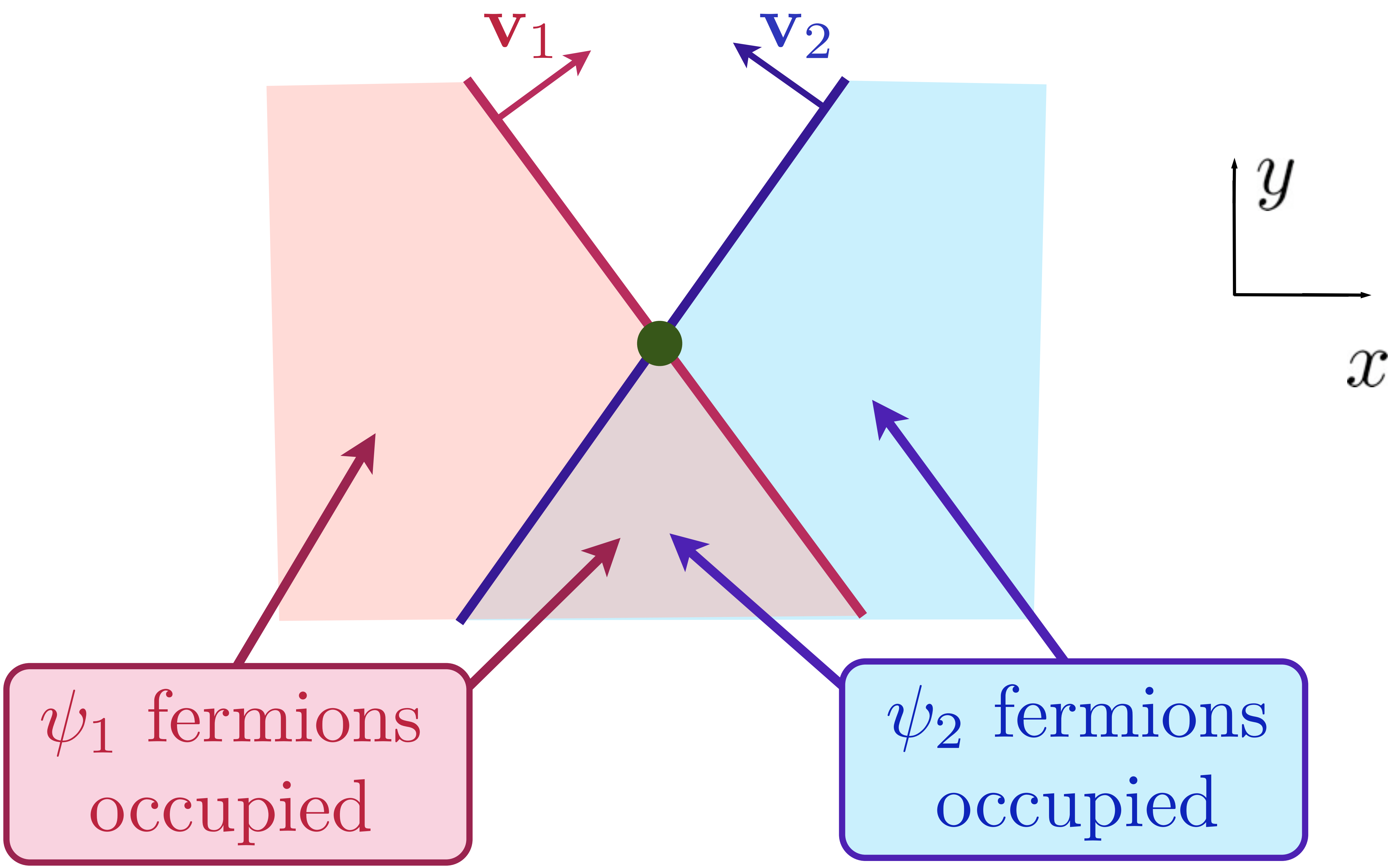

$$\mathcal{L}_f = \psi_{1\alpha}^{\ell\dagger}\left(\zeta\partial_\tau - i\mathbf{v}_1^\ell\cdot\boldsymbol{\nabla}_r\right)\psi_{1\alpha}^\ell + \psi_{2\alpha}^{\ell\dagger}\left(\zeta\partial_\tau - i\mathbf{v}_2^\ell\cdot\boldsymbol{\nabla}_r\right)\psi_{2\alpha}^\ell$$

SDW order parameter: $\mathcal{L}_\varphi = \frac{1}{2}\left(\boldsymbol{\nabla}_r\vec{\varphi}\right)^2 + \frac{s}{2}\vec{\varphi}^2 + \frac{u}{4}\vec{\varphi}^4$

$$\mathcal{L}_f = \psi_{1\alpha}^{\ell\dagger}\left(\zeta\partial_\tau - i\mathbf{v}_1^\ell \cdot \boldsymbol{\nabla}_r\right)\psi_{1\alpha}^\ell + \psi_{2\alpha}^{\ell\dagger}\left(\zeta\partial_\tau - i\mathbf{v}_2^\ell \cdot \boldsymbol{\nabla}_r\right)\psi_{2\alpha}^\ell$$

SDW order parameter: $\mathcal{L}_\varphi = \frac{1}{2}\left(\boldsymbol{\nabla}_r \vec{\varphi}\right)^2 + \frac{s}{2}\vec{\varphi}^2 + \frac{u}{4}\vec{\varphi}^4$

"Yukawa" coupling: $\mathcal{L}_c = -\vec{\varphi} \cdot \left(\psi_{1\alpha}^{\ell\dagger}\vec{\sigma}_{\alpha\beta}\psi_{2\beta}^\ell + \psi_{2\alpha}^{\ell\dagger}\vec{\sigma}_{\alpha\beta}\psi_{1\beta}^\ell\right)$

$$\mathcal{L}_f = \psi_{1\alpha}^{\ell\dagger}\left(\zeta\partial_\tau - i\mathbf{v}_1^\ell\cdot\boldsymbol{\nabla}_r\right)\psi_{1\alpha}^\ell + \psi_{2\alpha}^{\ell\dagger}\left(\zeta\partial_\tau - i\mathbf{v}_2^\ell\cdot\boldsymbol{\nabla}_r\right)\psi_{2\alpha}^\ell$$

SDW order parameter: $\mathcal{L}_\varphi = \frac{1}{2}\left(\boldsymbol{\nabla}_r\vec{\varphi}\right)^2 + \frac{s}{2}\vec{\varphi}^2 + \frac{u}{4}\vec{\varphi}^4$

"Yukawa" coupling: $\mathcal{L}_c = -\vec{\varphi}\cdot\left(\psi_{1\alpha}^{\ell\dagger}\vec{\sigma}_{\alpha\beta}\psi_{2\beta}^\ell + \psi_{2\alpha}^{\ell\dagger}\vec{\sigma}_{\alpha\beta}\psi_{1\beta}^\ell\right)$

Large *N* expansion

ψ_1 ——— ψ_2 ———

factor of N for each fermion loop

$\vec{\varphi}$ - - - - - - - - -

$\sim 1/N$

Breakdown of naive $1/N$ expansion

M. Metlitski

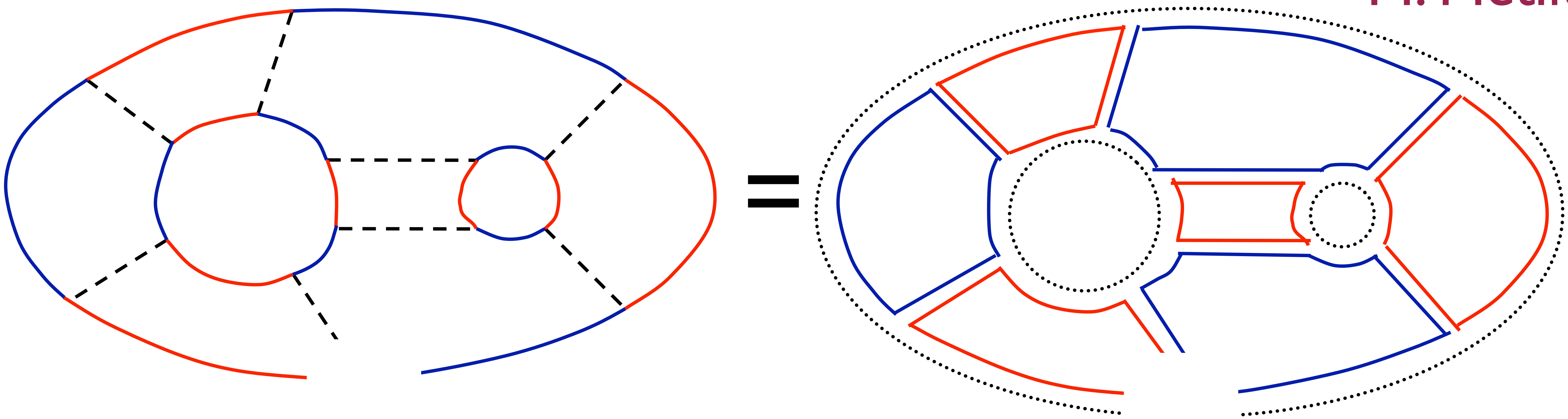

$$\text{Actual order} \sim \frac{1}{N^0}$$

Graph is **planar** after turning fermion propagators also into double lines by drawing additional dotted single line loops for each fermion loop

Sung-Sik Lee, *Phys. Rev.* B **80**, 165102 (2009); M. Metlitski and S. Sachdev, to appear

Breakdown of naive $1/N$ expansion

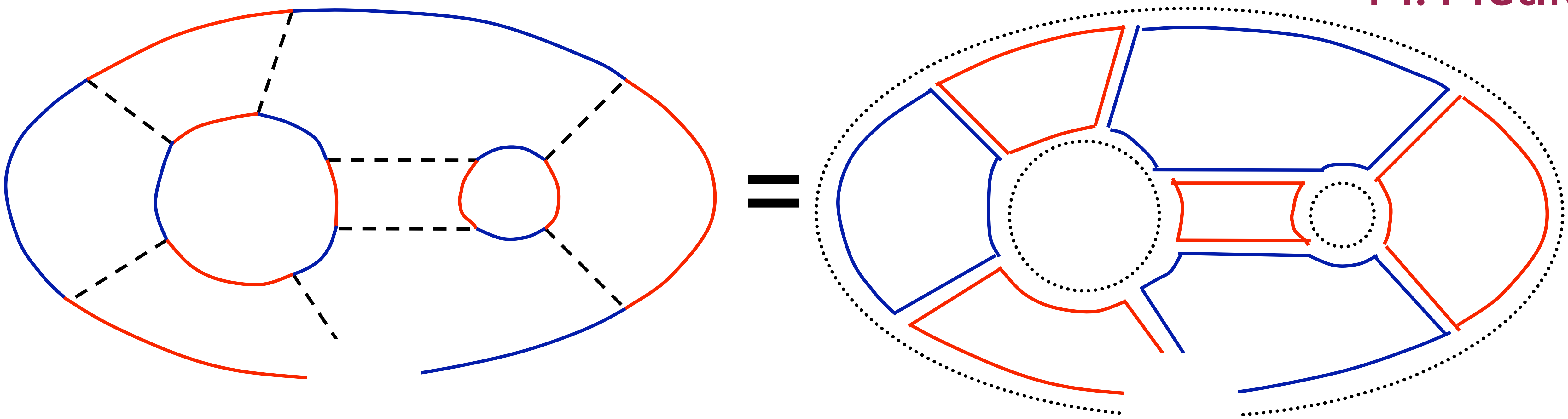

$$\text{Actual order} \sim \frac{1}{N^0}$$

A consistent analysis requires resummation of all planar graphs

Breakdown of naive $1/N$ expansion

M. Metlitski

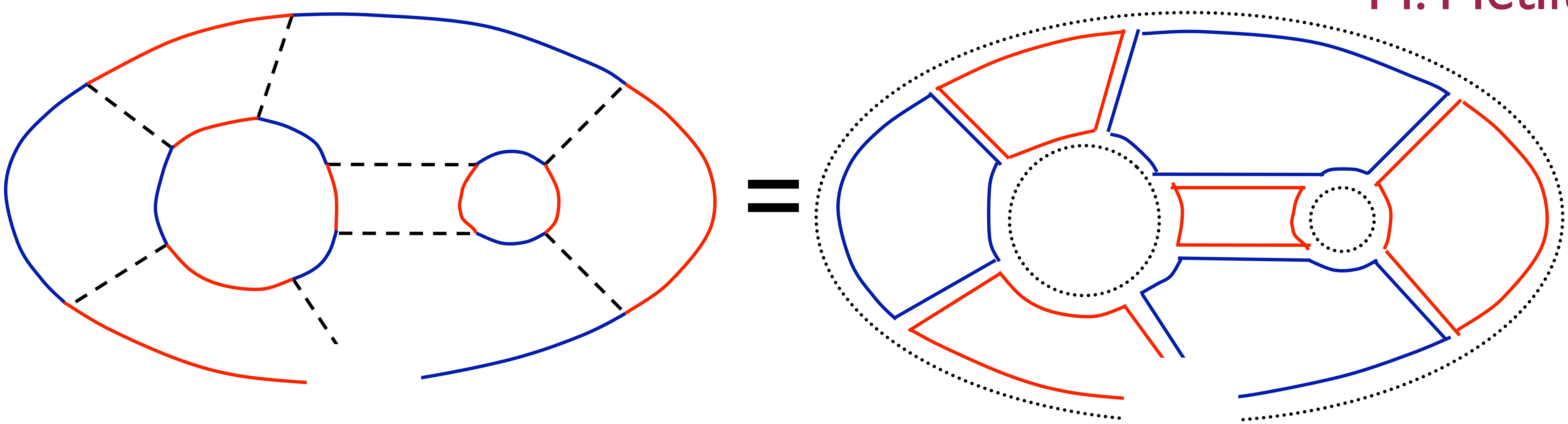

$$\text{Actual order} \sim \frac{1}{N^0}$$

A string theory for the Fermi surface ?

Conclusions

General theory of finite temperature dynamics and transport near quantum critical points, with applications to antiferromagnets, graphene, and superconductors

Conclusions

The AdS/CFT offers promise in providing a new understanding of strongly interacting quantum matter at non-zero density

Conclusions

Identified quantum criticality in cuprate superconductors with a critical point at optimal doping associated with onset of spin density wave order in a metal

Elusive optimal doping quantum critical point has been "hiding in plain sight".

It is shifted to lower doping by the onset of superconductivity